UNIVERSITÉ DU QUÉBEC À MONTRÉAL

ET

INSTITUT NATIONALE POLYTECHNIQUE DE LORRAINE (France)

DISTRIBUTION DE L'OR DE TYPE OROGÉNIQUE LE LONG DE GRANDS COULOIRS DE DÉFORMATION ARCHÉENS : MODÉLISATION NUMÉRIQUE SUR L'EXEMPLE DE LA CEINTURE DE L'ABITIBI

THÈSE

PRÉSENTÉE EN COTUTELLE

COMME EXIGENCE PARTIELLE

DU DOCTORAT EN RESSOURCES MINÉRALE

PAR

OLIVIER RABEAU

FÉVRIER, 2010

RÉSUMÉ

Cette thèse visait à mieux définir les méthodes de ciblage et apporter des éléments de réponse sur la genèse des gisements d'or de type orogénique en périphérie des grands couloirs de déformation archéens par le biais d'approches numériques novatrices. Cette thèse est présentée sous forme de trois articles. Le premier article traite de la distribution mathématique des gisements aurifères de type orogénique le long des grands couloirs de déformation. Une approche permettant de d'établir que la localisation des gisements se situant le long de structure de premier ordre n'est pas indépendante de la localisation de ses voisins a été développée. Cette approche permet de donner des éléments de réponse sur la formation de ces gisements et de générer des probabilités de découvertes à l'échelle régionale. La deuxième partie de cette présente une méthode l'évaluation du potentiel minéral sous couverture sédimentaire en 3D. Les teneurs aurifères compilées dans le secteur ont permis d'évaluer et de quantifier les relations spatiales existantes entre certaines entités géologiques et les emplacements minéralisés afin de cibler les endroits à haut potentiel. Enfin, les travaux présentés dans le dernier chapitre visent à délimiter les zones possédant une perméabilité structurale accrue lors de l'épisode de déformation contemporain à la mise en place de gisements aurifères de type orogénique. Une modélisation géomécanique 3D qui tient compte des propriétés physiques des roches a été effectuée sur un segment de faille choisi en utilisant un code d'élément fini. La déformation s'effectue en attribuant sur chaque discontinuité structurale des vecteurs ou des champs de déplacement en fonction des observations de terrain.

ABSTRACT

This thesis had the objective to define targeting methods adapted to orogenic gold deposits hosted in greenstone belts and to better understand the formation mechanism of these deposits using a numerical approach. The work accomplished is presented in three distinct articles. The first article aimed to determine if a mathematical relation can characterize the spatial distribution of orogenic gold deposits along a crustal scale fault zone within or if the localization of a deposit is independent of the position of each other. A uniform law was fitted between the frequency and the curvilinear inter-distance between successive orogenic gold occurrences along the CLLF for distances ranging from 315 to 5600 m. This approach gave insights on the formation mechanism and allowed the generation of a probability map for undiscovered deposits at a regional scale. The second chapter of this thesis focuses on a sector of the Cadillac Larder Lake Fault that was considered as having a high potential for discovery using the methodology presented in the last chapter. Compiled assays allowed the evaluation of the spatial association of certain geological features with orogenic gold mineralizations to allow targeting high potential areas. Finally, the work presented in the last chapter aimed at identifying dilatant zones during the deformation that is contemporaneous to the orogenic gold deposit formation. A 3D geomechanical modelling which takes rock properties into account was performed on a chosen segment of a fault zone using a finite element code. The deformation was induced using displacement vectors or fields interpreted from field data.

Remerciements

Je tiens avant tout à remercier Alain Cheilletz et Michel Jébrak qui ont dirigé mes travaux et m'ont fourni de précieux commentaires tout au long de cette thèse. Je remercie aussi grandement Jean-Jacques Royer pour ses conseils, et Marc-Olivier Titeux qui m'a beaucoup aidé lors de mes travaux de modélisation géomécanique. Merci aussi à Marc Legault qui m'a permis de démystifier la géologie du Sud de l'Abitibi et la métallogénie aurifère, à Guillaume Caumon qui m'a conseillé sur mes travaux de modélisation et à Anne-Laure Tertois de chez Paradigm qui m'a aidé à générer mon Solid Model

Cette thèse a été possible grâce à Denis Bois, directeur de l'URSTM-UQAT, qui a cru en moi et qui a tout mis en œuvre pour que je puisse entreprendre et mener à terme ce travail. Je tiens à le remercier pour sa confiance, son soutien et la liberté d'action qu'il m'a donnée. Je tiens aussi à remercier l'UQAT, le réseau DIVEX et le Ministère des ressources naturelles et de la Faune secteur mines qui m'ont donné le support technique et financier pour entreprendre ce travail.

Une reconnaissance particulière va à Robert Marquis qui a cru en mes capacités et qui m'a convaincu qu'il était possible de faire une thèse tout en ayant des enfants (tu avais tout de même embelli l'affaire !). Merci à l'équipe de l'UQAT et particulièrement à Francine (PB), ma coéquipière, qui m'a démarré en modélisation

géologique et qui a été pour moi une vraie défricheuse. Merci aussi à Jean Goutier avec qui j'ai discuté de nombreuse fois de géologie abitibienne et de sombréro. Je tiens aussi à remercier les autres gens du secteur Mines du MRNF (passé et présent) avec qui je travaille quotidiennement : Pat, Gabriel, Charles, Sylvain, Ali, Émilie, Claude, Johanne, Daniel, Serge, Pierre R, Hannafi, Prof. Marc, Jean, Mélanie, Lucie, Fabien, Ginette, les 2 Pierre de Montréal et François.

L'accueil chaleureux que j'ai reçu en France ne peut passer sous silence. Chacun de mes séjours de travail a été marqué par une ambiance remarquable. J'y ai côtoyé des personnes que je ne suis pas près d'oublier. Mille fois merci à Alain et Chantal avec qui j'ai passé de merveilleux moments d'un côté de l'Atlantique comme de l'autre. Leur gentillesse, leur générosité et leurs attentions ont permis à notre famille de se sentir chez soi de l'autre côté de l'océan. Ils nous ont reçus dans leur demeure et initiés à la réalité française ainsi qu'aux subtilités de la cuisine gauloise. Je n'ai connaissance d'aucun autre directeur de recherche ayant passé sa soirée de Noël à jouer de l'accordéon à une petite fille de 18 mois afin permettre à son étudiant daller assister sa femme à son accouchement. Je me considère chanceux et privilégié que nos chemins se soient croisés, je leur suis très reconnaissant pour tout ce qu'ils ont fait pour moi. Pierre et Marc-O, merci pour les quelques discussions sérieuses qu'on a pu avoir, mais surtout pour m'avoir fait rire et passer des moments inoubliables chez vous. J'espère avoir la chance de vous faire apprécier mon pays comme vous m'avez fait apprécier le vôtre et je vous souhaite beaucoup de bonheur dans l'avenir.

Merci aussi aux gens de l'équipe Gocad avec qui j'ai aussi passé de bons moments : Guillaume, Sarah, Anlor, Tobias, Manu, Luc, Christian, Pauline et tous les autres que j'ai moins bien connus faute de temps. Merci aussi aux dévouées Fatima et Mme Cugurno qui ont été très patientes avec moi et qui m'ont aidé à démêler la bureaucratie universitaire française.

Merci aussi aux compagnies minières qui ont participé au projet en me permettant d'avoir accès à leurs données et à Paradigm et Mira Géoscience qui m'ont donné accès aux licences des logiciels.

Ce travail n'aurait jamais été possible sans le support de ma famille. Clément et Éliane sont arrivés dans ce monde alors que leur père était déjà inscrit en thèse, leur joie de vivre et leur amour se sont avérés être une contribution essentielle à son achèvement. Merci à mes parents pour leur appui. Finalement, un énorme merci à ma blonde, Marie-Odile, qui a accepté de m'épauler et de me suivre dans cette aventure avec les sacrifices qui y étaient rattachés. Son soutien, son amour et sa présence à mes côtés ont été inestimables et irremplaçables.

TABLE DES MATIÈRES

Liste des figures

Liste des tableaux

Contribution des auteurs

Cette thèse est présentée sous forme d'articles scientifiques. J'ai effectué la plus grande partie des travaux en tant que premier auteur de ces articles. Je me dois par contre de souligner la participation des autres auteurs qui ont apporté une contribution dans l'interprétation des données ainsi que dans la relecture critique du texte de cette thèse. Les noms des gens ayant contribués sont énumérés au début de chaque article en tant que co-auteurs. Cette section vise à mettre en valeur la contribution spécifique de chacun des participants au travail accompli.

Dans la première partie de la thèse traitant de la distribution des gisements le long de la Faille Cadillac-Larder Lake, Jean Jacques Royer (ENSG-CRPG) a contribué à l'analyse spatiale des données et m'a aidé dans la réflexion permettant de dégager la loi mathématique expliquant la distribution spatiale des gisements. Alain Cheilletz (ENSG-CRPG) et Michel Jébrak (UQÀM) ont contribué en effectuant des lectures critiques sur le manuscrit.

Le second chapitre est le fruit du traitement d'une importante base de données et comprend la participation d'un bon nombre de personne. Marc Legault, à l'époque à l'emploi du Ministère des Ressources naturelles et de la Faune, a contribué en révisant la cartographie de surface ainsi que la caractérisation des minéralisations

aurifères dans le cadre de ses fonctions. Li Zhen Cheng (UQAT) a contribué à l'interprétation géophysique en profondeur et a effectué les inversions gravimétriques et magnétiques. Jean-Jacques Royer, Michel Jébrak et Alain Cheilletz ont effectué une lecture critique du manuscrit.

Finalement, le dernier chapitre de cette thèse qui renferme des travaux basés sur la modélisation géomécanique a été fait avec la collaboration de Marc-Olivier Titeux (ENSG-CRPG) qui m'a conseillé lors des étapes de modélisation et de paramétrisation. Michel Jébrak, Jean-Jacques Royer, Guillaume Caumon (ENSG-CRPG) et Alain Cheilletz ont effectué des lectures critiques du manuscrit.

Introduction

Les gisements d'or de type orogéniques comptent pour plus de 30% de la production mondiale en Au (Frimmel, 2007). Ces gisements épigénétiques sont retrouvés partout sur la planète dans des lithologies très variées tant en âge qu'en composition (Goldfarb et al. 2001). Une association particulière est par contre observée avec les ceintures de roches vertes archéennes où la majorité de ces gisements sont retrouvés. Au sein des ceintures de roches vertes archéennes, les gisements de type orogéniques présentent une association spatiale importante avec les failles majeures (Goldfarb et al., 2005 ; Goldfarb et al., 2001 ; Groves et al., 1998 ; Groves et al., 2003 ; Weinberg et al., 2004). On observe d'ailleurs plusieurs dépôts d'or de type orogénique qui s'alignent le long de ces failles ainsi que de leur extension verticale dans les terrains archéens à petite échelle. Ces failles majeures agissent souvent comme zones de sutures entre des terrains d'affinité différente. Ces structures qui sont souvent d'importance crustale sont dites de premier ordre et possèdent une expression en surface de plusieurs dizaines de kilomètres et une épaisseur pouvant atteindre quelques centaines de mètres (Goldfarb et al., 2005). Elles sont généralement subverticales, parallèles à subparallèles à la stratigraphie locale et deviennent listriques à très grandes profondeurs (Wyman and Kerrich, 1988). Elles représentent, pour la plus part, l'expression de plusieurs structures segmentées possédant une

évolution complexe et multiphasée sur plusieurs millions d'années (Goldfarb et al., 2001). Ces failles comportent un intérêt économique majeur puisqu'il est reconnu qu'elles agissent comme conduits principaux pour la circulation de fluides hydrothermaux possédant une source profonde (Beaudoin et al., 2006 ; Goldfarb et al., 2001 ; Goldfarb et al., 1991 ; Groves et al., 2000 ; Groves et al., 2003 ; Kerrich et al., 2000). Ces structures majeures agissent, en fait, comme système de type « pompe et valve » auprès des fluides minéralisateurs aurifères (Cox et al., 2001 ; Sibson et al., 1988).

Les failles de premier ordre dans les ceintures de roches vertes archéennes s'intègrent dans un réseau de failles et de fractures important comprenant aussi des failles de moins grande portée de deuxième et de troisième ordre. Ces dernières sont décrites comme étant respectivement parallèles et obliques au grain structural (Robert and Poulsen, 2001). Malgré leur rôle essentiel dans le transport des fluides aurifères, les failles majeures (de premier ordre) ne sont pas hôtes de la majorité des dépôts connus d'or de type orogénique. En fait, il est supposé que les failles de premier ordre amènent les fluides de source profonde jusqu'aux failles de 2e et 3e ordre de la croûte supérieur où les métaux précipitent (Eisenlohr et al., 1989; Kerrich and Feng, 1992). Les structures de dilatation servant à la précipitation des substances économiques à partir des fluides hydrothermaux sont variées et comprennent aussi les charnières de plis anticlinaux, les fractures associées aux contrastes de compétence entre les unités et les intersections de failles.

Malgré un contrôle d'ordre structural très important et l'évidence du rôle prédominant des failles de premier ordre, la distribution des dépôts d'or de type orogénique est en fait très irrégulière. L'activité des zones de déformation en tant que conduits pour les fluides minéralisateurs est hétérogène dans le temps et dans l'espace. On retrouve, en effet, des zones très riches en minéralisations et des secteurs qui en sont exempts. Typiquement, à une échelle régionale, les gisements aurifères très riches se concentrent en amas, les camps miniers, d'environ 100 à 1000 km^2 (Hodgson, 1993). Au sein de ces camps miniers, la distribution est dépendante de certains facteurs précis favorisant la circulation et la précipitation des métaux. Ces facteurs peuvent être très différents d'un terrain à l'autre malgré certains principes structuraux et géométriques qui restent similaires (Groves et al., 2000). Cette irrégularité dans la distribution des minéralisations est principalement due aux variations locales de perméabilité permettant la circulation de fluides et les dépôts de minéralisations.

Ce travail vise à effectuer l'étude de la distribution des gisements d'or de type orogénique le long de grands couloirs de déformation archéens par une approche numérique. En premier lieu, ce travail présente une étude da la distribution spatiale à grande échelle des gisements aurifères connus le long d'un couloir de déformation archéen majeur. Cette approche vise à établir s'il existe une relation mathématique caractérisant la distribution spatiale des gisements d'or orogénique le long de grand couloir de déformation archéen ou si la localisation d'un gisement est indépendante de la position spatiale des autres. Ce type d'approche, basée sur une distribution

géographique systématique, permet d'apporter des éléments de réponse en ce qui concerne le mode de formation des gisements aurifères de type orogénique et peut être exploité comme un outil d'exploration utile à l'échelle régionale. La deuxième partie de cette thèse aborde l'évaluation de potentiel par le biais de la modélisation régionale en 3D d'un segment d'une faille archéenne de premier ordre identifiée comme possédant un fort potentiel pour la présence de gisements non découverts à cause d'une couverture sédimentaire protérozoïque qui complique l'exploration. Ce chapitre vise à dresser le lien entre la présence de minéralisation le long de zones de suture archéennes ainsi que de leurs failles subsidiaires et la présence de certains éléments géologiques précis. L'association spatiale entre ces facteurs et les minéralisations aurifères a par la suite été pondérée et utilisée dans la génération de cartes de potentiel minéral en 3D spécifique à l'emplacement étudié. Finalement, un segment choisi d'un couloir de déformation archéen sera utilisé afin d'effectuer une modélisation géomécanique. Ce chapitre se base sur la notion que les pressions tectoniques et lithostatiques infligées à un volume rocheux entraînent des migrations de fluides des zones à hautes pressions vers les zones à basses pressions. Considérant que l'or s'est mis en place dans les ceintures de roches vertes suite à la majorité de la déformation tectonique, il est raisonnable de croire qu'en déformant une représentation 3D de la géologie présente aujourd'hui en utilisant les indicateurs cinématiques observables sur le terrain, il sera possible de développer un outil permettant la prévision de l'emplacement des zones de circulation hydrothermale lors de la mise en place de l'or.

Époque de mise en place de l'or de type orogénique

Cette thèse utilise une approche numérique afin d'effectuer l'étude de la distribution des gisements aurifères de type orogénique le long de grands couloirs de déformation archéens. Ce type d'étude implique une très bonne connaissance de la géologie de la ceinture de roches vertes hôte. Cette géologie est étudiée en fonction de la géométrie des entités observables présentement. L'utilisation d'observations et de données provenant de la ceinture de roche verte afin d'interpréter des modèles géologiques 2D ou 3D et de les mettre en relation avec les minéralisations aurifères implique que la géométrie observable aujourd'hui doit être similaire à celle présente lors de la mise en place. L'époque de mise en place de l'or de type orogénique par rapport à l'évolution tectonique de la ceinture est donc un élément crucial.

Cette thèse se concentre sur la distribution des gisements d'or orogénique au sein de la Sous-province archéenne de L'Abitibi. L'apparition tardive des minéralisations aurifères de type orogénique dans l'évolution tectonique des ceintures de roches vertes archéennes comme celle de l'Abitibi a été établie par plusieurs auteurs en se fiant principalement à des observations de terrain et à l'âge relatif des minéralisations par rapport aux unités datées les recoupant (Groves et al, 2000, Goldfarb et al., 2005, Dubé et Gosselin, 2007). Il a été statué que l'événement minéralisateur principal se serait produit à la fin de l'événement compressif Nord-Sud qui est responsable de l'orientation est-ouest des unités de la ceinture (Robert et al., 2005). Ceci implique

donc une mise en place tardive par rapport à la déformation. Même si certaines minéralisations semblent plus précoces (Couture et al. 1994) ou montrent des évidences de déformation ainsi que de remobilisation importante, cette étude fait la supposition que l'événement hydrothermal principal ayant engendrée la formation de la très grande majorité des gisements orogénique s'est produit tardivement dans l'évolution tectonique.

Ayant établi que la géométrie structurale observable est très similaire à celle présente lors de la circulation des fluides minéralisateurs et la mise en place des gisements d'or de type orogénique (Groves et al., 2000). Il est donc scientifiquement possible d'utiliser des cartes géologiques, des sections ou des modèles géologiques 3D représentant la géométrie actuelle afin d'effectuer la simulation des conditions physiques présentes lors de la mise en place des minéralisations (Groves et al., 2000 ; Weinberg et al., 2004).

Références

Beaudoin, G., Therrien, R., and Savard, C., 2006, 3D numerical modeling of fluid flow in the Val-d'Or orogenic gold district: major crustal shear zones drain fluids from overpressured vein fields: Mineralum Deposita, v. 41, p. 82-98.

Cox, S. F., Knackstedt, M. A., and Braun, J., 2001, Principles of structural control on permeability and fluid flow in hydrothermal systems., in Richards, J. P., and Tosdal, R. M., eds., Structural controls on ore genesis, volume 14. Reviews in Economic geology., Society of Economic Geologists.

Couture, **J.-F.,** Pilote, P., Machado, N., Desrochers, J.-P**. 1994,** Timing of gold mineralization in the Val-d'Or District, southern Abitibi Belt; evidence for two distinct mineralizing events, *Economic Geology*; v. 89; no. 7; p. 1542-1551

Dubé, B. et Gosselin, P., 2007, Greenstone-hosted quartz-carbonate vein deposits, *in* Goodfellow, W.D., ed., Mineral Deposits of Canada: A Synthesis of Major Deposit-Types, District Metallogeny, the Evolution of Geological Provinces, and Exploration Methods: Geological Association of Canada, Mineral Deposits Division, Special Publication No. 5, p. 49-73.

Eisenlohr, B. N., Groves, D. I., and Partington, G. A., 1989, Crustal-scale shear zones and their significance to Archaean gold mineralization in Western Australia: Mineralium Deposita, v. 24, p. 1-8.

Frimmel, 2007, Earth's continental crustal gold endowment, Earth and Planetary Science Letters 267, 1-2, 1, p. 45-55

Goldfarb, R. J., Baker, T., Dubé, B., Groves, D. I., Hart, C. R. J., and Gosselin, P., 2005, Distribution, Character, and Genesis of Gold Deposits in Metamorphic Terranes, p. 407-450.

Goldfarb, R. J., Groves, D. I., and Gardoll, S., 2001, Orogenic gold and geological time: a global synthesis: Ore Geology Reviews, v. 18, p. 1-75.

Goldfarb, R. J., Snee, L. W., Miller, L. D., and Newberry, R. J., 1991, Rapid dewatering of the crust deduced from ages of mesothermal gold deposits: Nature, v. 354, p. 296-298.

Groves, D. I., Goldfarb, R. J., Gebre-Mariam, M., Hageman, S. G., and Robert, F., 1998, Orogenic gold deposits: A proposed classification in the context of the crustal distribution and relationship to other deposit types: Ore Geology Reviews, v. 13, p. 7-27.

Groves, D. I., Goldfarb, R. J., Knox-Robinson, C. M., Ojala, J., Gardoll, S., Yun, G. Y., and Holyland, P., 2000, Late-kinematic timing of orogenic gold deposits and significance for computer-based exploration techniques with emphasis on the Yilgarn Block, Western Australia: Ore Geology Reviews, v. 17, p. 1-38.

Groves, D. I., Goldfarb, R. J., Robert, F., Hart, C. R. J., and, 2003, Gold deposits in metamorphic belts: overview of current understanding, outstanding problems, future reaserch, and exploration significance.: Economic Geology, v. 98, p. 1-29.

Hodgson, C. J., 1993, Mesothermal Lode-gold Deposits, in Kirkham, R. V., Sinclair, W. D., Thorpe, R. I., and Duke, J. M., eds., Mineral Deposit Modeling, Special Paper 40, Geological Association of Canada, p. 635-678.

Kerrich, R., and Feng, R., 1992, Archean geodynamics and the Abitibi-Pontiac collision: implications for advection of fluids at transpressive collisional boundaries and the origin of giant quartz vein systems: Earth-Sci. Rev., v. 32, p. 33-60.

Kerrich, R., Goldfarb, R. J., Groves, D. I., and Garwin, S., 2000, The Geodynamics of World-Class Gold Deposits: Characteristics, Space-Time Distribution, and Origins., in Hageman, S. G., and Brown, P. E., eds., Gold in 2000, 13, Reviews in Economic geology, p. 500-551.

Sibson, R. H., Robert, F., and Poulsen, K. H., 1988, High-angle reverse faults, fluid-pressure cycling, and mesothermal gold-quartz deposits: Geology, v. 16, p. 551-555.

Weinberg, R. F., Hodkiewicz, P. F., and Groves, D. I., 2004, What controls gold distribution in Archean terranes? Geology, v. 32, p. 545-548.

Wyman, D., and Kerrich, R., 1988, Alkaline Magmatism, Major Structures, and Gold Deposits: Implications for Greenstone Belt Gold Metallogeny: Economic Geology, v. 83, p. 454-461.

Chapitre 1: Spatial Distribution of Orogenic Gold Deposits along Major Archean Faults

1.1 Introduction générale

Ce chapitre est consacré à l'étude de la distribution statistique des minéralisations aurifères de type orogénique le long de grands corridors de déformation archéens. L'objectif principal de ce travail est de déterminer s'il existe une relation mathématique décrivant la distribution spatiale des gisements d'or de type orogénique le long de couloirs de déformation archéens majeurs ou si la position de chacun des gisements est indépendante de celle des autres.

Les travaux présentés se concentrent sur les failles Cadillac Larder Lake et Porcupine-Destor dans la ceinture de roches vertes de l'Abitibi dans la Province du Supérieur au Canada. Ces failles représentent des structures majeures visibles sur plusieurs dizaines de kilomètres et ayant contrôlé l'évolution hydrothermale d'une importante portion de croûte à l'Archéen. De plus, une importante base de données est déjà existante le long de ces couloirs de déformation qui permet ce type d'étude. Afin de prendre en compte la zone de dommage des failles, une zone tampon de 1 km a été créée le long des deux failles et tous les gisements inclus dans cette zone ont été

considérés dans l'étude. Un total de soixante-douze et vingt gisements connus le long des failles Cadillac-Larder Lake et Porcupine-Destor ont respectivement été utilisés afin de vérifier si leur distribution spatiale pouvait être considérée comme aléatoire ou si elle respectait une logique cohérente.

Une distribution de type log-uniforme a été trouvée entre la fréquence cumulative d'occurrence et l'inter-distance curvilinéaire entre les gisements.de type orogénique pour des inter-distances variant entre 315 et 5600 m le long de la Faille Cadillac-Larder Lake. Puisque les gisements sont moins nombreux le long de la Faille Porcupine-Destor, l'étude de cette dernière a servi à valider les résultats obtenus pour la Faille Cadillac-Larder Lake. Les résultats le long de ces failles ont été interprétés comme suggérant une influence structurale très importante sur la mise en place des minéralisations aurifères de type orogénique. En fait, les auteurs suggèrent que les emplacements minéralisés pourraient représenter des zones de relâchement de pression hydrostatique et que la distribution représenterait des ruptures structurales le long de la faille Cadillac-Larder Lake. Ces ruptures dues à des surpressions de fluides hydrothermaux créeraient des zones de perméabilité structurale importante et permettraient la circulation des fluides et le dépôt des minéralisations par relâchement de pression. Les résultats suggèrent que les zones d'influence de ces relâchements décroissent de façon logarithmique.

Finalement, une probabilité a été dérivée de la loi log-uniforme afin de générer une carte de potentiel en minéralisations aurifères de type orogénique régionale. Cette carte est basée sur la localisation des dépôts connus et permet une approche prédictive régionale qui peut s'avérer utile puisqu'elle permet de travailler avec une grande variété d'environnements géologiques et de cibler des territoires à plus fort potentiel en minéralisations sur une grande étendue.

Spatial Distribution of Orogenic Gold Deposits along Major Archean Faults

Olivier Rabeau
Université du Québec en Abitibi-Témiscamingue, Unité de recherche et de services en technologie minérale, 445 boul. de l'Université, Rouyn-Noranda, QC, Canada, J9X 5E4, Tel: (819) 354 4514 #248, Fax : (819) 354 4508 - olivier.rabeau@uqat.ca

Jean-Jacques Royer
CRPG, Centre de Recherche Pétrographique et Géochimique, Nancy Université, BP 20, 54501 Vandœuvre-lès-Nancy Cedex, France - royer@crpg.cnrs-nancy.fr

Michel Jébrak
UQAM, Université du Québec à Montréal, Département de Sciences de la Terre et de l'Atmosphère, 201, avenue du Président-Kennedy, PK-615, Montréal, QC, Canada, H2X 3Y7 - michel.jebrak@uqam.ca

Alain Cheilletz
CRPG, Centre de Recherche Pétrographique et Géochimique, Nancy Université, BP 20, 54501 Vandœuvre-lès-Nancy Cedex, France - cheille@crpg.cnrs-nancy.fr

Keywords: orogenic gold, spatial distribution, Cadillac Larder Lake Fault, hydrothermal flow, Archean

1.2 Abstract

The Cadillac-Larder Lake Fault zone located in the Abitibi Greenstone Belt in Canada was selected to determine if a mathematical relation can characterize the spatial distribution of orogenic gold deposits along a crustal scale fault zone within an Archean greenstone belt or if the localization of a deposit is independent of the position of each other. The Cadillac-Larder Lake Fault is a typical example of a large crustal scale fault zone which controlled the hydrothermal evolution of a large part of an important greenstone Belt. The extensive database of gold deposits compiled along this major structure makes it suitable for a study on the spatial distribution of ore deposits.

A buffer zone of 1 km was calculated around the fault trace and all deposits located within this zone were projected on the fault trace. A total of seventy two gold deposits were used to determine the spatial relationship. A uniform law was fitted between the frequency and the curvilinear inter-distance between successive orogenic gold occurrences along the CLLF for distances ranging from 315 to 5600 m. These results suggest that the spatial distribution of gold deposits may be attributed to structural failure and that the influence of lithological variation at a regional scale has a very low impact on the localization of gold mineralization along a crustal scale fault zone. The structural failure allowing fluid circulation during compression may be

induced by hydrostatic overpressure along a major Archean within the fault zone. The logarithmic distribution of inter-distances between deposits may explain that pressure release decreases following logarithmic law. Finally, probability was derived from the log uniform distribution to create a regional probability map along the Cadillac Larder Lake Fault Zone that is based on the location of known deposits.

1.3 Introduction

At mining camp scale, exploration geologists can rely on certain recurring features to evaluate the emplacement of orogenic gold mineralizations within Archean Greenstone belts. Many works on mineral potential mapping (Groves et al., 2000) or concerning controls on hydrothermal fluid flow (Cox et al, 2001; Sibson, 2001; Micklethwaite and Cox, 2004) have refined these exploration guidelines. The efficiency of predictive approaches relying on geological features is highly dependent on the location and dimension of the area being prospected. Similar approaches applied to a regional present a higher degree of difficulty because of the variety of geological environments.

Major crustal scale fractures such as the Boulder-LeFroy in the Yilgarn Craton or the Cadillac Larder Lake and the Destor-Porcupine faults in the Superior Craton represent, in a regional perspective, the main metallotect for orogenic gold deposits in

Archean greenstone belts. These structures spatially control the distribution of gold deposits acting as conduits that channel deep seated hydrothermal fluids (Goldfarb et al., 2001; Groves et al., 2003; Kerrich et al et al., 2000). Even tough, the association between these important structures and their vertical extension with orogenic gold mineralizations is clear, the distribution of deposits along the major structures still remains heterogonous and presents an apparently irregular pattern. Only a few studies have addressed the problem of regional distribution of orogenic gold deposits along major fault zones (Groves et al., 1998; Weinberg et al. 2004) within prolific Archean Greenstone Belts.

The main objective of this work is to determine if a mathematical relation can characterize the spatial distribution of orogenic gold deposits along a crustal scale fault zones or if the localization of a deposit is independent of the position others. The study will focus on the main fault zone in the Abitibi Subprovince in terms of gold production, the Cadillac–Larder Lake Fault (CLLF) (fig, 1-1). This structure is a typical example of a large crustal scale fault within an Archean greenstone Belt and the extensive database of gold deposits compiled along this major structure makes it suitable for a study on the spatial distribution of ore deposits.

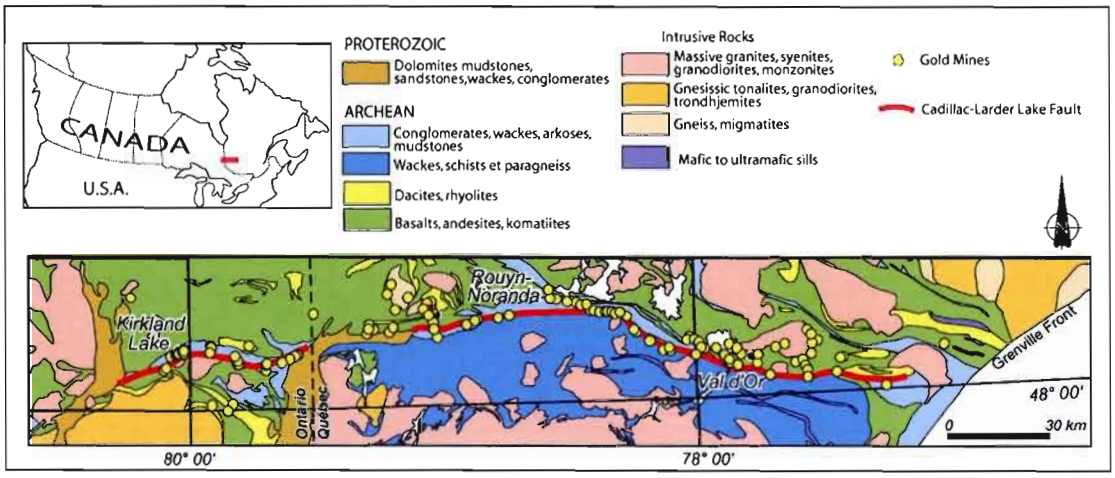

Figure 1-1: Simplified geology surrounding the Cadillac-Larder Lake Fault Zone (red) with localization of gold mines (yellow dots) and copper and zinc mines (red squares)

1.4 Geological setting

The Archean Abitibi and Pontiac Subprovinces (Figure 1-1) are located in the southern part of the Superior Craton. The Abitibi Subprovince is renowned as one of the richest gold and base metal producing region of the world. This plutonic and supracrustal belt is mainly composed of volcanic rocks ranging from komatiites to rhyolite, sediments intruded by many plutonic bodies with ages varying in a range of 2670 to 2759 Ma (Goutier and Melançon, 2007 and references therein). The Abitibi Subprovince has been defined as a collage of two arcs, the older Northern and

younger Southern volcanic zones (Chown et al., 1992). However, recent studies indicate that the Abitibi Subprovince could be much more complex than a simple collage of younger volcanic episodes onto old ones (Thurston, 2008). In many cases, geochronological data show a dismembering of older volcanic episodes with rifting during extrusion of younger volcanics (Goutier et al., 2008). Two main faults cross cut the Abitibi Green stone belt, Cadillac Larder Lake Fault (CLLF) and the Porcupine Destor Fault (PDF). The Pontiac Subprovince is (2,685 Ma to 2,672 Ma; Davis, 2002) located South of the Abitibi Subprovince is mainly composed of highly folded and deformed turbiditic sediments with rare horizons of mafic to ultramafic volcanics. .

In the Province of Quebec, the limit between these two Subprovinces is marked by one of the most important crustal scale fault zones in the area, the Cadillac Larder Lake Fault (Fig. 1-1). This major structure has been interpreted as a suture zone separating these terrains of different affinity (Daigneault & Mueller, 2004, Kerrich & Feng, 1992). The CLLF has a lateral extent of more than 200 km and can be identified from the city of Matachewan in Ontario to the city of Val-d'Or in Quebec. More than 2000 Mt of gold have been extracted from its vicinity from many world class mining camps (>100 Mt) such as Val-d'Or, Malartic, Cadillac, Larder Lake and Kirkland Lake (Poulsen et al., 2000)

Recent studies (Benn and Plesher 2005) based on analogue modeling, gravity models, seismic data and recent field work have interpreted the western segment of the CLLF and Porcupine Destor Fault located 200 km North as shallowly rooted fold-related structures. A consensus has been established on the fact that the eastern part of the CLLF actually represents a transcrustal structure marking the Boundary between the Pontiac Abitibi and the Pontiac Subprovinces (Dimroth et al., 1982) which lie respectively north and south of the CLLF.

1.5 Distribution of orogenic gold deposits along the CLLF

Spatial distribution of mineral deposits has been of great interest for the exploration and the research community even considering that mine or deposit distribution can only give an evaluation of the true metallic distribution of an area considering undiscovered deposits and economic factors. A systematic geographical distribution of mineralizations can be exploited as a valuable regional exploration tool and analogues to evaluate natural resource potentiality in under explored regions presenting similar geological context (McCammon, 1993). The mathematical function that determines the spatial distribution of orogenic gold mineralization can be used to determine fault segment which are the most favorable for undiscovered deposits along important Archean structures. Furthermore, the distribution of mineral deposits can provide insights on the formation of gold deposits.

A fractal approach was considered to explain the spatial distribution of precious metals within the Sierra Nevada (Carlson, 1991) and gold deposits in the Zimbabwe craton (Blenkinsop and Sanderson, 1999). The distribution of Archean orogenic gold deposits in the vicinity of crustal scale fault zone has also been tested along the Boulder-Lefroy Fault zone in Australia by Weinberg et al (2004) which noted a link with the presence of a gold mine and geological complexity. The approach proposed in this study is focussed on the distance separating each deposit from its neighbors and the possible relation with the distribution of mineralizing fluids pathways in structural dilation sites

1.6 Available Data and Methodology

The spatial analysis of the distribution orogenic gold deposits along the CLLF was undertaken using information contained in the public database of the *Ministry of Natural Ressources and Fauna of Quebec*. The study focuses on the segment where the CLLF marks the boundary between the Abitibi and Pontiac. The length of this segment of the CLLF represents about 160 km and almost 80% of its total length.

The CLLF is often represented as a line on the 2D map even though the associated damage zone of this major structure represents a much larger area, corresponding to many hundred meters. To account for the thickness of the deformation zone and the

multiple splays directly associated to the CLLF, a one kilometer buffer zone was established around the map trace of the CLLF in the sector of interest. All deposits located within this zone were used to conduct the spatial analysis. Mineralized occurrences defined by a single sample or a drill hole interception were not taken into account. The final deposit database is presented in table 1.

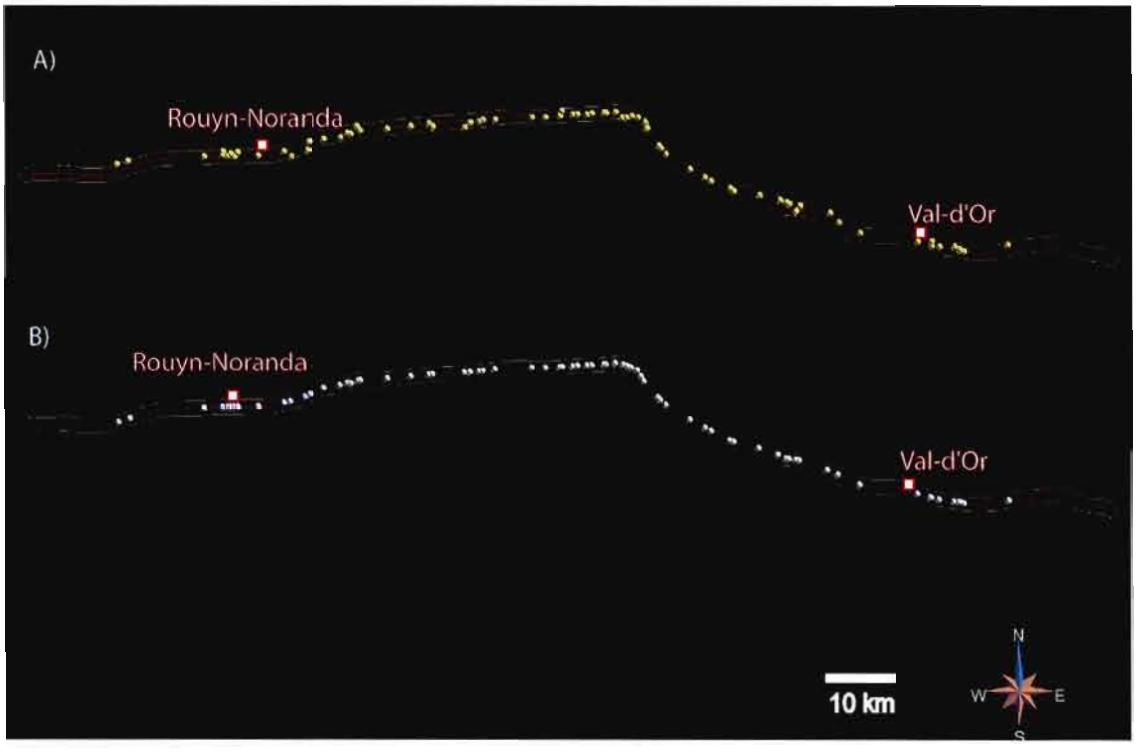

Figure 1-2: A) Distribution of orogenic gold deposits used in the study (yellow dots) and Cadillac-Larder-Lake fault zone (red line) with 1000 m buffer zone (yellow line). B) Projected known gold deposits

The deposit database was filtered to conduct the analysis only on deposits belonging to the orogenic gold type, and avoid incorporating other mineralization types with distinct characteristics, source, timing, and formation mechanism. Other types of gold mineralizations encountered in the study area are mainly volcanic massive sulfides or porphyry type deposits. Individual studies of deposits were used to determine the type of mineralization (Couture, 1996, Legault & Rabeau, 2006; Pilote et al., 2000; Lafrance et al., 2003; , Poulsen et al., 2000; Robert et al. 2005; Dubé and Gosselin, 2007). Certain known characteristics of orogenic gold deposits were also used to discriminate orogenic gold deposits from other types of gold mineralization. The metal content was the main discriminating factor on the basis that f the mineralizing fluids involved in the formation of orogenic gold have very low salinity deposits implying low base metal content (Groves et al., 2003).

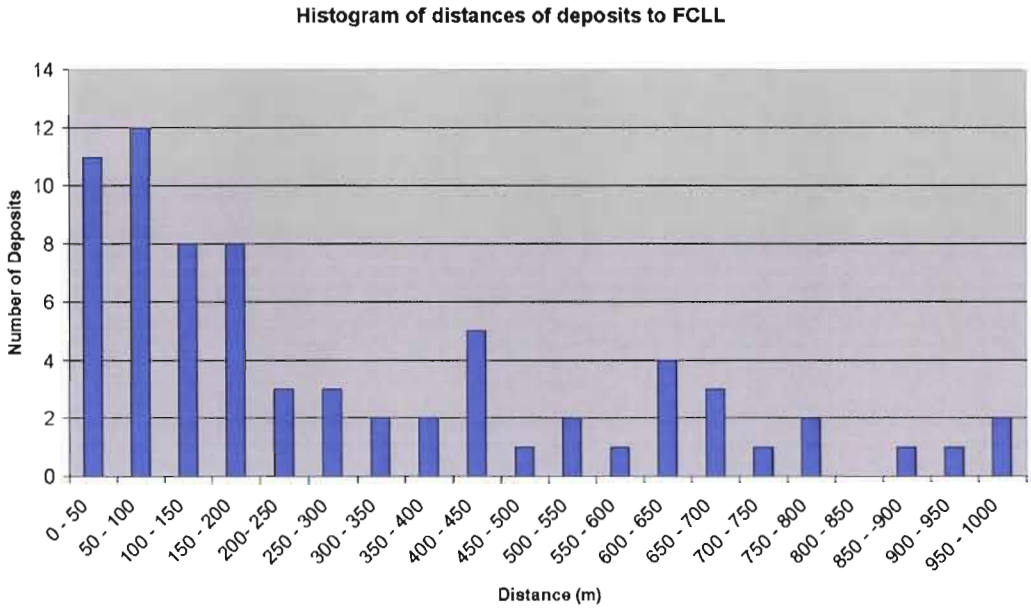

Figure 1-3: Distance of deposits to the Cadillac-Larder-Lake Fault

A total of 72 orogenic gold deposits identified along the investigated distance on the CLLF were used to conduct the spatial analysis. At regional scale all of these deposits can be represented as points on a 2D map. A map presenting the location of these deposits is presented in figure 1-2a. Most gold deposits are located less than 440 m from the CLLF with a mean distance of 290 m (Fig. 1-3). These orogenic gold deposits were then projected on the line representing the CLLF (figure 1-2B) and the curvilinear distance between each of the deposits was calculated following the fault trace (table 1). The methodology does not use the Euclidian distance, but the curvilinear distance calculated along the fault. A mean distance of 1950m was calculated between deposits. The cumulative frequency distribution F_d was

calculated and plotted against the log of the measured curvilinear inter distance *d* between successive Au deposits along the CLLF (figure 1-4). A theoretical distribution model defined for curvilinear distances *d* ranging from 315 m to 5615 m, was fitted using a mean squares method on the observed frequency distribution according to the following linear model (R^2 = 0.993, N = 65). This theoretical distribution model $F_D[d]$ is based on a Log-uniform distribution. The details of this type of distribution are presented in annexe 1. The following equation defines the theoretical distribution model:

$$F_D(d) = P(D \leq d) = a\,Log_{10}(d) - b \quad d \in [315m, 5615m] \text{ (eq. 1)}$$

$$a = 0.793_{\pm 0.008} \qquad b = 1.966_{\pm 0.026}$$

Mineralized Body	Deposit Type	Curvilinear Distance (m)	Distance to CLLF (m)	ESTN	NORD
Lac Sanies Zone Est	Deposit	0	1001	625066	5338534
Lac Fortune	Deposit with tonnage	1708	939.3	626711	5338979
Rivière Adeline	Deposit	11135	146.6	637976	5339618
Bazooka	Deposit with tonnage	2738	206.7	640711	5339829
Mc Donough	Deposit	66.5	679.0	640761	5340304
Augmitto	Deposit with tonnage	702	76.0	641487	5339710
Durbar	Deposit with tonnage	423.4	359.5	641906	5339999
Cinderella	Deposit	546.1	62.0	642461	5339584
Goldbar	Deposit	448	517.0	642911	5340169

Astoria	Closed mine	3508.9	34.5	645961	5339735
Lac Bouzan	Deposit	3925.4	130.9	649811	5340330
Dransfield zone	Deposit	950.5	796.9	650931	5339620
Pepmont	Deposit	2146	652.8	653191	5340525
Dovercliff	Deposit with tonnage	889.8	321.2	653366	5341735
MineMcWatters	Closed mine	2205.1	245.0	655531	5342080
Mine New Rouyn Merger	Closed mine	2414	399.5	658011	5342330
Mine O'Neill-Thompson	Closed mine	1200	130.9	659011	5342930
East O'Neill	Deposit with tonnage	521.1	204.9	659521	5342795
Davidson Fault	Deposit	1154	444.4	660436	5343820
Davidson Creek	Deposit	377.9	178.0	660911	5343280
Mine Heva	Closed mine	4014.6	162.7	664901	5343535
Mine Hosco	Closed mine	3467	133.4	668361	5343880
Bouzan-Or	Deposit	2698	16.0	671030	5344271
Maracambeau	Deposit	548.3	449.1	671611	5343845
Paquin	Deposit with tonnage	4633.9	854.4	676261	5343730
Calder Bousquet (1)	Deposit	840.7	250.9	677061	5344380
Calder Bousquet (2 and5)	Deposit	1295	148.7	678356	5344595
Calder Bousquet (4)	Deposit with tonnage	547.3	40.8	678886	5344770
Cavanagh	Deposit	1761	252.0	680661	5344780
Lac Norman	Deposit with tonnage	5459	106.0	686071	5345140
Brown-Bousquet	Deposit	1988	91.6	688056	5345132
Bouscadillac	Deposit with tonnage	2139	55.6	690196	5345284
Brown-Cadillac	Deposit	344.8	649.9	690486	5346010
Mine Thompson Cadillac	Closed mine	1586	62.7	692111	5345539
Mine O'Brien	Closed mine	694.6	52.1	692801	5345579
Zone 36 Est	Deposit with tonnage	1376	58.6	694189	5345538
Mine Kewagama	Closed mine	690.7	46.0	694870	5345674
Mine Central Cadillac	Closed mine	1791	27.0	696656	5345756
Mine Gallant	Closed mine	352.8	28.9	697018	5345729
Mine Pandora No 3	Closed mine	1364	24.5	698361	5345899

Mine Pandora No 4	Closed mine	1222	683.6	699311	5345075
Pandora No 1	Deposit	670.5	402.3	700011	5345129
Mine Pandora No 2	Closed mine	590.9	68.5	700761	5345334
Tonawanda	Deposit	925.9	281.0	701715	5345144
MineLapaCadillac	Closed mine	741.3	719.7	702773	5344429
Maritime Cadillac	Deposit	986.9	462.8	702991	5343574
Mine Pan-Canadian-No	Closed mine	3162.1	184.5	704666	5341186
MinePaCanadiannNo 2	Closed mine	526.9	189.8	705061	5340834
Mine Pan-Canadian No 1	Closed mine	1189	10.3	705810	5339979
Parbec Malartic	Deposit with tonnage	4128	98.0	709351	5337869
East Amphi	Closed mine	2490	97.4	711527	5336715
Western Porphyry Zone	Deposit with tonnage	1028	182.4	712451	5336179
Mine Barnat	Closed mine	3028.2	160.3	715261	5335189
Mine East Malartic	Closed mine	630.2	72.8	715791	5334779
New Senator Rouyn	Deposit with tonnage	3786	308.3	719586	5334229
Mine Malartic Gold Fields No 2	Closed mine	2880	616.7	722611	5333535
Mine Malartic Gold Fields (No 1)	Closed mine	1419	776.0	723547	5333249
Chabela	Deposit with tonnage	398.2	586.8	723915	5333027
Harpers Malartic	Deposit	1078	403.3	724863	5331936
Dubuisson Gold Fields	Deposit	487.5	523.2	725517	5332750
Propriété Audet	Deposit with tonnage	4340	980.9	729932	5331760
Quebec Explorers	Deposit with tonnage	1770	191.7	731190	5330364
Gold Stack-Cadillac	Deposit	3795.2	103.0	734344	5328877
Centremaque	Deposit	8767.1	22.5	742949	5327592
Orenada No.4	Closed mine	1989	6.2	744997	5327006

Mine Mid-Canada	Closed mine	143.2	604.8	745005	5327634
Orenada No.2	Deposit	1165	185.3	746151	5326918
Oramaque: PorphiryZone	Deposit	2258.3	411.3	748406	5326882
Oramaque-Cadillac: Northern Zone	Deposit	743.5	142.0	749112	5326549
Oramaque-Cadillac: Schist Zone	Deposit	216.2	15.6	749314	5326339
Sabourin Creek	Deposit	506.4	54.7	749797	5326252
Mine Akasaba	Closed mine	6665.3	607.0	756126	5327166

Table 1-1: Deposits located in a 1000m buffer zone of the Cadillac-Larder Lake Fault Zone that where used in the study (ESTN and NORD given in UTM Nad 83)

Limiting the fit to the inter distance in the interval [315, 5615m] disqualified 7 deposits form the statistics. These deposits do not fit the theoretical distribution. As seen on figure 1-4, a group of three deposits (Lac Sanies, Mc Donough, and Mid-Canada Mine), on the lower left side of the cumulative frequency curve, represents deposits whose projected inter curvilinear distance along the CLLF is too small (less than 150m). Since the methodology presented in this paper involves the projection of deposits on the fault trace, deposits which are aligned orthogonally to the fault may appear to be very close to each other. Further more, deposits which are very close to one and other may represent the same mineralized body. The second group, situated on the upper right side of the cumulative frequency curve, corresponds to four deposits (Lac Norman, Mine Akasaba, Centremaque, and Rivière Adeline) whose

projected inter curvilinear distance is greater (over 5,400m) than expected by the theoretical model $F_D\,[d]$. This could be interpreted by the presence of potentially undiscovered deposits located between these deposits.

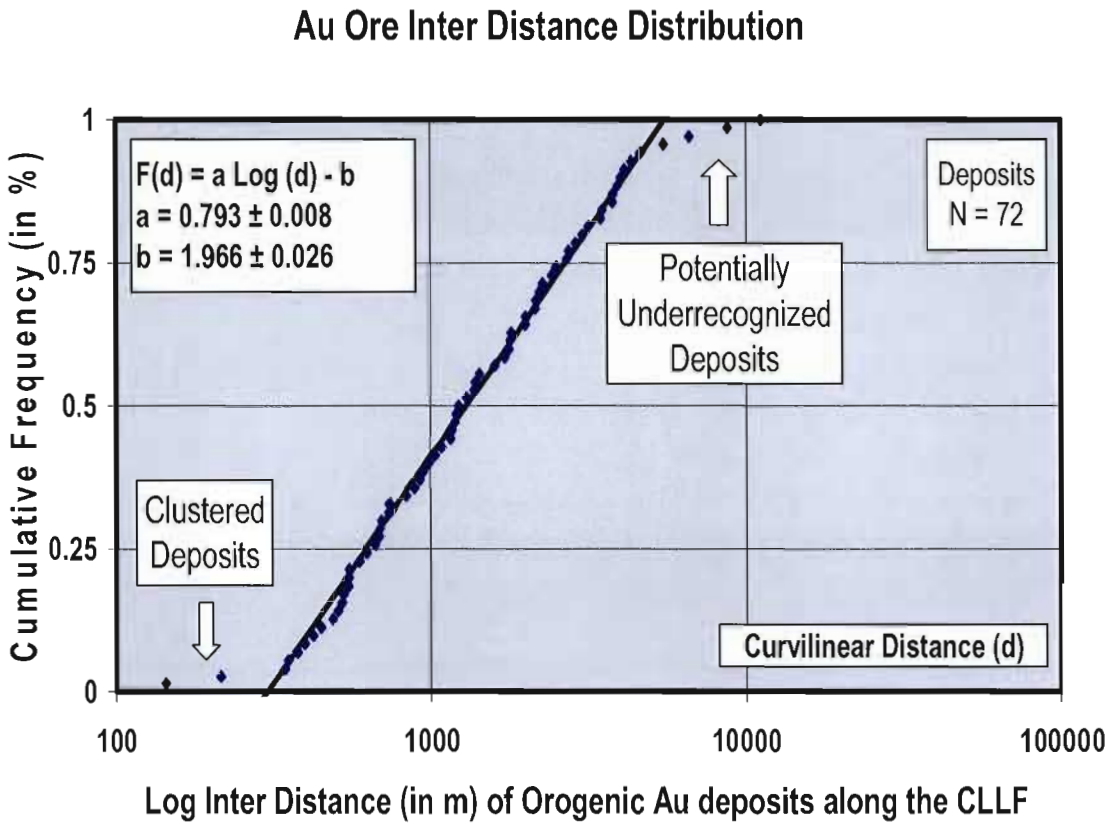

Figure 1-4: Cumulative distribution of the inter curvilinear distance between orogenic Au deposit along the eastern segment of the CLLF.

1.6.1 Validation of the spatial distribution

To test the theoretical Log-uniform distribution model $F_D\ [d]$ for orogenic gold deposits along the CLLF, the same methodology was applied on the Porcupine Destor Fault. This fault zone located north of the CLLF and is considered as the second major fault zone in the Abitibi Greenstone Belt and also host many important mining camps.

In order to preserve a homogeneous database, only the eastern segment of the PDF located within the Quebec Province was used to conduct the validation. A total of 29 deposits of the orogenic gold type and were within the 1 km buffer zone. From this total, 9 were not considered since their curvilinear inter-distance to their neighbor was less than 50 m. From the remaining deposits a Log-uniform law could be plotted between the cumulative frequency and the curvilinear distance (eq. 2) for the interval of 256 to 7895 m. The figure 1-5 presents the graph for the gold deposits of the PDF with the ones of the CLLF.

$$F_D(d) = a\,Log_{10}(d) - b \qquad d \in [256m, 7895m] \qquad \text{(eq. 2)}$$

$$a = 0.778 \qquad b = 1.983$$

Since the log uniform distribution of the FDP is only based on 20 deposits, it has to be considered with caution since it implies an important uncertainty on the results. It is only presented for validation purposes of the log uniform distribution of orogenic gold deposits along major fault zones.

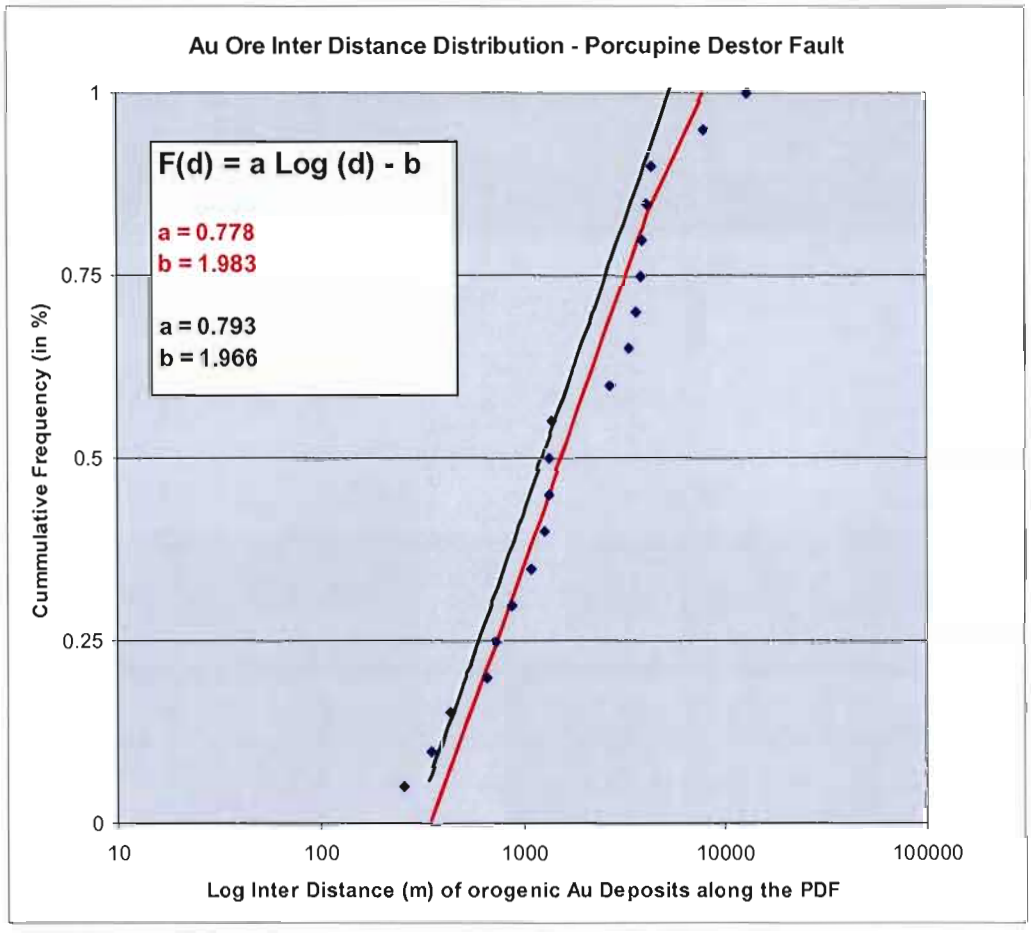

Figure 1-5: Cumulative distribution of the inter-curvilinear distance between orogenic Au deposit along the eastern segment of the PDF (data blue dots and the fitted log uniform law in red) presented with the results for the CLLF.

1.7 Discussion

Orogenic gold deposits mainly form within compressional / transpressionnal tectonic regimes (Goldfarb et al., 2001). This type of epigenetic gold deposits result from the circulation of large quantity of hydrothermal fluids. These hydrothermal fluids are interpreted to originate from prograde metamorphic chemical reactions involving dehydration in reaction to the compressionnal tectonic regime. In order to form economical concentrations of metals, the fluid flow, fundamentally controlled by permeability variations (Cox et al., 2001), has to be focused in restrained zones. In areas composed of lithologies with low primary permeability, the pathways used by the fluid flow are controlled by fault zones (Weinberg et al., 2004). Mineralizing fluids are channeled in first order fault zones and mineralizations are usually deposited in dilation sites located in second to third order fault although some important mineralizations (such as the Ker-Adisson Mine in Ontario or the Lapa Mine in Quebec) are located within first order faults.

These deep seated fluids are channeled through crustal scale fractures by a system of fault-valve action (Sibson et al., 1988). In a context of important fluid release, Sibson and Scott (1998) have proposed that fault strength attains a maximum between the middle and the base of the frictional seismogenic zone, and diminishes to very low values when fluid pressure is close to lithostatic values. In this tectonic context, near

lithostatic fluid pressure can bring existing fluid channeling structures to yield and create drainage paths by which pressure is released. The fluid flow may then cause an instant drop in fluid pressure and result in hydrothermal precipitation (Cox, 2001).

The results presented in this study show a uniform *log(d)* law relation of the curvilinear inter-distance of successive orogenic gold occurrences along a first order fault zone for distances ranging from 315 to 5600 m. The cumulative frequency distribution calculated of the inter-Euclidian distance exhibits a more complex shape similar to a log-normal distribution. The fit obtained with the curvilinear distance emphasizes the major role of the fault in the formation of orogenic gold deposits and the circulation of deep seated hydrothermal fluids. Considering that the distances were measures along a crustal scale fault zone that controlled the hydrothermal evolution of a large portion of Archean continental crust, this mathematical distribution can be expected to give insights on fluid circulation within similar structures.

The results presented in this study suggest that structural failure is the main factor controlling the distribution of orogenic gold deposits along crustal scale fault Archean fault zone. In fact, the influence of lithological variation at a regional scale seems to have a very low impact on the localization of orogenic gold mineralizations. Important variations of lithological units occur along the CLLF and the distribution

seems to be uniform along the full length of the fault. The uniform *log (d)* distribution emphasizes the role of structural failure in distribution of gold.

Furthermore, the results can give insight on the zone of influence of a fault failure in response to near lithostatic fluid pressure. Figure 1-4 suggests that structural failure induced by hydrostatic overpressure along a major Archean fault zone follows a logarithmic distribution of inter-distances. If we consider that the location of mineralization corresponds to the mark of pressure valve release mechanism, the results of this study suggest that the relaxation in the stress induced by the pressure release decreases following a log-uniform law.

1.7.1 Regional potential mapping using structural failure location

The location of known deposit should correspond to the localization of a structural failure du to near lithostatic fluid pressure. The cumulative frequency distribution F_D *[d]* of the curvilinear distances D between two neighbor deposits is the proportion of occurrences which were found within a distance d of a known deposit. By considering the number of deposits in the study, this relation can be interpreted as the conditional probability of finding a mineralized occurrence at a distance less than d from a known mineralized occurrence along a fault zone. The theoretical fitted distribution F_D *[d]* was used to evaluate the probability of potentially unrecognized

mineralized occurrences within the close vicinity of the CLLF. Deposits presenting inter-distance greater than predicted by the theoretical model (Fig. 1-4) were interpreted as indicating potential zones with possible unrecognized mineralized occurrences. To determine the probability distribution, the trace of the CLLF was regularly sampled every 10m in order to calculate the curvilinear distance to the nearest known projected deposit. This curvilinear distance was interpolated laterally on a regular grid band of 2km in extension and centered on the CLLF, giving the distance *d* to the nearest known deposit of any locations situated in this zone (Fig. 1-6A). The *log(d)* uniform distribution model was then used to derive a probability map along the full length of the Eastern segment of the CLLF. Figure 1-6b presents those results for various levels of confidence.

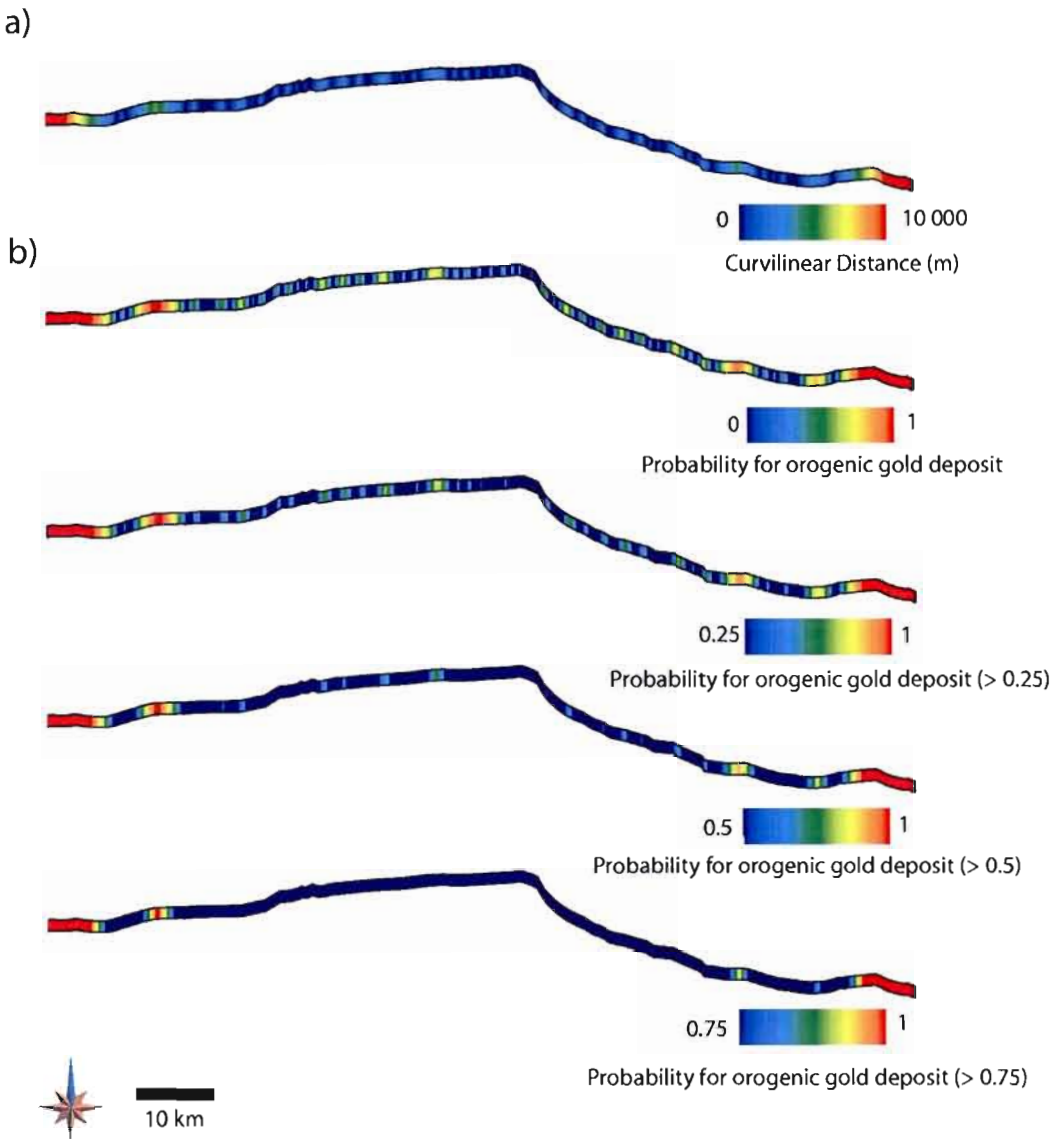

Figure 1-6: a) Curvilinear inter distance between known orogenic gold mineralizations mapped on the trace (1 km buffer) of the Cadillac Larder Lake Fault trace. b) Derived probability maps of potentially unrecognized orogenic Au mineralization occurrences for various confident levels varying from 0 to 1.

The results presented in Figure 1-6 have to be interpreted with caution. Since the methodology used inter distance calculation between deposits, the distance measured for deposits located on the extremities of the faults are biased. Consequently, the part of the CLLF located near the Grenville front presents a higher occurrences inter distance compared to the rest of the fault, and therefore a highest derived probability, because no deposits are present passed the Grenville Front. The Eastern part of the studied portion of the CLLF presents the same bias but it is important to note that the Kerr Addison deposits is located only a few kilometers from the Ontarian border and that there is truly a lack of deposits in this area since the CLLF is covered by the Proterozoic sediments of the Gowganda Formation (Rabeau et al., 2009) which renders classical exploration techniques difficult.

1.8 Conclusions

The study helped to highlight the relationship between structural failure and the location of mineralized occurrences. These zones of failure have the potential to focus large volumes of hydrothermal fluids which are essential in the formation of orogenic gold deposits. The influence on regional stress of a structural failure du to fluid overpressure along a crustal scale fault zone appears to decrease following a log-uniform law. These results imply that the nature of the lithological units along the fault zone have little influence on the location of mineralized occurrences.

Considering a uniform formation mechanism, the methodology presented in this study can be used as a guideline to delineate zones of high potentiality for orogenic gold mineralizations near Archean fault zones. The use of this methodology implies a well detailed database of known deposits. Further test should be undertaken to verify if the same uniform-log law can be observed on second and third order fault zones.

1.9 Acknowledgements

This work was supported by the University of Quebec in Abitibi-Témiscamingue, the DIVEX consortium and the Ministère des Ressources naturelles et de la Faune du Québec.

1.10 References

Carlson, C., 1991 Are gold deposits in the crust fractals? A study of gold mines in the Zimbabwe craton, Geological Society, London, Special Publications, January 1, 1999; 155(1): 141 – 151

Benn, K, Plesher, A. P., 2005, A detachment fold model for fault zones in the Late Archean Abitibi greenstone belt, Tectonophysics, Volume 400, Issues 1-4, p. 85-104

Blenkinsop, T. G. and Sanderson, D. J., 1999; Are gold deposits in the crust fractals? A study of gold mines in the Zimbabwe craton Geological Society, London, Special Publications, 155(1): 141 – 151

Carlson, C. A., 1991, Spatial distribution of ore deposits, Geology; v. 19; no. 2; p. 111-114

Chown, E. H., Daigneault, R., Mueller, W. & Mortensen, J. K. 1992. Tectonic evolution of the Northern Volcanic Zone, Abitibi Belt, Quebec. *Canadian Journal of Earth Sciences* 29, 2211-2225.

Couture, J.-F. 1996. Gisements metalliques du district de Rouyn-Noranda. In: *Métalogénie et évolution de la région de Rouyn-Noranda* (edited by Couture, J.-F. & Goutier, J.) MB 96-06. Ministère des Ressources naturelles du Québec, 11-18.

Cox, S. F., Knackstedt, M. A. & Braun, J. 2001. Principles of structural control on permeability and fluid flow in hydrothermal systems. In: *Structural controls on ore genesis* (edited by Richards, J. P. & Tosdal, R. M.). *Reviews in Economic geology.* volume 14. Society of Economic Geologists.

Daigneault, R. & Mueller, W. U. 2004. Abitibi greenstone belt plate tectonics: the diachronous history of arc development, accretion and collision. In: *The Precambrian Earth: Tempos and events* (edited by Eriksson, P., Altermann, W., Nelson, D., Mueller, W. U., Catuneaunu, O. & Str and, K.). *Development in Precambrian Geology* 12. Elsevier, 88-103.

Daigneault, R., Mueller, W. U. & Chown, E. H. 2002. Oblique Archean subduction: accretion and exhumation of an oceanic arc during dextral transpression, Southern Volcanic Zone, Abitibi Subprovince, Canada. *Precambrian Research* 115(1-4), 261-290.

Davis, D. W. 2002. U-Pb geochronology of Archean metasedimentary rocks in the Pontiac and Abitibi subprovinces, Quebec, contraints on timing, provenance and regional tectonics. *Precambrian Research* 115, 97-117.

Dimroth, E., Imreh, L., Rocheleau, M. & Goulet, N. 1982. Evolution of the south-central part of the Archean Abitibi Belt, Quebec. Part I: Stratigraphy and paleogeographic model. *Canadian Journal of Earth Sciences* 19(9), 1729-1758.

Dubé, B., Gosselin, P., 2007, Greenstone-hosted quartz-carbonate vein deposits, in : Mineral Deposits of Canada: A Synthesis of Major Deposit-Types, District Metallogeny, the Evolution of Geological Provinces, and Exploration Methods, Godfellow, W.D, ed., Geological Association of Canadca, Mineral Deposit Division, Special Publication No. 5, p. 46-73.

Eisenlohr, B. N., Groves, D. I. & Partington, G. A. 1989. Crustal-scale shear zones and their significance to Archaean gold mineralization in Western Australia. *Mineralium Deposita* 24, 1-8.

Goldfarb, R. J., Groves, D. I. & Gardoll, S. 2001. Orogenic gold and geological time: a global synthesis. *Ore Geology Reviews* 18, 1-75.

Goutier, J., McNicoll, V., Dion, C., Legault, M., Ross, P.-S., Mercier-Langevin, P., Monecke, T., Thurston, P.C., Ayer, J.A., 2008, Une Nouvelle Stratigraphie du Groupe de Blake River: Deex Grands Épiosdes Volcaniques et quatres épisodes de Minéralisations en SMV, abstract, GAC-MAC, Quebec 2008, p. 64

Groves, D. I., Goldfarb, R. J., Gebre-Mariam, M., Hageman, S. G. & Robert, F. 1998. Orogenic gold deposits: A proposed classification in the context of the crustal distribution and relationship to other deposit types. *Ore Geology Reviews* 13(1-5), 7-27.

Groves, D. I., Goldfarb, R. J., Knox-Robinson, C. M., Ojala, J., Gardoll, S., Yun, G. Y. & Holyland, P. 2000. Late-kinematic timing of orogenic gold deposits and significance for computer-based exploration techniques with emphasis on the Yilgarn Block, Western Australia. *Ore Geology Reviews* 17, 1-38.

Groves, D. I., Goldfarb, R. J., Robert, F., Hart, C. R. J. &. 2003. Gold deposits in metamorphic belts: overview of current understanding, outstanding problems, future reaserch, and exploration significance. *Economic Geology* 98, 1-29.

Kerrich, R. & Feng, R. 1992. Archean geodynamics and the Abitibi-Pontiac collision: implications for advection of fluids at transpressive collisional boundaries and the origin of giant quartz vein systems. *Earth-Sci. Rev.* 32, 33-60.

Kerrich, R., Goldfarb, R. J., Groves, D. I., Garwin, S. (2000). The Geodynamics of World-Class Gold Deposits: Characteristics, Space-Time Distribution, and Origins. In: Gold in 2000 (eds. Hageman, S. G. & Brown, P. E.). Reviews in Economic geology, 13, p. 500-551.

Lafrance, B., Moorhead, J. & Davis, D. W. 2003. Cadre géologique du camp minier de Doyon-Bousquet-LaRonde. Ministère des Ressources naturelles, Québec, 43 pages.

Legault, M. & Rabeau, O. 2006. Étude Métallogénque et modélisation 3D de la Faille Cadillac dans le secteur de Rouyn-Noranda. In: *RP 2006-03*. Ministère des Ressources naturelles et de la Faune du Québec, 8.

McCammon, R.B., 1993. Prospector II-an expert system for mineral deposits models. In:
Kirkham, R.V., Sinclair, W.D., Thorpe, R.I., Duke, J.M. (Eds.), Mineral Deposit Modeling. Geological Association of Canada, Special Paper 40, 679-684.

Micklethwaite, S., Cox, S.F., 2004, Fault-segment rupture, aftershock-zone fluid flow, and mineralization, *Geology*, v. 32; no. 9; p. 813-816

Pilote, P., Beaudoin, G., Chabot, F., Crevier, M., Desrochers, J.-P., Giovenazzo, D.,

Lavoie, S., Moorhead, J., Mueller, W. U., Pelz, P., Robert, F., Scott, C., Tremblay, A. & Vorobiev, L. 2000. Géologie de la région de Val-d'Or, Sous-province de l'Abitibi - Volcanologie physique et évolution métallogénique. Ministère des Ressources naturelles, Québec, 110 pages.

Poulsen, K. H., Robert, F. & Dubé, B. 2000. Geological classification of Canadian gold deposits. Geological Survey of Canada, 106 pages.

Sibson, R.H., 2001, Seismogenic framework for hydrothermal transport and ore deposition. Richards, J.P. and Tosdal, R.M. Review in Economic Geology, 14; Structural controls on ore genesis. pp. 1-24.

Rabeau, O, Legault, M., Cheilletz, A, Jébrak, , L. Z., Royer, J.J., 2009, Gold potential of a hidden Archean fault zone: the case of the Cadillac-Larder Lake Fault , accepted, Journal of Mining and Exploration geology

Robert, F Poulsen, H, Cassidy, KF, CJ, 2005 , Gold metallogeny of the Yilgarn and Superior cratons, Economic Geology One Hundredth Anniversary volume , 2005

Thurston, P.C., Goutier, J., McNichol, V., Legault, M., 2008, Mafic Dykes cutting the Blake River Group, Abitibi Subprovince, abstract, GACMAC 20008

Weinberg, R. F., Hodkiewicz, P. F. & Groves, D. I. 2004. What controls gold distribution in Archean terranes? Geology 32(no. 7), 545-548.

1.11 Annexe 1

Log - Uniform distribution

A random function D is said to be 'Log-uniform distributed' on the interval $[d_{min}, d_{max}]$ if its Cumulative Distribution Function (*cdf*) $F_D(d)$ is defined by :

$$\begin{aligned} &F_D(d) = 0 && d \le d_{\min} \\ &F_D(d) = P(D \le d) = a\ln(d) - b && d \in [d_{\min}, d_{\max}] \\ &F_D(d) = 1 && d_{\max} \le d \end{aligned} \tag{1}$$

where $ln(d)$ is the natural logarithm of d, a and b are constants which depend on the limits d_{min} and d_{max} of the interval on which the distribution is defined. The probability distribution function (*pdf*) $f_D(x)$ of D is defined as the derivative of $F_D(x)$:

$$\begin{aligned} &f_D(x) = 0 && x \notin [d_{\min}, d_{\max}] \\ &f_D(x) = \frac{dF_D(x)}{dx} = \frac{a}{x} && x \in [d_{\min}, d_{\max}] \end{aligned} \tag{2}$$

As a Probability Distribution $f_D(d)$ must sum to *1* over its interval of definition, the constants a and b are related to d_{min} and d_{max} by the following relationships :

$$\frac{1}{a} = \ln\left(\frac{d_{\max}}{d_{\min}}\right) \qquad b = a\ln(d_{\min}) \qquad d_{\min} = \exp\left(\frac{b}{a}\right) \qquad d_{\max} = d_{\min}\exp\left(\frac{1}{a}\right) \tag{3}$$

Denoting $\Delta d = d_{max} - d_{min}$ and $d_m=(d_{max} + d_{min})/2$ the range and the mid value of the definition interval $[d_{min}, d_{max}]$ of D, respectively, the mean μ_D and standard deviation σ_D of a log-uniform distributed variable D are equal to :

$$\mu_D = a\,\Delta d = \Delta d \,\ln\left(\frac{d_{\max}}{d_{\min}}\right)^{-1} \qquad \sigma_D = C_V\,\mu_D \qquad C_V = \frac{\sigma_D}{\mu_D} = \sqrt{\frac{d_m}{\mu_D} - 1} \tag{4}$$

where C_V is the variation coefficient of the random variable D. The above definitions show that the key parameters for a log-uniform distribution are the limit of the definition interval d_{min} and d_{max}.

In the text, the log-uniform distribution D is defined using the decimal logarithm (instead of the natural one), as the decimal logarithm is more commonly used in the geoscientist community:

$$\begin{aligned} &F_D(d) = 0 && d \le d_{\min} \\ &F_D(d) = P(D \le d) = a' \log_{10}(d) - b && d \in [d_{\min}, d_{\max}] \\ &F_D(d) = 1 && d_{\max} \le d \end{aligned} \tag{5}$$

This definition is equivalent, it is only needed to substitute the constant $a' = a\ ln(10)$, and use log_{10} instead of ln in the above equations.

Chapitre 2: Gold potential of a hidden Archean fault zone: the case of the Cadillac-Larder Lake Fault

2.1 Introduction générale

Cette section présente sous forme d'article des travaux portant sur l'évaluation du potentiel minéral sous couverture sédimentaire et contrôles sur les minéralisations aurifères de type orogénique à une échelle locale.

La compilation des données géologiques, géophysiques, structurales et géochimiques et leur intégration au sein d'un modèle géologique 3D a permis d'évaluer le potentiel aurifère dans les environs d'une importante zone de faille archéenne sous couverture protérozoïque. Cette méthodologie a été développée en utilisant le cas de la Faille Cadillac-Larder Lake (FCLL) dans la région de Rouyn-Noranda. Puisque plus de 2000 t d'Or ont été extrait à proximité de la FCLL, l'objectifs des travaux est l'évaluation du potentiel aurifère en profondeur de ce segment. Un modèle géologique 3D (50 x 9 x 1.5 km) incluant le segment sous couverture de la FCLL a été construit en utilisant l'ensemble des données géologiques disponibles et 23 coupes géologiques. La géologie du socle archéen sous la couverture protérozoïque a été interprétée avec des inversions géophysiques, des forages (42 au total) et les contacts

géologiques exposés. Les teneurs aurifères dans le secteur ont été filtrées et ajusté à une grille régulière de 250 x 250 x 250 m afin d'évaluer et de quantifier les relations spatiales existantes entre certaines entités géologiques et les emplacements minéralisés en utilisant la méthode du *poids de la preuve*. Les failles de direction Est-Ouest, les intersections de failles ainsi que certaines lithologies possédant une porosité primaire importantes comme les certains tuf du Groupe de Blake River et les sédiments du Timiskaming se sont montrés très prospectifs avec des valeurs de $W_+ >$ 0.24. Ces entités géologiques ont ensuite été utilisées par le biais d'un indice de combinaison pour évaluer le potentiel en or de type orogénique sous le couvert sédimentaire. Cette méthodologie permet une optimisation des campagnes d'exploration puisque les zones pour lesquelles la probabilité de minéralisations a été évaluée à la plus haute valeur représentent 1% du volume initial.

Gold potential of a hidden Archean fault zone: the case of the Cadillac-Larder Lake Fault

Olivier Rabeau
Université du Québec en Abitibi-Témiscamingue, Unité de recherche et de services en technologie minérale, 445 boul. de l'Université, Rouyn-Noranda, QC, Canada, J9X 5E4, Tel: (819) 354 4514 #248 Fax: (819) 354 4508 - olivier.rabeau@uqat.ca

Marc Legault
MRNFQ, Ministère des Ressources naturelles et de la Faune du Québec, 70, boul. Québec, Rouyn-Noranda, QC, Canada, J9X 6R1 – marc.legault@mrnf.gouv.qc.ca

Alain Cheilletz
CRPG, Centre de Recherche Pétrographique et Géochimique, Nancy Université, BP 20, 54501 Vandœuvre-lès-Nancy Cedex, France - cheille@crpg.cnrs-nancy.fr

Michel Jébrak
UQAM, Université du Québec à Montréal, Département de Sciences de la Terre et de l'Atmosphère, 201, avenue du Président-Kennedy, PK-615,1Montréal, QC, Canada, H2X 3Y7 - michel.jebrak@uqam.ca

Jean-Jacques Royer
CRPG, Centre de Recherche Pétrographique et Géochimique, Nancy Université, BP 20, 54501 Vandœuvre-lès-Nancy Cedex, France - royer@crpg.cnrs-nancy.fr

Li Zhen Cheng
Université du Québec en Abitibi-Témiscamingue, Département de Sciences Appliquées 445 boul. de l'Université, Rouyn-Noranda, QC, Canada, J9X 5E4 – li_zhen.cheng@uqat.ca

Key Words: Orogenic gold, 3D Geomodeling, Spatial Analysis, Cadillac-Larder Lake Fault, Mineral potential map

2.2 Abstract

By compiling geological, structural, geophysical and geochemical information into a 3D geological model, we evaluated the orogenic gold potential in the vicinity of a hidden segment of an important Archean fault zone - the Cadillac Larder Lake Fault (CLLF) in the region of Rouyn-Noranda. The segment of CLLF in the present study is partly covered by Proterozoic sedimentary rocks. Since more than 2000 t Au have been extracted along the CLLF, our objective is to evaluate the gold potential at depth for a poorly known segment of this fault. A 3D geological model (50 x 9 x 1.5 km^3) including the covered segment was built through the compilation and homogenisation of the available geological data and the construction of 23 cross sections. The geology under the Proterozoic cover was evaluated using geophysical inversions, drill holes (42 in total) and surrounding geology. All available assays were filtered and upscaled to a 250 x 250 x 250 m regular cell grid to determine and quantify spatial relationships between geological features and mineralized occurrences using the weights of evidence method. Structural features, such as EW trending faults and fault intersections, and certain lithologies with a high primary porosity, such as volcanoclastics of the Blake River Group and Timiskaming sedimentary rocks, proved to be very prospective yielding favorable factors with a weight of evidence index greater than $W_+ > 0.24$. These salient features were then assigned a combination index for ultimately evaluating the orogenic gold potential under the

sedimentary cover. The zones resulting in an optimisation of exploration targeting were attributed the highest probability representing ~ 1% of the initial volume,

2.3 Introduction

Mineral discoveries along known metallotects in highly explored regions are becoming fewer and costlier as they often require deeper and riskier exploration campaigns. However, when used to their full potential, the large amounts of accumulated data in vastly prospected sectors can enhance mineral exploration by improving targeting for deep seated deposits. This paper presents an example of optimized use of this data with a 3D quantitative method to reduce discovery costs for gold exploration, at depth, in the vicinity of a hidden segment of an important Archean fault zone.

Transcrustal scale fault zones within Archean greenstone belts are commonly of great economic importance because of their spatial association with orogenic gold deposits (Groves, 1993; Kerrich et al., 2000; Goldfarb et al., 2001; Dubé and Gosselin, 2007). The location and geometry of these major fault zones are crucial for gold prospecting even if a minority of gold deposits is directly hosted within these structures. The Cadillac–Larder Lake Fault (CLLF; Fig. 2-1) located in the Abitibi Subprovince of the Superior province is a typical example of a large transcrustal fault zone which

hosts many world class mining camps (>100 Mt) such as Val-d'Or, Malartic, Cadillac, Larder Lake, Kirkland Lake and Matachewan (Poulsen et al., 2000). However, gold deposits are not distributed regularly along the CLLF. The segment located between the town of Cadillac and the Quebec-Ontario border presents a very poor gold endowment compared to other segments of comparable length. This lack of known gold deposits can be partially attributable to the Proterozoic sedimentary cover which masks the CLLF for more than 30 km. Thickness of the sedimentary cover is locally greater than 700 m and making usual exploration methods inadequate.

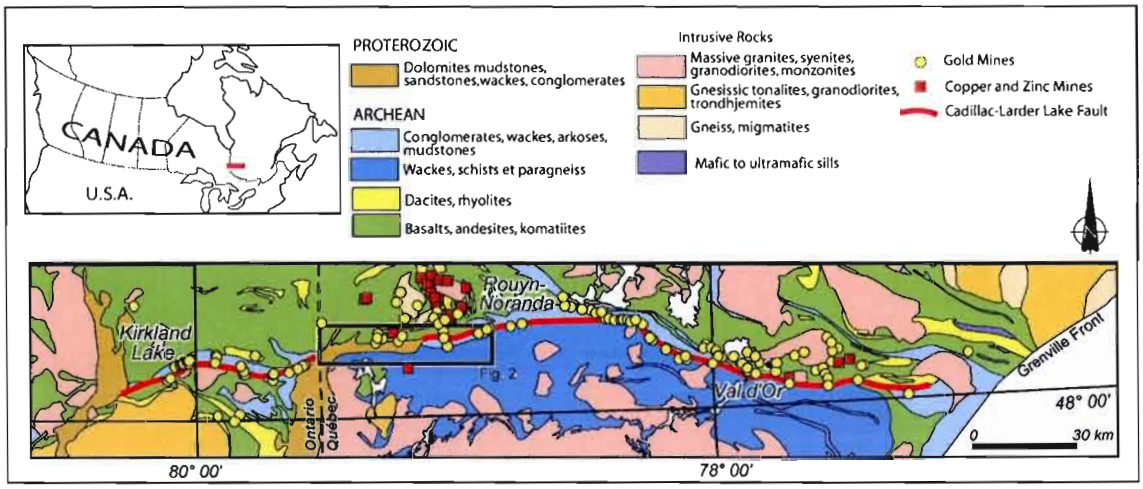

Figure 2-1: Simplified geological map along the Cadillac-Larder Lake Fault (CLLF) showing the location of past and present gold, copper and zinc mines.

The aim of this work is to define a methodology using the Gocad ® 3D modeling software (Mallet, 1992b), to combine geological, geophysical and geochemical data

to identify high potential zones at depth along a lesser known segment of the CLLF. A 3D regional geological model for a partly covered 50 km segment along the CLLF and its adjacent structures was built. This model includes a 3D representation of the Archean-Proterozoic unconformity and an interpretation of the Archean units and structures underneath the cover. The geophysical data were used to validate and interpret the geological model. The regional model provides a platform to conduct a 3D spatial analysis on a compiled gold assay database to identify the geological features controlling the distribution of gold mineralizations. The spatial association of these geological features with gold was then quantified using the weights of evidence method and a knowledge base approach was used to generate exploration targets at depth underneath the sedimentary cover using combination factors.

2.4 Geological Setting

The Archean Abitibi Greenstone Belt located in the southern part of the Superior Craton is composed of an assemblage of plutonic (50 %), volcanic (40 %) and sedimentary (10 %) rocks. The 50 x 9 km study area is situated along the limit between the Abitibi and the Pontiac Subprovinces (Dimroth et al., 1982; Couture et al., 1996; Thurston et al., 2008b) which lie respectively north and south of the CLLF (Fig. 2-2). The northern part of the Pontiac Subprovince is mainly composed of highly folded and deformed turbiditic sedimentary rocks (< 2685 Ma; Davis, 2002)

with some horizons of mafic to ultramafic volcanics and cross-cutting syenite and granite. In the Abitibi Subprovince, most volcanic rocks range in composition from komatiite to rhyolite. A majority of the volcanics present in the study area are part of the Blake River Group. An age of 2701 Ma was reported for rocks of the Blake River Group near the study area (Lafrance et al., 2005).

The McWatters Formation, observed south of the CLLF, is mainly composed of volcanic rocks which are suggested as equivalent to volcanic rocks of the Pontiac Subprovince (Morin et al., 1993). The Piché Formation is composed of ultramafic to mafic volcanic rocks wedged within the CLLF. The Cadillac Group (< 2687 Ma; Davis, 2002, Lafrance et al., 2005, Mercier-Langevin et al., 2007) is located in the northeastern corner of the study area and consists mainly of a mudstone and wacke assemblage. The Archean sedimentary rocks adjacent to the CLLF are part of the Timiskaming Group and composed of unsorted polygenic conglomerates, sandstone and local interdigitation of alkaline volcanic rocks (2677 to 2670 Ma; Corfu et al. 1991, Davis, 2002, Ayer et al. 2005)

Many dykes and sills of gabbroic to dioritic composition crosscut the study area. Their relative age suggests a synvolcanic to syntectonic emplacement (Thurston et al., 2008a). Minor alkaline and cal-alkaline intrusions are observed on both sides of the CLLF. An age of 2685 to 2672 Ma was found for certain of these intrusions (Corfu et al. 1989, Wilkinson et al., 1999, Davis, 2002).

Proterozoic sediments of the Gowganda Formation at the base of the Cobalt Group lie unconformably on the Archean basement in the western and central part of the study area. This formation consists mainly of a basal conglomerate overlain by wackes, mudstones and sandstones which mask the CLLF and the Archean basement for over 30 km. A Rb-Sr isochron gave an age of 2288 Ma for the Gowganda Formation (Fairbairn et al., 1969). Two inliers in the Cobalt Group expose the Archean basement in the central part of the study area (Legault and Rabeau, 2006). All Achean rocks are crosscut by N-S and N-E trending Proterozoic diabase dikes.

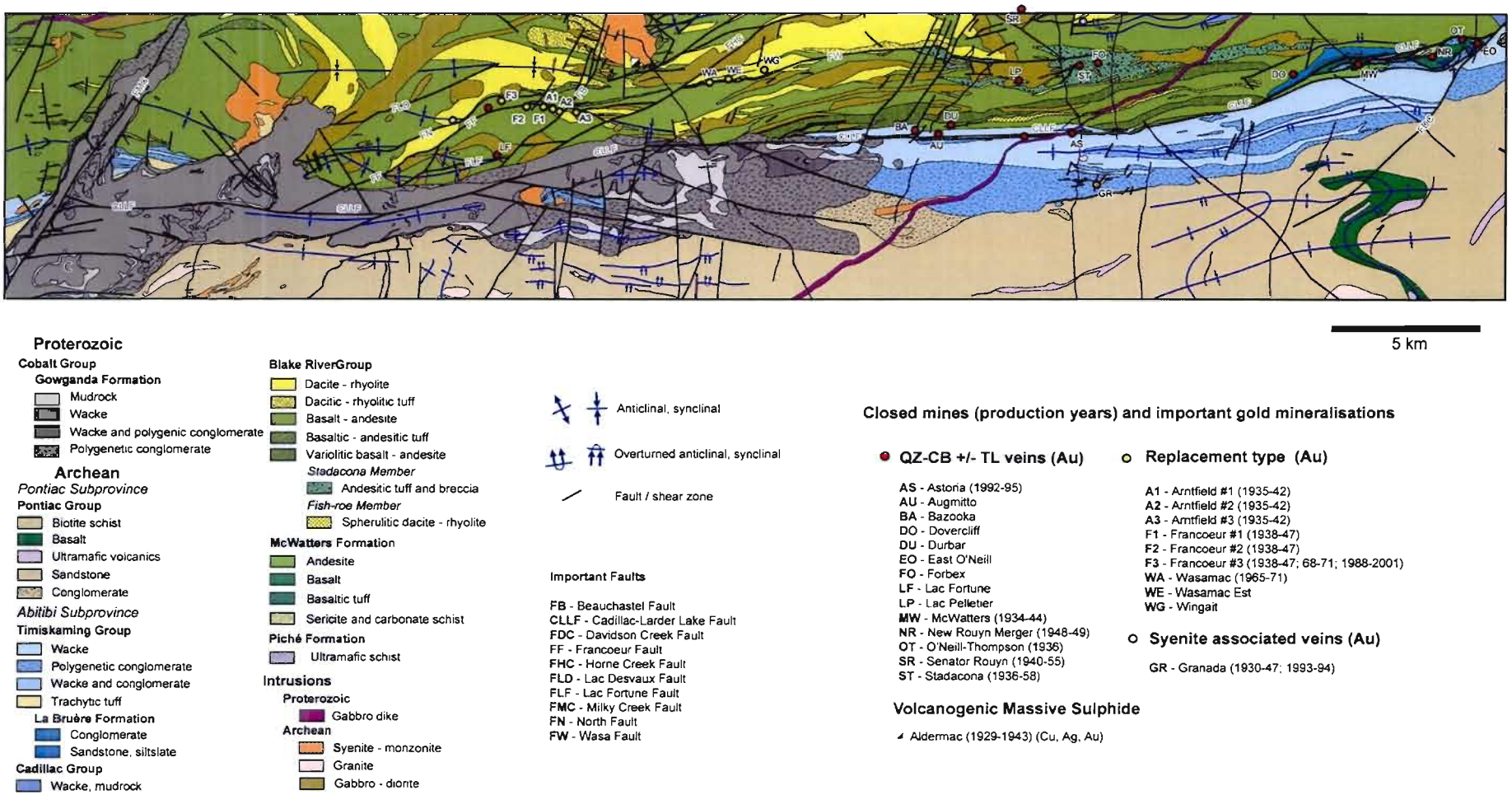

Figure 2-2: Geological map of the study area with location of mines and mineral deposits (modified from Legault and Rabeau, 2007)

The tectonic evolution of the study area is associated with numerous events of thrusting and dextral transpression (Daigneault et al., 2002, Daigneault and Mueller, 2004). The first episode is characterized by the accretion of the Pontiac and Abitibi Subprovinces (2680 – 2,690 Ma), followed by dextral strike-slip movement along the CLLF which led to the formation of the Timiskaming Group (2670 – 2680 Ma). Renewed thrusting (2661 – 2670 Ma), exhumation of the Pontiac Subprovince (2642 – 2661 Ma) and late dextral transpression (< 2642 Ma) complete the tectonic events along the CLLF.

2.4.1 Regional Gold Metallogeny

Although no mines are currently active in the sector, 50 t Au have been extracted along the CLLF in the study area (Couture, 1991). Additionally, a world class deposit, the Kerr-Chesterville (336 t Au; 1930-1996 (Guindon et al., 2007)), occurs along the western extension of this segment of the CLLF in Ontario. Four different types of gold mineralizations have been recognized in the study area (Legault and Rabeau, 2007): (1) Gold-rich quartz-carbonate ± tourmaline ± sulfides constitute the most represented type (70 %). Typical examples are the Stadacona, Astoria and Senator-Rouyn mines (Couture, 1996). (2) Replacement type deposits (~20 %) is associated with a strong pervasive albite/sericite, carbonate alteration and disseminated sulphides. The Francoeur and Wasamac deposits (Couture et Pilote, 1993) are representative examples. (3) Mineralization spatially associated with

syenitic intrusions (~5%) includes two subtypes: *quartz-carbonate veins* such as the Granada Mine (Couture and Willoughby, 1996) and in a lesser manner *disseminated sulphides* enriched in Au-Cu- (Couture and Marquis, 1996; Legault and Lalonde, in prep.). (4) Volcanogenic massive sulphide (VMS) deposits related polymetallic mineralization (~5%) are also encountered in the study area (Legault and Rabeau, 2007). Additionally, some occurrences of epithermal-type mineralization have been observed north of the study area near the transcrustal Porcupine-Destor Fault (Legault et al., 2005) but have not been described near the CLLF.

More than one type of mineralization can coexist in a single deposit as observed in the Kerr-Chesterville deposit located within the CLLF west of the study area. This deposit (the second largest along the CLLF) is composed of a quartz-*carbonate vein type* (carbonate ore) and a *replacement type* (flow ore) (Kishida and Kerrich, 1987; Smith *et al.*, 1990).

Most of the gold mineralisation considered in this study belongs to a broad class of orogenic gold deposit types. These deposits are characterized by epigenetic, structurally controlled mineralization located in accretionary orogens that formed over a large crustal-depth range from deep seated fluids (Groves et al., 1998). The quartz-carbonates vein, replacement and veins associated to syenite types fit with this definition.

Orogenic gold mineralizations post-date regional metamorphism, plutonism and early phases of orogenic deformation (Groves et al., 2000; Goldfarb et al. 2001) combined with their location within a craton imply that the present geometry of the host terrains can be considered as very similar to the one present during ore formation. At local scale, displacement may be observed on ore but at regional scale the displacement should be minor.

2.5 Geological Modeling

Geological modeling enhances the geological understanding of a specific region by allowing interpretations using all available geoscientific data in a 3D environment. A thorough comprehension of the geological setting and an abundance of quality 3D data are prerequisites for the construction of such models. As opposed to a 2D environment, the 3D approach offers the benefit of avoiding bias generated by projection of data on the surface and allows the calculation of true distances between objects taking depth and 3D geometry into account (Fig. 2-3). The geology and structural context of the study area are well defined and its proximity to the prolific Rouyn-Noranda central camp provides access to a multitude of high quality data for the sector (Table 2-1). These data were first compiled with standardized units and referenced using the UTM NAD83 spatial projection.

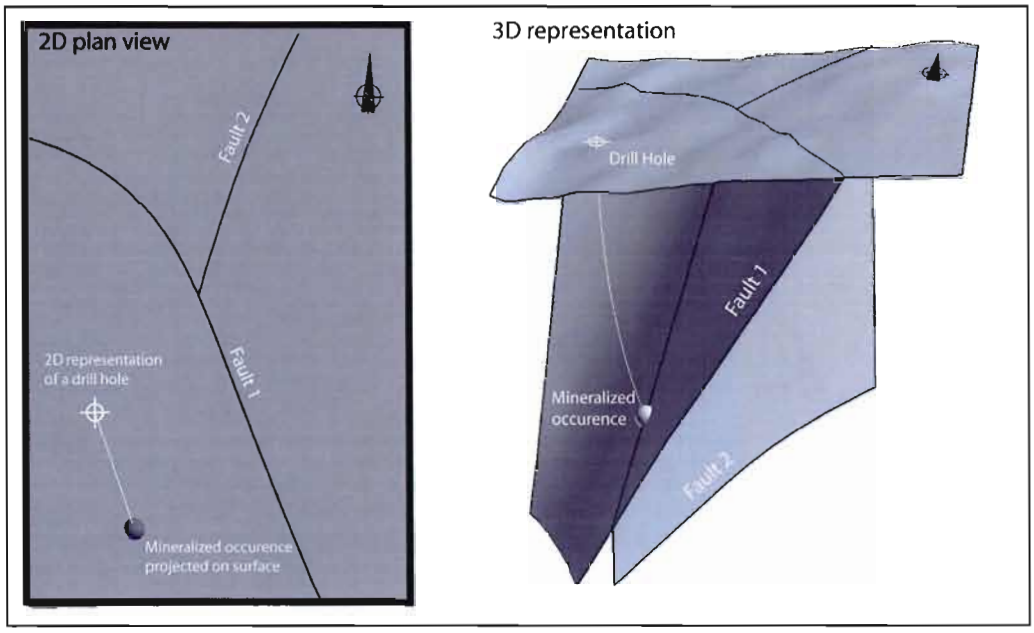

Figure 2-3: Illustration of the advantages of having a 3D representation versus a 2D map. A 3D approach allows a better visualizing capacity of spatial relationships as shown by the connection between the intersection of faults 1 and 2 and the mineralized occurrence. A 3D representation also avoids distortion due to projections to surface and data stacking (as seen with the drill hole representation on both images) and offers the possibility of calculating true distances between geological features.

Data type	Quantity / type	Source
Drill holes	> 9000	Mining companies, compilation of historical data
Gold assays	> 209 000	Mining companies, compilation of historical data
Structural data	> 1600	Compilation maps (CG 32D/02, 03, 04); Leduc (1986); Legault and Rabeau (2006, 2007)
Geological map	1 :50 000 map	Legault and Rabeau (2006)
Magnetic map	MegaTEM survey (north) Provincial survey (south)	XStrata, unpublished data (2002); Dion and Lefebvre (1997)
Gravimetric measurements	1249 stations	Dion (1993)
Digital elevation map	308 100 points	USGS (http://edc.usgs.gov/products/elevation/gtopo30/gtopo30.html)

Table 2-1: Data used to construct the geological model

A 3D geological model (50 x 9 x 1.5 km^3) was built based on 23 vertical cross-sections (Fig. 2-4a) at a mean spacing of 2 km. The sections were interpreted by recent geological mapping in the study area (Legault and Rabeau, 2006, 2007), and compiled structural and drill hole data (2-1). These sections then served as geometrical constraints for building triangulated surfaces representing the boundaries of geological units (Fig. 2-4b). The creation of triangulated surfaces respecting the range of constraints of available data was carried out using the Discrete Smooth Interpolation method (Mallet, 1992; Fig. 2-4c). Finally, a volumetric model was derived from the partition of space by the surface model (Fig. 2-4c) composed of the ribbons representing geological contacts and faults.

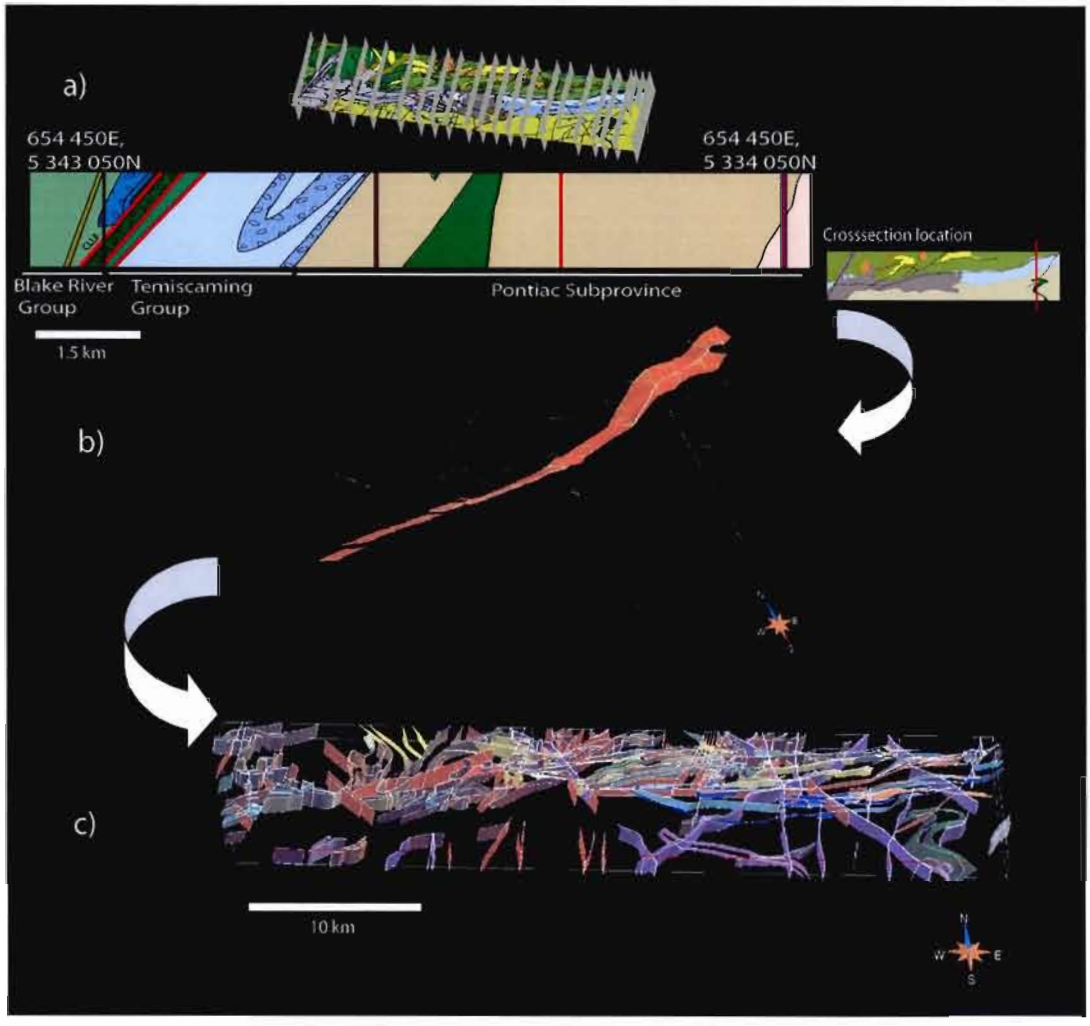

Figure 2-4: a. Location and example of the interpreted cross sections; b. Surface representation of the CLLF being constructed by joining the dip interpretations in each cross section; c. Surface model of the study area (without the Proterozoic sedimentary cover and Archean units underneath).

2.5.1 Modeling the Archean-Proterozoic Unconformity and the Hidden Archean Units

One of the main challenges in the modeling process was the evaluation of the geometry of the unconformity between the Proterozoic cover and the Archean units underneath using structural data and very sparse data derived from drill-holes performed in the sedimentary cover (Fig. 2-5). A total of 418 surface bedding measurements were used to estimate the shape of the unconformity at depth. The structural data show that the Proterozoic sedimentary formation has a basin-like shape with very shallow dipping borders (Fig. 2-5a). The geometry of the unconformity was refined using 81 compiled diamond drill holes from which 42 intercept the base of the Proterozoic cover (Fig. 2-5b). The surface representing the unconformity was built to accommodate both sets of data giving priority to drill hole control points. The final estimation shows that, in the study area, the Cobalt Group has a thickness of up to 790 m in its western portion and becomes shallower towards the east where two inliers are present (Fig. 2-5c).

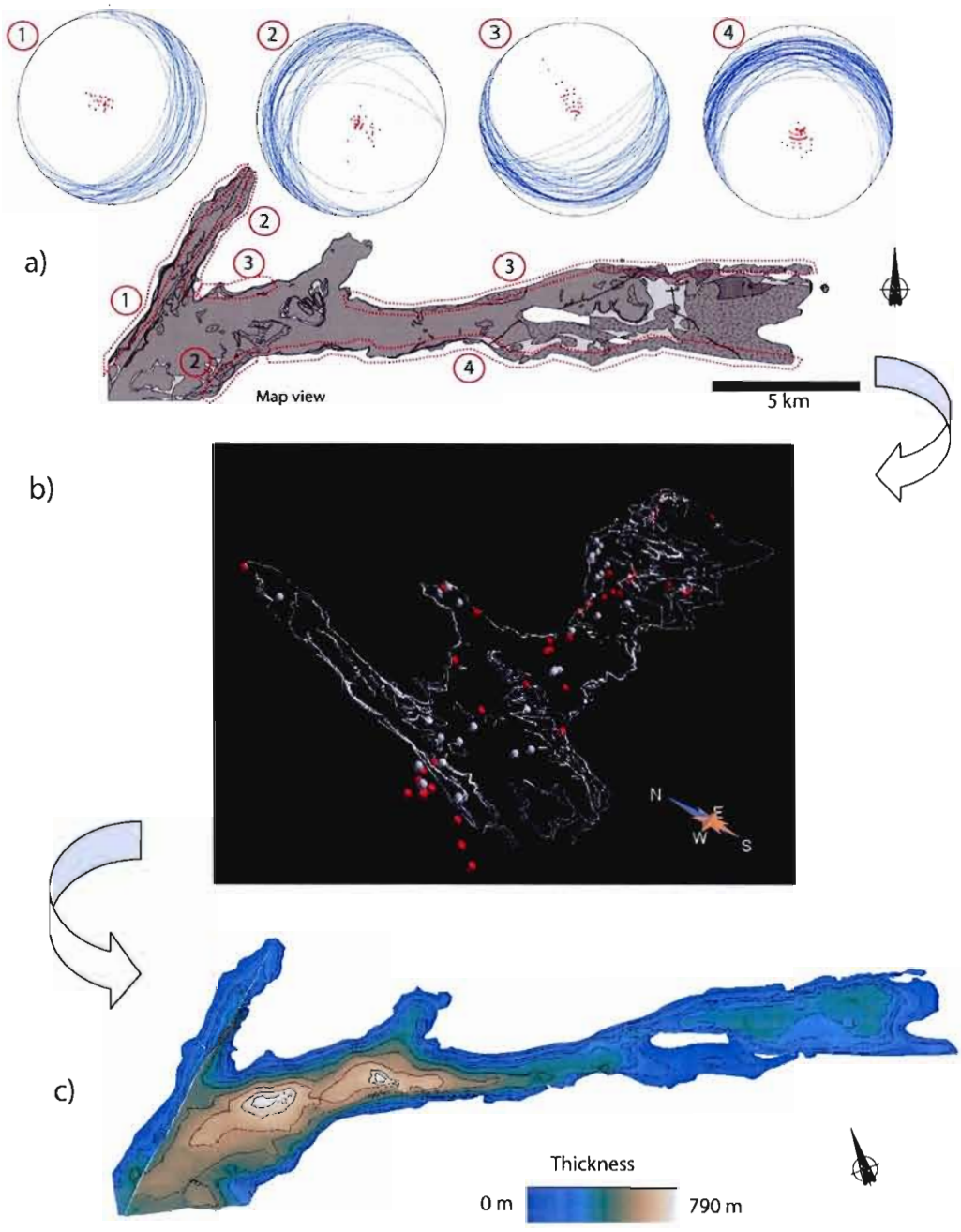

Figure 2-5: Data used to model the 3D geometry of the Archean-Proterozoic unconformity consisted of bedding measurements at the borders of the Cobalt Group (map view) (a) and drill holes within the Cobalt sediments (b). The intersections of

the Archean-Proterozoic unconformity are shown in red whereas drill holes that did not intersect Archean basement are shown in grey (oblique view). c. Model of the thickness of the Proterozoic cover.

The 42 drill holes that intersect the unconformity also provide valuable information for the interpretation of the geology underneath the sediments (Fig. 2-6a). In combination, magnetic data could be used to evaluate the location of contacts of certain highly magnetic units (e.g., ultramafic rocks in the Pontiac, syenites) in sectors where the sedimentary cover is thin because of the very low magnetic susceptibility (measured to < 0.001 SI) of the Cobalt Group. The gravimetric data were mainly used to determine the trace of the CLLF (Fig. 2-7) which separates two contrasting Subprovinces in terms of their nature and density: the volcanic rocks of the Blake River Group to the north, compared with the less dense sedimentary rocks of the Pontiac Subprovince to the south.

The major part of the covered sector is occupied by metamorphosed sediments and ultramafic lavas of the Pontiac Subprovince. The lithologies composing the Blake River Group only occupy the northern part of the covered Archean basement. The Timiskaming sediments are intersected along the CLLF on the full length of the covered Archean basement. They were interpreted on both sides of the CLLF but only on its hanging wall in the central part of the covered area. The alkaline volcanic rocks of this group are intersected by drill holes over a large area in the western part

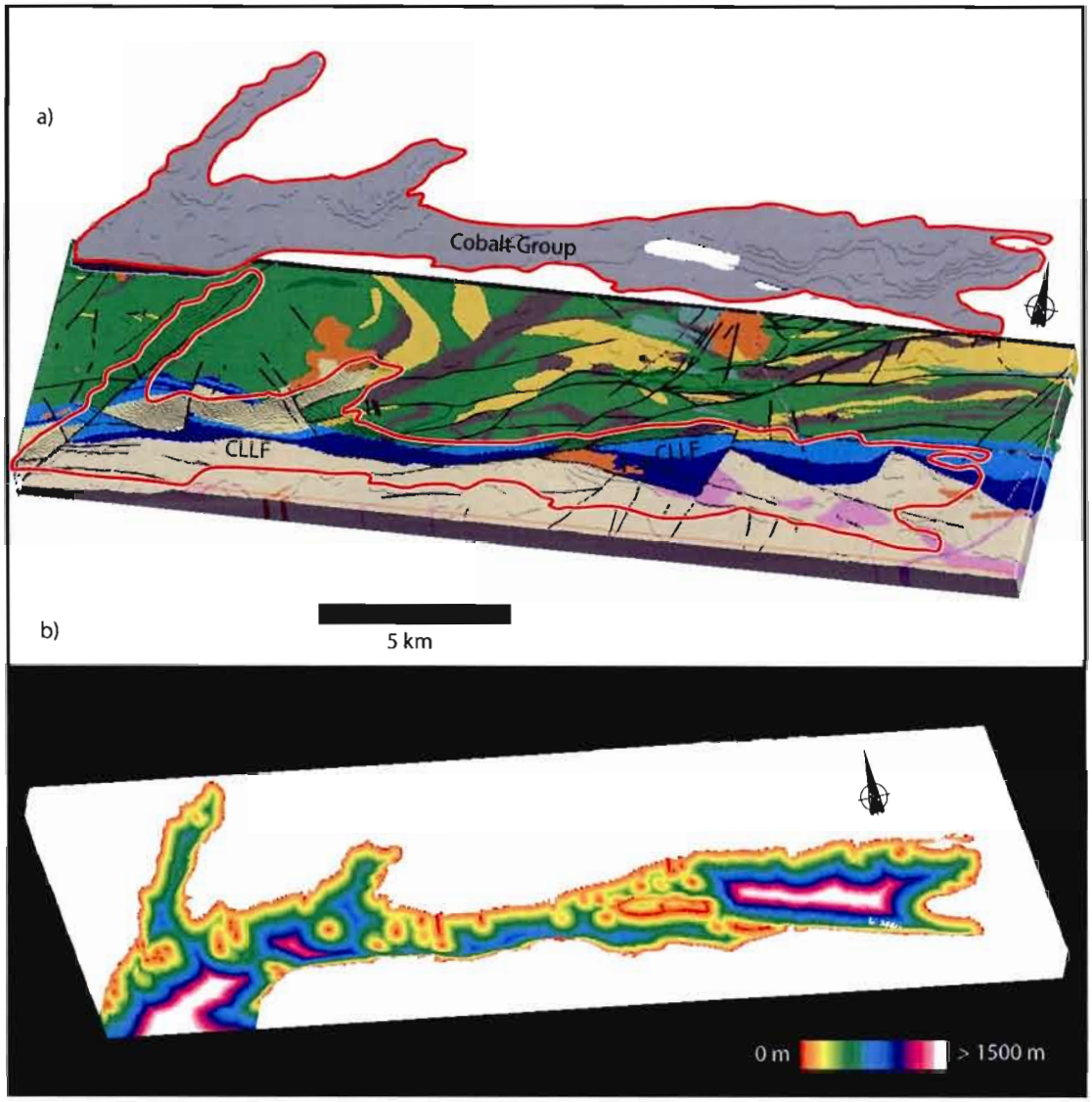

Figure 2-6: a. Geological model of the units lying underneath the Cobalt Group. b. Calculated distance to drill hole data and observed contacts near the edge of the Proterozoic sedimentary cover, the two main constraints for the interpretation the underlying 3D geological map. The distance to these control points can be considered as an indication of the degree of uncertainty in the model

of the unexposed Archean rocks. Finally, two syenite intrusions have been intersected underneath the Cobalt Group.

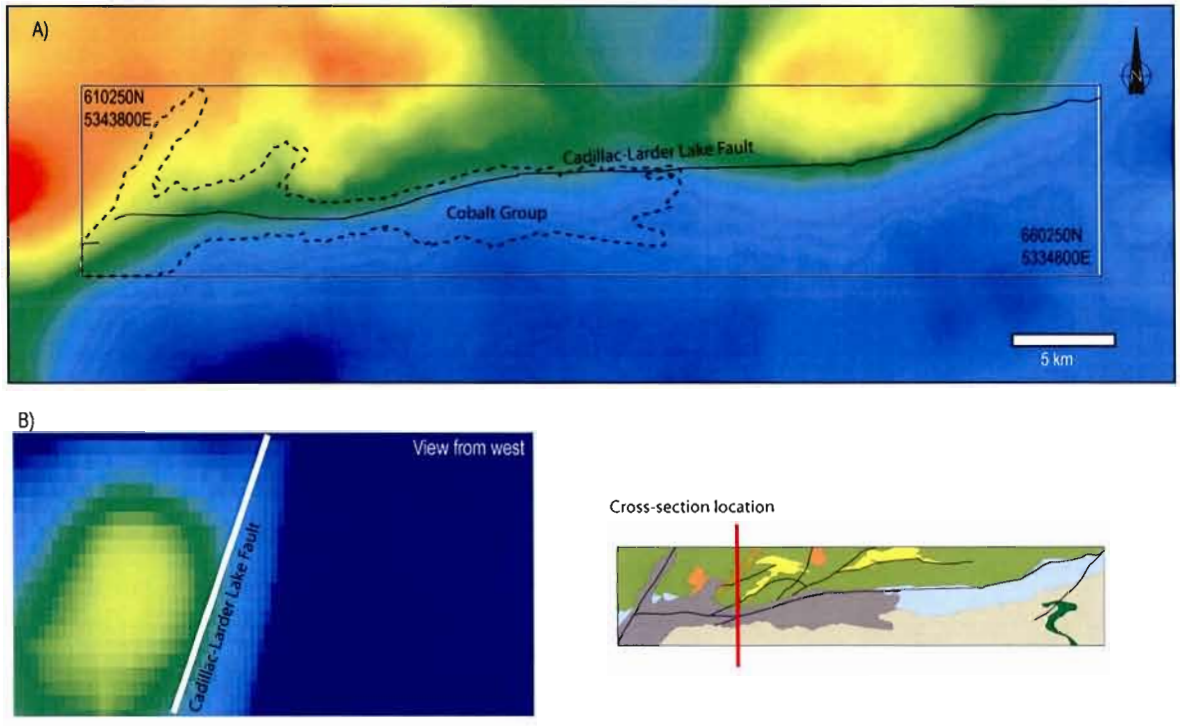

Figure 2-7: a. Map of the residual gravimetric anomaly. b. Section of the unconstrained inversion of the gravimetric data showing the general attitude of the CLLF under the Cobalt Group sediments.

The interpretation of the nature and geometry of the hidden Archean units is locally based on sparse and heterogeneously distributed data. To distinguish sectors where the interpretations are based on hard data from others, the degree of confidence linked to interpretations was quantified (Fig. 2-6b). The two main constraints for the

interpretation of the geometry of the Archean–Proterozoic discontinuity and the underlying 3D geological map are drill hole data and observed contacts near the edge of the Proterozoic sedimentary cover. Because the reliability of the interpretations is directly linked to the distance from these control points, this property was calculated and added in the geological model. A high degree of confidence can be attributed to interpretations in sectors coloured in red, located less than 100 m from a control point, whereas the ones coloured in white are located more at than 1.5 km from a control point implying that the geological interpretation is highly subjective.

2.5.2 Geophysical Inversion

The gravity and magnetic data were inverted to recover the density and the magnetic susceptibility distribution in three dimensions in order to assist in interpreting the 3D geometry of certain geological entities. The airborne magnetic data of the northern half of the study area were acquired via MEGATEM technology with 125 m line spacing (Xstrata, unpublished data, 2002), whereas the data from the southern part are from a wider-spaced (200 m) public database of the Ministry of Natural Resources and Fauna of Quebec (Dion and Lefebvre, 1997). The ground gravity data represent the compilation of two databases from the Ministry of Natural Resources and Fauna of Quebec and the Geological Survey of Canada, where the distribution of the

stations are heterogeneous and mostly located along roads and lake shores (Dion, 1993).

The inversion of gravity data defines a density distribution model that provides the best fit to the observed data on surface. The inversion algorithm used (GRAV3D) was developed at the University of British Columbia (Li and Oldenburg, 1998). The elevated density contrast between the units of the Pontiac and the Abitibi Subprovinces allows proper estimation of the dip of the CLLF along the total length of the model. The 3D inversion results confirm that the CLLF is steeply dipping (~ 75° N) underneath the Proterozoic cover (Fig. 2-7b). This result is consistent with the magnetic data inversion.

The inversion of magnetic data allows evaluation of the distribution of the magnetic susceptibility associated with different lithologies. The 3-D inversion (University of British Columbia code: MAG3D developed by Li and Oldenburg, 1996) was used to invert the data without considering geological constraints. The non-uniqueness of the results obtained in the magnetic interpretation was addressed by favoring a solution with emphasis on a deeper explanation of the susceptibility distribution. The results of the 3D inversion refined the dip of late NE-SW trending structures (Fig. 2-8) such as the Milky Creek, Beauchastel, Horne Creek and Davidson Creek Faults.

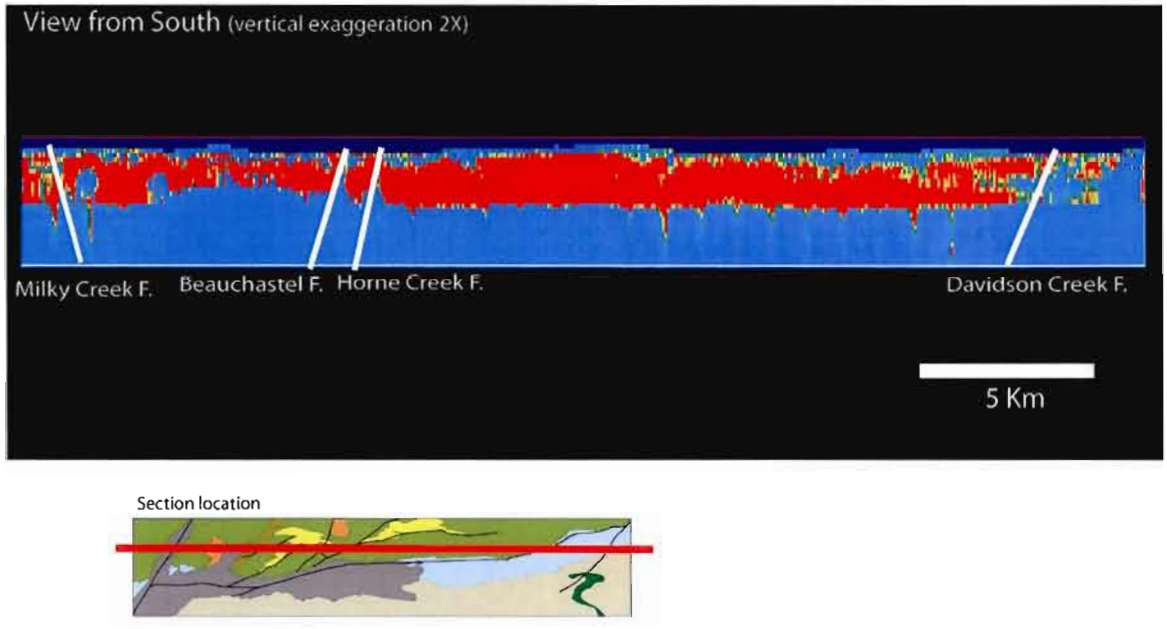

Figure 2-8: Longitudinal section of the unconstrained inversion of the magnetic data which allows interpretation of the dip of the Milky Creek, Beauchastel, Horne Creek and Davidson Creek Faults at depth

2.6 Spatial Analysis of Mineralized Occurrences

Computer-based methodologies such as 3D modeling can be used as predictive tools by uncovering repetitive controls on mineralization. A common method used to delineate prospective areas is to carry out a spatial analysis on a training set of data to identify factors controlling the distribution of known deposits and to use this knowledge on lesser known regions.

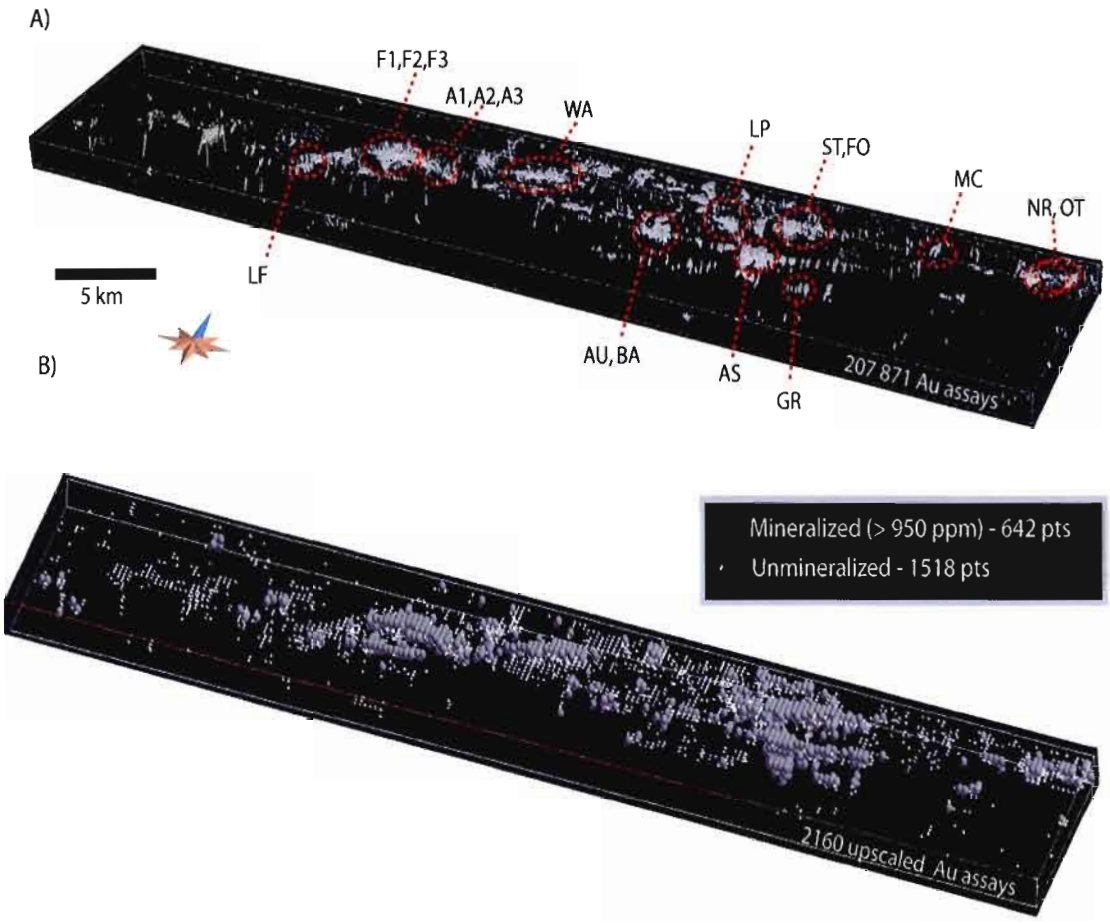

Figure 2-9: a. Location of all gold assays and of major deposits: Francoeur 1, 2 and 3 (F1, F2, F3); Arntfield 1, 2, and 3 (A1, A2, A3); Fortune Lake (LF); Augmitto (Au); Bazooka (BA), Astoria (AS); Granada (GR); Stadacona (ST); Forbex (FO); McWatters (MC); New Rouyn-Merger (NR) and O'Neail-Thompson (OT). b. Upscaled assays with a grid of 250 x 250 x 250 m showing mineralized (> 950 ppb) and unmineralized occurrences

The 3D geological model was used to test the spatial association of specific geological features with gold occurrences. These occurrences were determined using almost 210,000 compiled gold assays. Samples analyzed for precious metals are generally well distributed within the study area even if certain sectors associated with closed mines or studied deposits over-represented (Fig. 2-9a). In order to properly evaluate the controls on orogenic gold mineralization, the database had to be filtered to remove assays derived from other mineralization types with distinct characteristics, source, timing and formation mechanism. These gold occurrences can belong to volcanogenic massive sulfide deposits, porphyry-type deposits associated with syenites, or epithermal-type deposits.

Individual studies of deposits were taken into account to discriminate orogenic gold deposits from other types (Barrett et al., 1992; Legault and Rabeau, 2007; Couture et al., 1996). Furthermore, certain known characteristics of orogenic gold deposits were used to discard assays linked to other types of gold mineralization. The low salinity of the mineralizing fluids involved in the formation of orogenic gold deposits implies low base metal content. In fact, ores typically have negligible values in Cu, Mo or Pb, Sn and Zn (Groves et al., 2003) as opposed to porphyries or VMS. Orogenic gold deposits also typically have a high Au/Ag ratio. More than 11,200 Cu and 18,000 Ag assay were used to discard 7,538 assays considered too rich in base metals or in Ag. The discarded assays were mainly located in the sector of the Aldermac Mine and of the Bay Renaud Syenite.

A regular grid covering the entire study area composed of 250 x 250 x 250 m cells was used to upscale the assay database to diminish the sampling bias on statistical calculations due to data clustering near known deposits (Fig. 2-9b). The size of cells was determined by iteration in order to define well known deposits while avoiding over-sampling. The mean, median, maximum and minimum of gold concentrations (ppb) in each cell were calculated. The maximum value of each cell was used to determine two data classes: the mineralized and unmineralized occurrences.

All sells containing a maximum gold concentration value of more than 950 ppb was considered as a mineralized occurrence. This threshold was set considering the minimum economic grade in Archean orogenic deposits (1.51 g / t Au in 2007 at the Sigma mine (Perreault, 2007) and an average grade of less than 2 g /t Au at the Archean Golden Mile deposit) and obligation to discriminate between anomalous gold concentrations and mineralized occurrences.

The unmineralized occurrences were defined by the remaining cells containing gold concentration values. This process defined 642 mineralized and 1518 unmineralized occurrences. A total of 54 unmineralized occurrences located in Proterozoic lithologies (32 in the sedimentary rocks of the Cobalt Group and 22 in the diabase dikes) were eliminated for the spatial analysis because they postdate the orogenic gold mineralization.

Using the 3D geological model and the upscaled and filtered assay database, an analysis was conducted to examine spatial associations of orogenic gold occurrences with pertinent geological features. These spatial associations were quantified using the *weights of evidence method* (Bonham-Carter et al., 1988). This method measures the degree of spatial association by a pair of weights (W+ and W-) calculated as follow:

$$W+ = ln[P(X|D)/P(X|\overline{D})]$$
$$W- = ln[P(\overline{X}|D)/P(\overline{X}|\overline{D})] \quad \text{(eq. 1)}$$

where D and $\overline{D}$ represent respectively the presence and absence of an occurrence. $P(X|D)$ corresponds to the probability of having a factor X in association with a mineralized occurrence D, and $P(\overline{X}|\overline{D})$ is the probability of not having factor X in association with an unmineralized occurrence.

A positive value of W^+ combined to a negative value of W^- indicates that the tested factor is positive evidence for the presence of orogenic gold. However, in the case of a negative correlation with gold deposits, W^+ would have a negative value and W^- would be positive. An absence of spatial association is implied if $W^+ = W^- = 0$. This methodology requires a sufficient number of reference ore deposits in order to calibrate the occurrence and non-occurrence probabilities. In order to use this

methodology, an extensive data training set is required. The *weighs of evidence method* will allow the evaluation of the degree of spatial association between mineralized occurrences and several geological parameters, such as distance to structural features, host rocks, and distance to intrusive bodies.

In order to quantify the uncertainty attached to each weight, a confidence interval was estimated for each W^+ and W^-, respectively, using a similar technique as the one applied for estimating interval for probabilities. Since weights of evidences W are calculated from the ratio of the conditioned probability such as $p = P(X/D) = P(X \cap D)/P(D)$, it is possible to estimate a confidence interval for the weights using classical rules for propagation errors with the confidence interval for each probability involved. The confidence interval ($\pm \varepsilon_p$) for probability p was estimated using the equation (Kendall, 1997):

$$\varepsilon_p = z_{\alpha/2} [p.(1-p)/n]^{1/2} \quad \text{(eq. 2)}$$

where p is the estimated probability, n the sample number, and $z_{\square/2}$ is the risk level defined by a normal distribution for a risk of 95% to be in the interval considered (in this case $z_{\alpha/2} = 1.96$).

The confidence interval ε_r for probability ratio $r = p/q$ was calculated using the following equation:

$$\varepsilon_r = r\,[\varepsilon_p/p + \varepsilon_q/q] \qquad \text{(eq. 3)}$$

The lower W_- and upper W_+ bounds of the confidence interval for the weight of evidence $W = ln[p/q]$ was estimated reporting the upper and lower values of p and q, respectively, in the definition:

$$W_- = ln\,[(p-\varepsilon_p)\,(q+\varepsilon_q)/] \qquad W_+ = ln\,[(p+\varepsilon_p)\,(q-\varepsilon_q)/] \qquad \varepsilon_w = [W_+ - W_-]/2 \qquad \text{(eq. 4)}$$

2.6.1 Lithologies

At greenstone belt-scale, orogenic gold mineralization can be hosted by any rock type (Hodgson, 1993); however, some lithologies are more commonly associated with deposits than others (Hodgson and Troop, 1988). This is explained by certain geochemistries that favor precipitation of gold from the hydrothermal fluid, or by competency contrasts that influence the geometry and density of fractures and correlative fluid circulation.

	Mineralized	Unmineralized	$W^+ \pm \sigma_w$	$W^- \pm \sigma_w$
Pontiac Group				
Sedimentary rocks	4	69	-2.02±2.46	0.04±0.61
Basalt	0	3	n.d.	n.d.
Ultramafic volcanics	0	2	n.d.	n.d.
Blake River Group				
Rhyolite	75	227	-0.28±0.36	0.04±0.34
Basalt	222	603	-0.17±0.25	0.10±0.24
Andesitic tuff	62	61	0.84±0.45	-0.06±0.5
Basaltic tuff	16	19	0.65±0.82	0.01±0.96
Rhyolitic tuff	15	27	0.24±0.77	-0.01±0.81
Andesite	0	2	n.d.	n.d.
Timiskaming Group				
Conglomerate, wacke	139	181	0.56±0.32	-0.11±0.34
Trachytic tuff	0	25	n.d.	n.d.
Piché Formation				
Ultramafic rocks	15	8	1.45±1.05	-0.02±1.15
Intrusive Rocks				
Syenite	4	37	-1.40±3.17	0.02±0.82
Gabbro	90	199	0.03±0.35	0.00±0.35
Felsic intrusions	0	1	n.d.	n.d.

Table 2-2: Spatial associations with mineralization (= favorable features).*

The 3D regional geological model of the CLLF was used to evaluate and quantify the spatial association of each major lithology with the mineralized occurrences (Table 2-

2). The lithologies presenting a spatial association with mineralized occurrences considering the uncertainty intervals on the calculated weights are: the ultramafic rocks of the Piché Formation (W_+ = 1.45±1.05, W_-= -0.02±1.15), the andesitic tuff of the Blake River Group (W_+ = 0.84±0.45, W_-= -0.06±0.5) and the sedimentary rocks of the Timiskaming Group (W_+ = 0.56±0.32, W_-= -0.11±0.34).

The other volcanoclastic rocks of the Blake River Group have a positive W_+ and a negative W_-, but have a low level of confidence according to the calculated uncertainty. The preferential association of gold mineralization with volcanoclastic rocks and weakly metamorphosed sediments illustrates the importance of primary permeability in the formation of orogenic gold deposits. The spatial association of mineralized occurrences within the Piché Formation is more likely explained by its location within the CLLF, which hosts numerous deposits. The spatial association of syenites with gold deposits is well documented (Hodgson and Troop, 1988; Robert, 2001) but the spatial analysis in this study fails to bring out this association. This can be explained by the fact that syenites associated with gold mineralizations are mostly of small dimension (less than 3 km^2; Legault and Lalonde (in prep)) and that these small intrusions tend to be under evaluated in a regional model, possibly due to the upscaling procedure used to estimate characteristics in the regular cell grid. Furthermore, because these intrusive bodies are also associated with other gold mineralization types, many of the gold assays associated with these intrusions were filtered out.

2.6.2 Faults and Fault Intersections

Structural features have an important control on orogenic gold deposit distribution. Major fault zones are thought to act as channel ways for gold-bearing hydrothermal fluids from deeper crustal levels (Kerrich et al., 2000) whereas second- and third-order faults, which host most of the gold endowment, are believed to form dilatational sites favorable for gold precipitation (Eisenlohr et al., 1989).

The faults located in the study area can be separated into two distinct groups based on their orientation. The east-west group contains faults having an orientation between N060° and N120° and represents 66 fault segments. The north-south group contains 94 faults with orientations between N315° and N045°. Each of these groups were tested individually for their spatial association with orogenic gold occurrences. The distances of the mineralized and unmineralized occurrences from each of the fault groups were calculated in the model. The statistical analysis showed that the mean distance of mineralized occurrences to E-W faults is 284 m, and 75% are within 360 m of one of these faults. A strong spatial association ($W_+ = 0.44 \pm 0.21$, $W_- = -0.71 \pm 0.24$) can be observed using a 360 m distance to E-W faults and the mineralized occurrences (Fig. 2-10a). The same statistical analysis of the distances between mineralized occurrences and N–S faults indicates a mean distance of 758 m and much less association with mineralized occurrences.

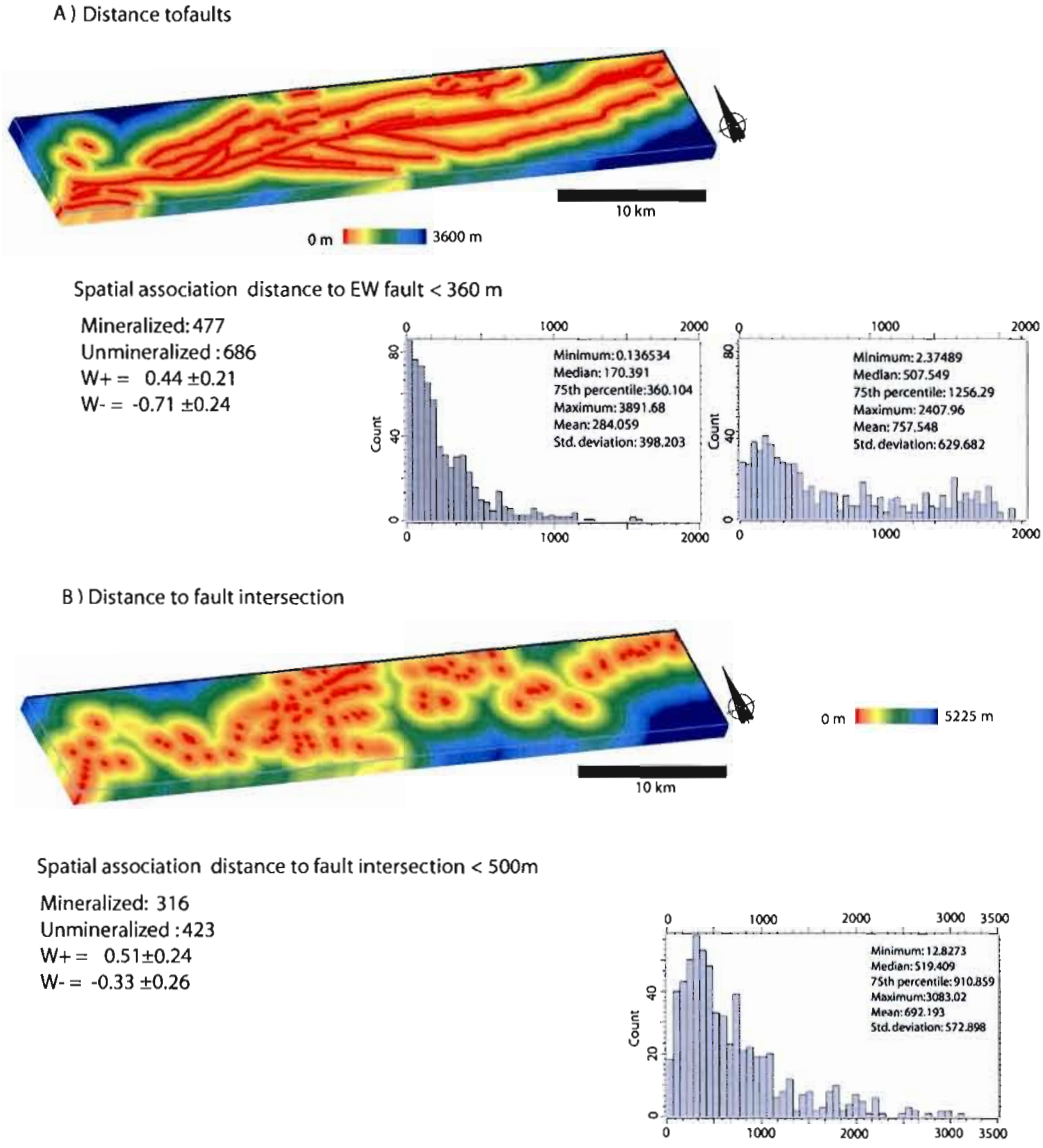

Figure 2-10: Calculated distance of mineralized occurrences to E-W faults (a) and to fault intersections (b). Histograms show the cumulative frequency of mineralized occurrences versus to the distance to both fault groups, and calculated weights with confidence intervals.

Localized zones where the fracture density is important become sectors of enhanced permeability leading to the circulation of large amounts of mineralizing fluids and gold precipitation (Tripp and Vearncombe, 2004). Fault intersections at a regional scale were therefore considered as areas of high fracture density.

Fault intersections can be represented in 3D space as lines. The distance between the generated lines and mineralized occurrences was computed in order to define the spatial association of fault intersections and gold deposits. A histogram showing the cumulative frequency of mineralized occurrences as a function of the distance to fault intersections shows a break at the median value of 519 m (Fig. 2-10b). This range was used in the calculation of weights and confirms a good spatial relationship with weights of evidence ($W_+ = 0.51 \pm 0.24$, $W_- = -0.33 \pm 0.26$).

2.6.3 Distance to Intrusive Rocks

It has been noted that the competency contrast of plutonic bodies with their host rock favors fracturing during deformation and creates dilatational sites (Groves et al., 2000). Hence, intrusive bodies can be favorable hosts for gold deposits. The spatial distribution of mineralized occurrences around each intrusive unit was tested and quantified. The lithologies considered for the calculation were: gabbros, felsic intrusions and syenites. The distance to each mineralized occurrences was calculated

for the closest intrusive body. Although 75% of all the occurrences are within 668 m of an intrusive body (Fig. 2-11), the calculated weights (W_+ = -0.04±0.22, W_-= 0.05±0.21) show that there is no spatial association between mineralized occurrences and intrusions, meaning that mineralized and unmineralized occurrences are located at the same distance from plutonic bodies.

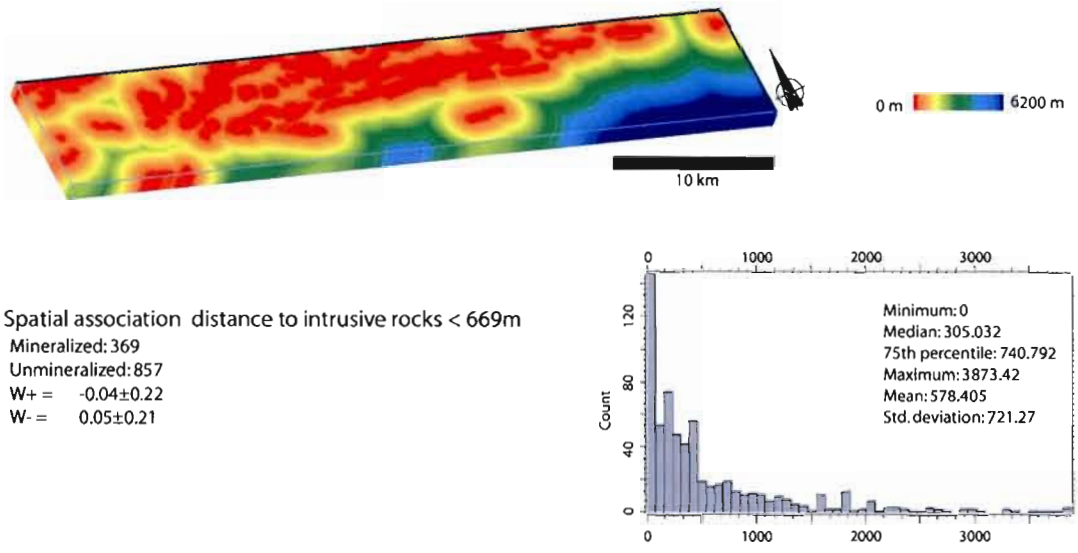

Figure 2-11: Calculated distance to intrusions with accompanying histogram showing the cumulative frequency of mineralized occurrences versus to the distance to the nearest intrusion, with calculated weights and confidence intervals.

2.7 3D Mineral Potential Mapping under the Proterozoic Cover

Hidden orogenic gold deposits can be considered to have common characteristics with known deposits in the same area. The geological model built under the Proterozoic cover was used to target areas using the aforementioned influential geological features and their quantified spatial association (Fig. 2-12). Geological features presenting a positive spatial association (Table 2-2) were used to define favourable zones.

	Combination Index
Structural features	
< 500 m to fault intersection	0.25
< 355 m to E–W Faults	0.5
Lithological features	
Temisiskaming sediments	0.25
Andesitic tuff	0.25
Uncertainty – Distance to control points	
250 m < Control point > 500 m	-0.15
500 m < Control point > 750 m	-0.2
Control point > 750 m	-0.3

Table 2-3: Combination index for each geological feature used for mineral potential mapping

A combination index having a value between 0 and 1 was assigned to each influential feature in such way that the cumulative value of the index is equal to 1 (table 2-3). This index allows the integration of the specific knowledge of the user while considering the degree of spatial association measured by the weights of evidence. The index value presented were established by considering that structural factors are the most significant because of their influence on the distribution of orogenic gold deposits and present the highest spatial association.

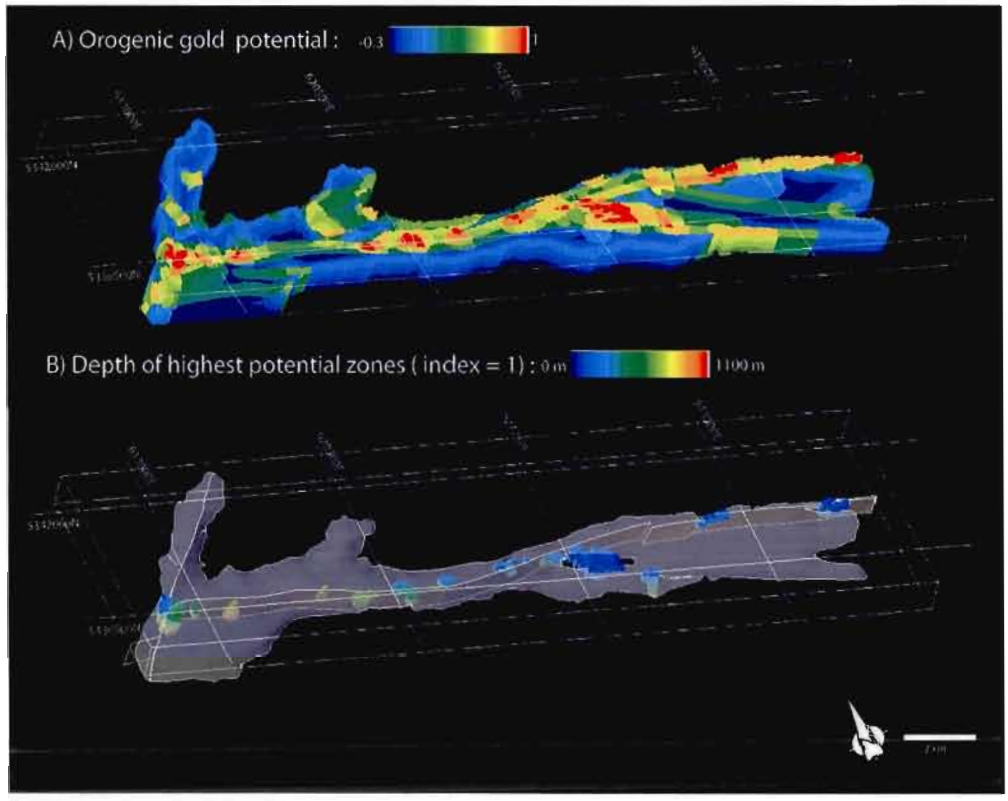

Figure 2-12: a. Mineral potential map for orogenic gold mineralization under the Proterozoic sedimentary cover. Index values vary from -0.3 to 1. b. Location in 3D of

zones with highest index value painted accordingly to their depth with respect to the unconformity contact and CLLF.

Most of the closed mines or well defined deposits are located on a fault zone: Francoeur, Wasamac, Arntrfield, Astoria, Augmitto, McWatters. A 0.5 combination index was assigned for cells located at less than 360 m from an E-W fault. A 0.25 combination index was also assigned to cells located at less than 520 m away from a fault intersection. In the geological model, mineralized occurrences are hosted in a unique lithology; consequently, cells located in a favourable lithology were assigned an index value of 0.25. The Piché Formation, located directly within the CLLF, was treated distinctly. An index value of 0 was attributed to cells within the Piché Formation because they already cumulate the 0.5 index assigned to E-W faults du to their spatial association to the CLLF.

The degree of confidence linked to geological interpretations under the Cobalt Group sediments (Fig. 2-6b) was also included in the generation of the 3D gold potential map to account for sectors where interpretations were made with less data. A value determined by the level of uncertainty in interpretations was subtracted from the cumulative index factor. The distance to the control points was considered as representative of the degree of uncertainty. The cumulative index of cells located less than 250 m away from a control point were left unchanged, whereas cells located

between 250 and 500, 500 and 750 m, and more than 750 m from a control point were given values of 0.15, 0.2 and 0.3 respectively subtracted from their combination index.

The end result of the combination of all the cumulative indexes (Fig. 2-12a) helps to discriminate zones of high potential for orogenic gold mineralizations. The 3D potential map focuses exploration by targeting high potential zones with consideration to uncertainty and therefore associated risk. The majority of the high potential zones are located along the CLLF because this fault zone has a favorable orientation and it also spatially controls one of the favorable lithologies, the Timiskaming Group. The final map shows that less than 6.25 % of the total volume has obtained a 0.75 cumulative index and less than 1 % than was granted a cumulative index value of 1. The depth of these exploration targets is essential to determine their potential economical value. Figure 2-12b presents the highest potential localities with a color code for depth. More than 75% of the targets presented are less than 650 m deep.

2.7.1 Cross-Validation of the 3D potential map

The capacity of the presented methodology to predict mineralized volumes was tested. Figure 2-13a presents the proportion of the total gold assays and of the

mineralized occurrence upscaled subset against the total combination index assigned to their location. The upscaled mineralized occurrences have a higher proportion of high cumulative combination index since the total assays database has not been filtered for non-orogenic gold occurrence. Eighty-five percent of the 642 defined mineralized occurrences present a spatial association with at least one of the 6 factors.

Figure 2-13b presents the proportion of the 642 mineralized occurrences and of the 14 mines exploited in the study area against the total volume of Archean basement covered by the 3D model sorted decreasingly accordingly to the cumulative value of the combination index. This graph shows that more than 90 % of the mines have been predicted less than 20% of the total surface area has been covered.

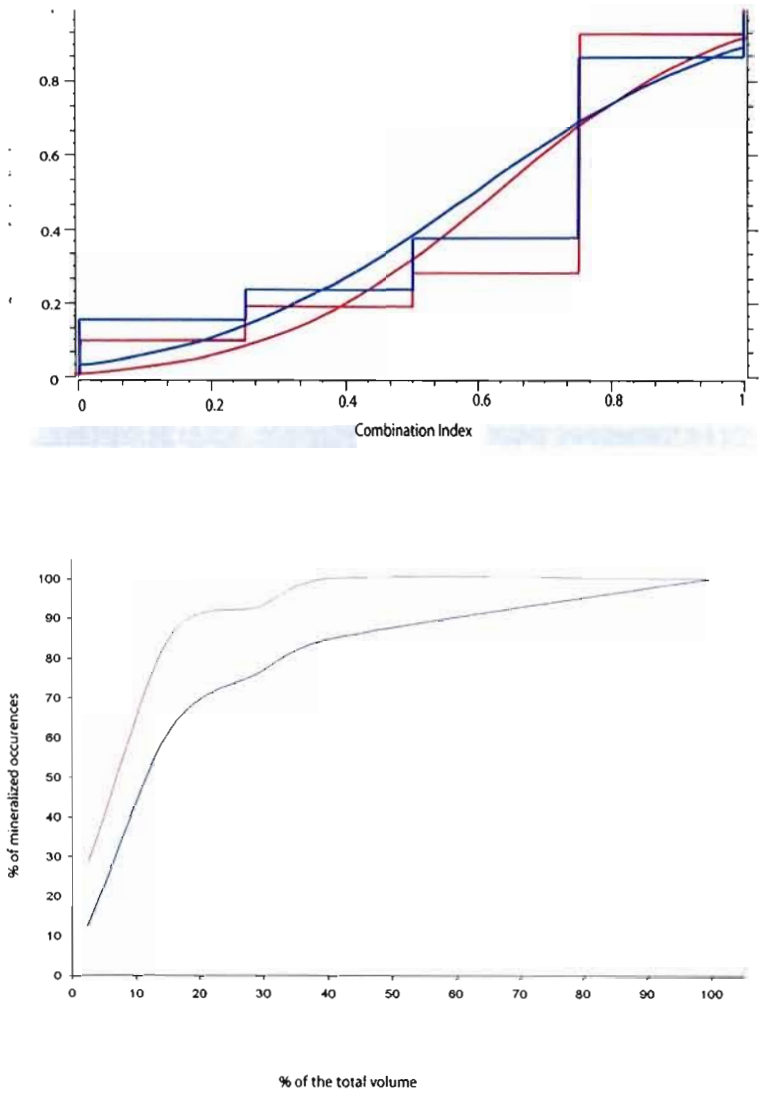

Figure 2-13: ***a***. *Graph presenting the percentage of all compiled gold grades (red) and of the mineralized occurrences determined by the upscalling method (blue) against the combination index value.* ***b***. *Graph presenting the proportion (%) of the mineralized occurrences determined by the upscalling method (blue) and of the 14*

mines present in the study area (red) against the total volume sorted decreasingly according to the combination factor value.

Finally, the only known orogenic gold mineralization of more than 1 g / t under the sedimentary rocks of the Cobalt Group is located at the eastern end of the Proterozoic cover on the eastern side of the Milky Creek Fault zone, and was delimited as a high potential zone with an index value of 1.

2.8 Conclusion

The integration of a detailed geological observations with structural measurements, drill hole data and geophysical interpretation has led to the construction of a realistic geological model. This model, coupled with compiled gold assays, was used to perform a spatial analysis to identify the controlling features of gold mineralizations and create a 3D mineral potential map under a hidden segment of a major Archean fault zone. The methodology suggested here uses a training set to evaluate features that influence the distribution of gold mineralization, but still relies on geological knowledge to assign an importance to each of these factors. This methodology based on Bayesian statistics and relying on 3D modeling is an efficient way to reduce risk in

regional exploration campaigns at depth, and is particularly useful in sectors in which traditional exploration methods are inappropriate but where data are abundant.

The methodology presented here has limitations in certain aspects. The main limitation is caused by uncertainties linked to interpretations at depth. Even though the methodology takes into account distances to control points under the Proterozoic cover, many interpretations on cross sections may influence the spatial relationships between geological features and mineralized occurrences, and were made with unequally distributed data. Another limitation is linked to the assay database. Because copper and silver were not analyzed systematically, assays from different deposit types may have been treated as orogenic deposits. Finally, the end result may vary by changing the importance given to each feature with the combination index, because the geologist's knowledge directly influences the end result.

2.9 Acknowledgements

This work was supported by the University of Quebec in Abitibi-Témiscamingue, the DIVEX consortium, and the Ministère des Ressources naturelles et de la Faune du Québec. The manuscript benefited from careful reviews by Eric De Kemp, Jeff Harris, Shoufa Lin and Jeremy Richards. The authors would like to thank Jean Goutier for his comments on part of the work presented. The assistance of Gabriel

Morin in the preparation and 3D integration of numerical data and of Johanne Jobidon for graphical design are also acknowledged. The following mining companies are also acknowledged for sharing data, information or expertise: Xstrata Copper, Richmont Mines, Alexis Mining Corporation, Iamgold, Jean Decarreaux, Yorbeau Ressources, West Cadillac Mining Corporation. Finally, Julie Gagné, Mark-Antony Canada and Pauline Mercier are thanked for their meticulous help compiling the data necessary for this study.

2.10 References

Barrett, T. J., Cattalani, S., Chartrand, F. and Jones, P, 1992, Massive sulfide deposits of the Noranda area, Quebec. II. The Aldermac mine: Canadian Journal of Earth Sciences, v. 28, p. 1301-1327.

Bonham-Carter, G. F., Agterberg, F. P. and Wright, D. F, 1988, Integration of Geological Datasets for Gold Exploration in Nova Scotia: Photogrammetric Engineering and Remote Sensing v. 54, p. 1585-1592.

Dubé, B., Gosselin, P., 2007, Greenstone-hosted quartz-carbonate vein deposits, in : Mineral Deposits of Canada: A Synthesis of Major Deposit-Types, District Metallogeny, the Evolution of Geological Provinces, and Exploration Methods,

Godfellow, W.D, ed., Geological Association of Canadca, Mineral Deposit Division, Special Publication No. 5, p. 46-73.

Corfu, F., 1993, The Evolution of the Southern Abitibi Greenstone Belt in Light of Precise U-Pb Geochronology: Economic Geology V.88, p. 1323-1340.

Couture, J.-F. 1991, Carte géologique des gîtes métallifères des districts de Rouyn Noranda et de Val-d'Or. DV 90-11. Ministère de l'Énergie et des Ressources du Québec.

Couture, J.-F, 1996, Gisements metalliques du district de Rouyn-Noranda. In: Métalogénie et évolution de la région de Rouyn-Noranda , ed. Couture, J.-F. and Goutier, J., MB 96-06. Ministère des Ressources naturelles du Québec, 11-18.

Couture, J.-F., Goutier, J. and Péloquin, A. S, 1996, Géologie de la région de Rouyn-Noranda, Québec. In: Métallogénie et évolution de la région de Rouyn-Norand, ed. Couture, J.-F. and Goutier, J., MB 96-06, Ministère des Ressources naturelles du Québec, 1-9.

Couture, J.-F. and Pilote, P, 1993, The Geology and Alteration Patterns of a Disseminated Shear Zone-Hosted Mesothermal Gold Deposits: The Francoeur 3 Deposit, Rouyn-Noranda, Quebec: Economic Geology, V. 88, p. 1664-1684.

Couture, J.-F. and Willoughby, N. O, 1996, Géologie du gisement Granada. In: Métallogénie et évolution de la région de Rouyn-Noranda, ed. Couture, J.-F. and Goutier, J., MB 96-06. Ministère des Ressources naturelles du Québec, p. 77-80.

Daigneault, R. and Mueller, W. U. 2004. Abitibi greenstone belt plate tectonics: the diachronous history of arc development, accretion and collision, The Precambrian Earth: Tempos and events, ed. Eriksson, P., Altermann, W., Nelson, D., Mueller, W. U., Catuneaunu, O. and Strand, K., Development in Precambrian Geology, v .12. Elsevier, p. 88-103.

Daigneault, R., Mueller, W. U. and Chown, E. H., 2002, Oblique Archean subduction: accretion and exhumation of an oceanic arc during dextral transpression, Southern Volcanic Zone, Abitibi Subprovince, Canada: Precambrian Research, v. 115, p. 261-290.

Dimroth, E., Imreh, L., Rocheleau, M. and Goulet, N.,1982, Evolution of the south-central part of the Archean Abitibi Belt, Quebec. Part I: Stratigraphy and paleogeographic model: Canadian Journal of Earth Sciences, v. 19, p.1729-1758.

Dion, D.J., Lefrebre, D., 1997, Données numériques (profiles) des levés géophysiques aéroportés du Québec (32D), Ministère des Ressources naturelles et de la Faune du Québec, DP-96-02.

Dion, D.J., 1993, Données gravimétrique dans la région de l'Abitibi (Chibougamau, Rouyn-Noranda, Val-d'Or) et de Manicouagan, Ministère des Ressources naturelles et de la Faune du Québec, MB 93-61X

Eisenlohr, B. N., Groves, D. I. and Partington, G. A., 1989, Crustal-scale shear zones and their significance to Archaean gold mineralization in Western Australia.: Mineralium Deposita, v. 24, p. 1-8.

Fairbairn, H. W., Hurley, P. M., Card, K. D. and Knight, C. J., 196,. Corroletion of Radiometric Ages of Nipissin Diabase and Huronian Metasediments with Proterozoic Orogenic Events in Ontario: Canadian Journal of Earth Sciences, v. 6, p. 489-497.

Guindon, D.L., Grabowski, G.P.B., Meyer, G. and Picotte, M.C.M., 2007, Report of Activities 2006, Resident Geologist Program, Kirkland Lake Regional Resident Geologist Report: Kirkland Lake District; Ontario Geological Survey, Open Report 6204, p. 42.

Goldfarb, R. J., Groves, D. I. and Gardoll, S., 2001, Orogenic gold and geological time: a global synthesis: Ore Geology Reviews, v. 18, p. 1-75.

Groves, D. I. 1993. The crustal continuum model for late-Archean lode-gold deposits of the Yilgarn Block, Western Australia: Mineralium Deposita, v. 28, p. 366-374.

Groves, D. I., Goldfarb, R. J., Gebre-Mariam, M., Hageman, S. G. and Robert, F., 1998, Orogenic gold deposits: A proposed classification in the context of the crustal distribution and relationship to other deposit types: Ore Geology Reviews, v. 13, p. 7-27.

Groves, D. I., Goldfarb, R. J., Knox-Robinson, C. M., Ojala, J., Gardoll, S., Yun, G. Y. and Holyland, P, 2000, Late-kinematic timing of orogenic gold deposits and significance for computer-based exploration techniques with emphasis on the Yilgarn Block, Western Australia: Ore Geology Reviews, v. 17, p. 1-38.

Groves, D. I., Goldfarb, R. J., Robert, F., Hart, C. R. J., 2003, Gold deposits in metamorphic belts: overview of current understanding, outstanding problems, future research, and exploration significance.: Economic Geology, v. 98, p. 1-29.

Hodgson, C. J., 1993, Mesothermal Lode-gold Deposits. Mineral Deposit Modeling, ed. Kirkham, R. V., Sinclair, W. D., Thorpe, R. I. and Duke, J. M., Special Paper 40. Geological Association of Canada, p. 635-678.

Hodgson, C. J. and Troop, D. G., 1988, A New Computer-Aided Methodology for Area Selection in Gold Exploration: a Case Study from the Abitibi Greenstone Belt: Economic Geology, v. 83, p. 952-977.

Kendall, M., Stuart, A., Ord, J. K., 1997, Kendall's Advanced Theory of Statistics: Classical Inference and the Linear Model. Vol. 2A, John Wiley & Sons Inc; 6th ed., 300p.

Kerrich, R., Goldfarb, R. J., Groves, D. I. and Garwin, S., 2000, The Geodynamics of World-Class Gold Deposits: Characteristics, Space-Time Distribution, and Origins, Gold in 2000, ed. Hageman, S. G. and Brown, P. E., v. 13. Reviews in Economic geology, p. 500-551.

Kishida, A. and Kerrich, R., 1987, Hydrothermal alteration zoning and gold concentration at the Kerr-Addison Archean lode gold deposit, Kirkland Lake, Ontario: Economic Geology, v. 82, p. 649-690.

Lafrance, B., Davis, D. W., Goutier, J., Moorhead, J., Pilote, P., Mercier-Langevin, P., Dubé, B., Galley, A. G. and Mueller, W. U., 2005, Nouvelles datations isotopiques dans la portion québécoise du Groupe de Blake River et des unités adjacentes. Ministères des Ressources naturelles et de la Faune, Québec, 15 p.

Leduc, M., 1986, Géologie de la région du lac Dasserat, Abitibi (Groupe de Blake River). Ministère de l'Énergie et des Ressources, Québec; MB 86-14, 180 p., 2 cartes.

Legault, M. and Lalonde A., in prep, Discrimination des syenites associés aux gisements aurifères de la Sous-province de l'Abitibi, Québec, Canada, Ministère des Ressources naturelles, RP-2008-XX

Legault, M. and Rabeau, 2007, Étude métallogénique et modélisation 3D dans la region de la Faille Cadillac dans le secteur de Rouyn-Noranda (phase 2), Ministère des Ressources Naturelles et de la Faune du Québec, 11 p.

Legault, M. and Rabeau, 2006, Étude métallogénique et modélisation 3D dans la region de la Faille Cadillac dans le secteur de Rouyn-Noranda (phase 1), Ministère des Ressources natureelle et de la Faune du Québec , 11 p.

Mallet, J. L. 1992a. Discrete Modeling for Natural Objects: Mathematical Geology, v. 29, p. 199-219.

Mallet, J. L. 1992b. Gocad: A Computer Aided Design Program for Geological Applications. Proceedings, Nato ASI Series C: Math Pys. Sci. Vol 354.

McNicoll, V., Dubé, B., Goutier, J., Mercier-Langevin, P., Dion, C., Monecke, T., Ross, P.S., Thurston, P, Percival, J., Legault, M., Pilote, P., Débard, J. Leclerc, F., Gibson, H., Ayer, J., 2008, New U-Pb Geochronology from theTGI-3 Abitibi/plan cuivre : Implications for geological Interpretations and Base Metal Exploration, abstract, GAC-MAC, Quebec 2008, p.110.

Mercier-Langevin, P., Dubé, B., Hannington, M. D., Davis, D. W., Lafrance, B., Gosselin, G., 2007 The LaRonde Penna Au-Rich Volcanogenic Massive Sulfide Deposit, Abitibi Greenstone Belt, Quebec: Part I. Geology and Geochronology : *Economic Geology*, v. 102, p. 585-609.

Morin, D., Jébrak, M., Bardoux, M. and Goulet, N., 1993, Pontiac metavolcanic rocks within the Cadillac tectonic zone, McWatters, Abitibi belt, Quebec: Canadian Journal of Earth Sciences, v. 30, p. 1521-1531.

Poulsen, K. H., Robert, F. and Dubé, B., 2000, Geological classification of Canadian gold deposits. Geological Survey of Canada, 106 p.

Robert, F., 2001, Syenite-associated disseminated gold deposits in the Abitibi greenstone belt, Canada: Mineralium Deposita, v. 36, p. 503-516.

Smith, J. P., Spooner, E. T. C., Broughton, D. W. and Ploeger, F. R., 1990, The Kerr Addison-Chesterville Archean Gold-Quartz Vein System, Virginiatown: Time Sequence and Associated Mafic "Albitite" Dyke Swarm, Geoscience Research Grant Program Summary of Research 1989-1990, ed. Milne, V. G., Miscellaneous Paper 150. Ontario Geological Survey, p. 175-199.

Thurston, P.C., Ayer, J.A., Goutier, J., Hamilton, M.A., 2008a, Depositional Gaps in Abitibi Greenstone Belt Stratigraphy: A Key to Exploration for Syngenetic Mineralization : Economic Geology. v. 103, p. 1097-1134

Thurston, P.C., Goutier, J., McNichol, V., Legault, M., 2008b, Mafic Dykes cutting the Blake River Group, Abitibi Subprovince, abstract, GACMAC 20008

Tripp G.I., and Vearncombe, J. R., 2004, Fault/fracture density and mineralization: a contouring method for targeting in gold exploration: Journal of Structural Geology v. 26, p. 1087-1108

Chapitre 3: 3D Strain Modeling Driven by Field Data in the Vicinity of the Cadillac Larder Lake Fault Zone: Insights on Archean Orogenic Gold Distribution

3.1 Introduction générale

Cette section présente sous forme d'article des travaux de modélisation mécanique orientés vers la définition de zones en dilation lors de l'épisode de déformation contemporain à la mise en place de l'or de type orogénique. Ces zones représentent des zones de perméabilité structurale accrue lors de l'épisode de déformation. Les zones pressentant une perméabilité structurale dans un contexte de surpressurisation des fluides peuvent indiquer les conduits potentiels empruntés par les fluides minéralisateurs. La méthodologie présentée s'appuie sur les observations structurales pour définir un déplacement dans le modèle. Cette méthodologie permet de définir une carte de potentiel en trois dimensions et de cibler les zones par où les fluides minéralisateurs auraient circulé en respectant les observations de terrain.

La modélisation de la déformation s'est effectué sur un segment choisi d'une faille d'importance crustale archéenne sur un secteur d'environ 11.75 x 7.2x 1 km en utilisant un code d'élément fini intégré au géomodelleur Gocad et développé par Muron (2005). La méthodologie choisie tient compte des hétérogénéités lithologiques des observations structurales de terrain. Des vecteurs et des champs de déplacement sont attribués à chaque discontinuité structurale en fonction des observations effectuées sur le terrain.

3D Strain Modeling Driven by Field Data in the Vicinity of the Cadillac Larder Lake Fault Zone: Insights on Archean Orogenic Gold Distribution

Olivier Rabeau
Université du Québec en Abitibi-Témiscamingue, Unité de recherche et de services en technologie minérale, 445 boul. de l'Université, Rouyn-Noranda, QC, Canada, J9X 5E4, Tel: (819) 354 4514 #248; Fax: (819) 354 4508 - olivier.rabeau@uqat.ca

Marc-Olivier Titeux
CRPG, Centre de Recherche Pétrographique et Géochimique, Nancy Université, BP 20, 54501 Vandœuvre-lès-Nancy Cedex, France - caumon@gocad.org

Michel Jébrak
UQAM, Université du Québec à Montréal, Département des Sciences de la Terre et de l'Atmosphère, 201, avenue du Président-Kennedy, PK-615,1Montréal, QC, Canada, H2X 3Y7 - michel.jebrak@uqam.ca

Jean-Jacques Royer
CRPG, Centre de Recherche Pétrographique et Géochimique, Nancy Université, BP 20, 54501 Vandœuvre-lès-Nancy Cedex, France - royer@crpg.cnrs-nancy.fr

Guillaume Caumon
CRPG, Centre de Recherche Pétrographique et Géochimique, Nancy Université, BP 20, 54501 Vandœuvre-lès-Nancy Cedex, France - caumon@gocad.org

Alain Cheilletz
CRPG, Centre de Recherche Pétrographique et Géochimique, Nancy Université, BP 20, 54501 Vandœuvre-lès-Nancy Cedex, France - cheille@crpg.cnrs-nancy.fr

Key Words: Orogenic gold, 3D Geomodeling, Finite element method, Cadillac-Larder Lake Fault, Strain modeling

3.2 Abstract

The use of numerical modeling for the prediction of epithermal deposits can be a valuable tool for the exploration community. The proposed approach will provide an assessment of the potential in orogenic gold mineralization for areas in the vicinity of Archean crustal scale fault zones. The methodology presented uses a finite element method to model the geomechanical reaction of a rock mass to displacements along fault zones. Movements along faulted discontinuities are parameterised based on field interpretations. A 3D strain analysis is then performed on the rock mass to identify zones in dilation during deformation. These zones are taught to represent potential l fluid focussing areas. The realistic three dimensional approach coupled with the use of field data highly contributes to reduce risk linked to an exploration campaign.

The methodology is tested on a 11x7x1 km segment of the Cadillac Larder Lake Fault. The Results provide valuable insights on the spatial distribution of structural permeability near a major Archean fault zone during the phase of deformation that led to the formation deposits. The distribution dilatant sites found through the geomechanical modeling is compared with the location of known gold deposits and to the location of sites enriched in carbonates to validate the different models tested and the methodology.

3.3 Introduction

As other epigenetic hydrothermal deposits, orogenic gold deposits (Groves et al., 1998) are generated by the circulation of enormous quantities of fluids. Economical concentrations of metals imply that the fluid flow has to be focused in restrained zones. These critical emplacements are fundamentally determined by permeability variations (Cox et al., 2001). In the case of orogenic gold deposits within Archean greenstone belts, the fluid flow is mainly focused in fault zones (Weinberg et al., 2004) since the host lithologies typically have low primary permeability. In a regional perspective, the main spatial control on deposit distribution is crustal scale fractures within Archean greenstone belts. These major structures acted as conduits that channel deep seated hydrothermal fluids (Goldfarb et al., 2001) (Groves et al., 2003); Kerrich et al., 2000). Some orogenic deposits are directly hosted within crustal scale faults but most of the gold endowment in Archean greenstone belts is located within adjacent second- and third-order faults that are believed to be more appropriate dilatational sites to host deposits (Eisenlohr et al., 1989). Even tough a strong structural control is well established for orogenic gold deposits (Robert et al., 2005), their distribution remains heterogeneous and difficult to foretell since permeability distribution is dependant on a combination of complex factors such as, rock rheology, geometry of the rock formation, fluid properties and stress.

The spatial association of orogenic gold mineralizing systems with structural features combined with the fact that they are formed at the end of a tectonic event implies that deformation induced permeability or structural dilation are a critical controls for fluid focusing and ore formation. The ability to predict structural permeability during deformation taking into account rock properties at a regional scale can lead to promising gold exploration targets in the vicinity of crustal scale fault zones.

In a compressional regime, fluids migrate from localities of high pressure to dilatational sites. The main objective of this work is to obtain a 3D distribution of dilatant zones during deformation trough and near a major Archean fault zone using field observations. These dilatant sites can be interpreted as potential fluid focussing environments. Field observations will mainly be used to construct a 3D representation of a segment of a major Archean fault zone and to determine the movements of structural blocs. The response of the rock mass to these displacements will be calculated with a geomechanical approach considering the heterogeneous rock properties. These results will afterwards be used to interpret the possible pathway of auriferous fluid flow following the distribution of structural permeability. The validation of this distribution will be done by testing the spatial association with a database of compiled gold assays and alteration indexes. The results will shed light on the main controls on the distribution of orogenic gold mineralizations and hydrothermal fluid circulation near crustal scale fault zones in Archean Greenstone Belts

This study focuses on the Cadillac–Larder Lake Fault (CLLFZ; Fig. 3-1) located in the Abitibi Subprovince of the Superior province which is a typical example of a large transcrustal fault zone that controlled the hydrothermal evolution of a large portion of continental crust. This fault hosts many world class mining camps (>100 Mt) such as Val-d'Or, Malartic, Cadillac, Larder Lake, Kirkland Lake and Matachewan (Poulsen et al., 2000).

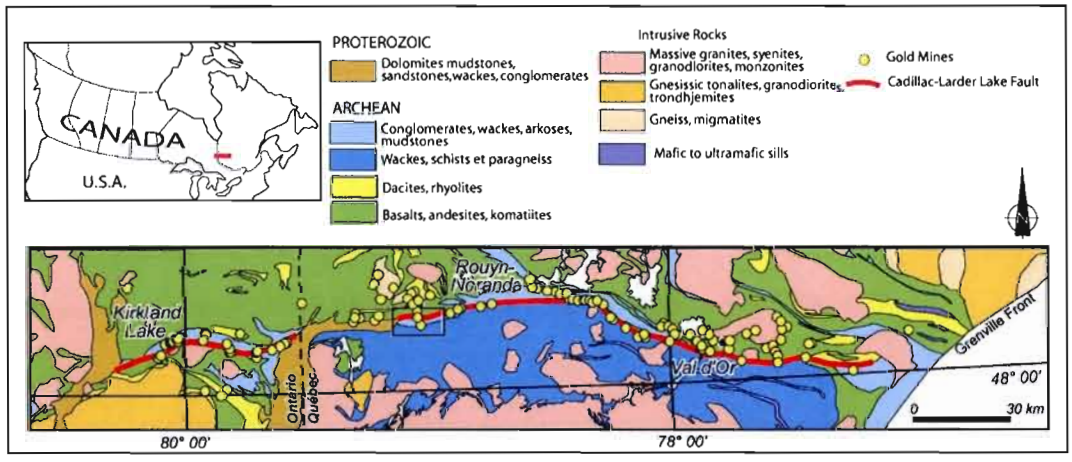

Figure 3-1: Simplified geological map along the Cadillac-Larder Lake Fault Zone (CLLFZ) showing the location of past and present gold mines.

3.4 Geological Setting

The 25 x 10 km study area is situated along the Cadillac Larder Lake Fault Zone which represents the limit between the Abitibi and the Pontiac Subprovinces (Dimroth et al., 1982; Couture et al., 1996; Thurston et al., 2008b) lying respectively north and south of the fault zone (Fig. 3-1). The part of the Pontiac Subprovince within the study area is mainly composed of highly folded and deformed turbiditic sedimentary rocks (< 2685 Ma; Davis, 2002) containing some horizons of mafic to ultramafic volcanics and cross-cutting syenite and granite. The Abitibi Subprovince contains mostly volcanic rocks ranging in composition from komatiite to rhyolite. The volcanics present in the study area are part of the Blake River Group. An age of 2701 Ma was reported for rocks of the Blake River Group near the study area (Lafrance et al., 2005; McNicoll et al., 2008).

The Piché Formation is composed of ultramafic to mafic volcanic rocks wedged within the CLLFZ. The Archean sedimentary rocks adjacent to the CLLFZ are part of the Timiskaming Group and composed of unsorted polygenic conglomerates, sandstone and local interdigitation of alkaline volcanic rocks (2677 to 2670 Ma; Corfu et al. 1993, Davis, 2002,). Many dykes and sills of gabbroic to dioritic composition crosscut the study area. Their relative age suggests a synvolcanic to syntectonic emplacement (Mueller et al., 2008; Thurston et al., 2008a). Minor

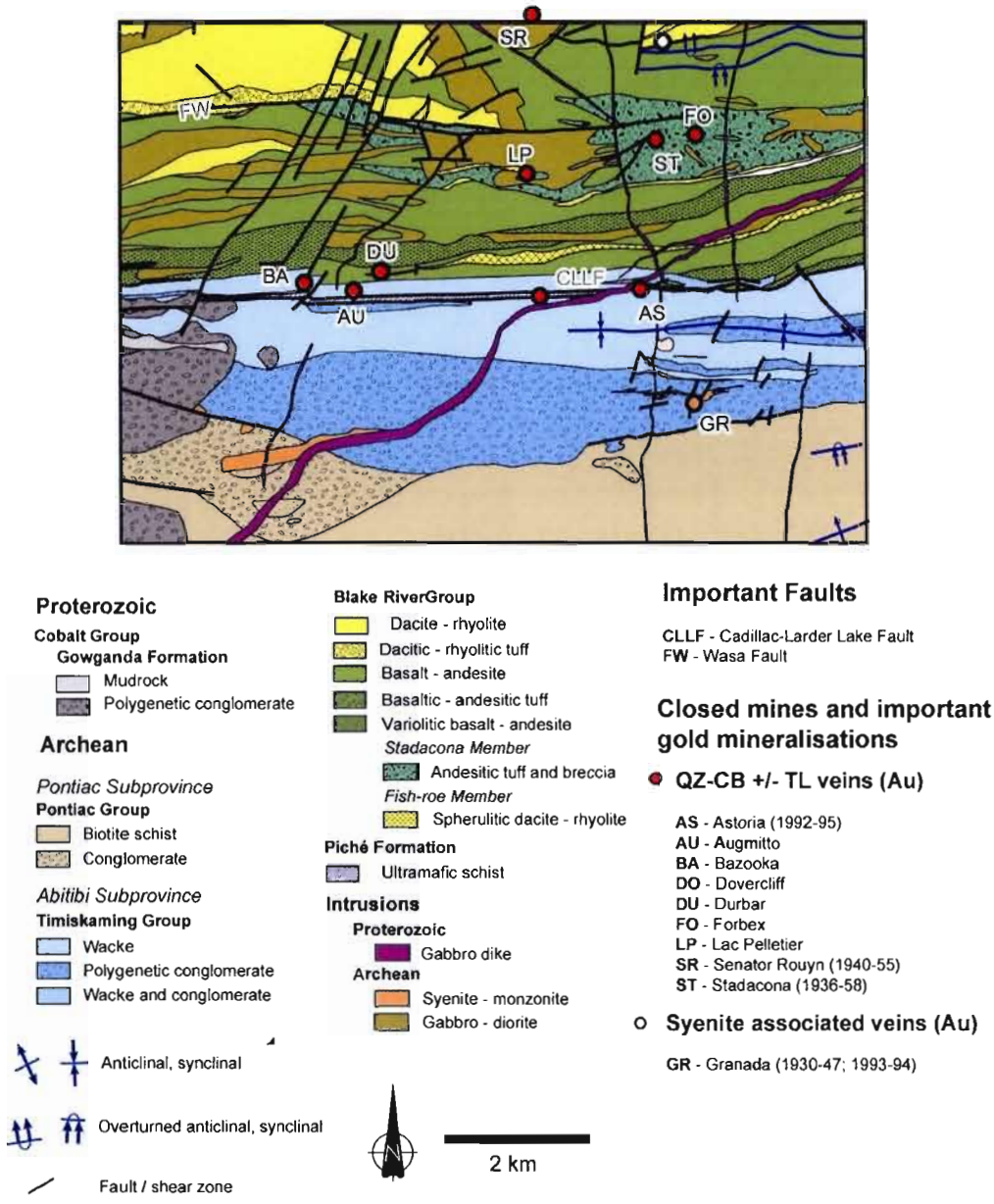

Figure 3-2: Geological map of the study area (modified from Rabeau et al., 2009 and Legault and Rabeau, 2007)

alkaline and cal-alkaline intrusions are observed on both sides of the CLLFZ. An age of 2685 to 2672 Ma was found for certain of these intrusions (Corfu et al. 1989, Davis, 2002).

Proterozoic sediments of the Gowganda Formation (2288 Ma; Fairbairn et al., 1969) at the base of the Cobalt Group lie unconformably on the Archean basement in the western and central part of the study area. This formation consists mainly of a basal conglomerate overlain by wackes, mudstones and sandstones which mask the CLLFZ and the Archean basement for over 30 km. Two inliers in the Cobalt Group expose the Archean basement in the central part of the study area (Legault and Rabeau, 2006). All Achean rocks are crosscut by N-S and N-E trending Proterozoic diabase dikes.

3.5 Tectonic evolution and timing of gold mineralizations

The tectonic evolution of the study area is associated with numerous events of thrusting and dextral transpression (Daigneault and Mueller, 2004; Robert et al., 2005). Figure 3-3 synthesises the main tectonic events in relation with the geological units and gold mineralizing events for the study area. The first episode of deformation D1 (2685 Ma) occasioned early folding, tilting and local thrusting (Robert et al., 2001). The 2677 to 2670 Ma fluvial-alluvial Timiskaming Group was deposited on

an unconformity as a result of uplift. This episode was followed by a North-south shortening, the main period of deformation D2 which is responsible for the East-west trend of the lithological units (Robert, 2001). The D2 compression progressed in a dextral transpression D3 which is identified by a sub-horizontal lineation on the principal deformation corridor, the CLLFZ.

Four different types of gold mineralizations have been recognized near the study area (Rabeau et al. 2009; Legault and Rabeau, 2007): (1) Gold-rich quartz-carbonate ± tourmaline ± sulphides constitute the most represented type (70 %). Typical examples are the Stadacona and Astoria mines (Couture, 1996). (2) Replacement type deposits (~20 %) are associated with a strong pervasive albite/sericite, carbonate alteration and disseminated sulphides. The Francoeur and Wasamac deposits (Couture and Pilote, 1993) are representative examples. (3) Mineralization spatially associated with syenitic intrusions (~5%) includes two subtypes: *quartz-carbonate veins* such as the Granada Mine (Couture and Willoughby, 1996) and in a lesser manner disseminated sulphides enriched in Au-Cu (Couture and Marquis, 1996; Legault and Lalonde, in prep.). (4) Volcanogenic massive sulphide (VMS) deposits related polymetallic mineralization (~5%) are also encountered in the study area (Legault and Rabeau, 2007).

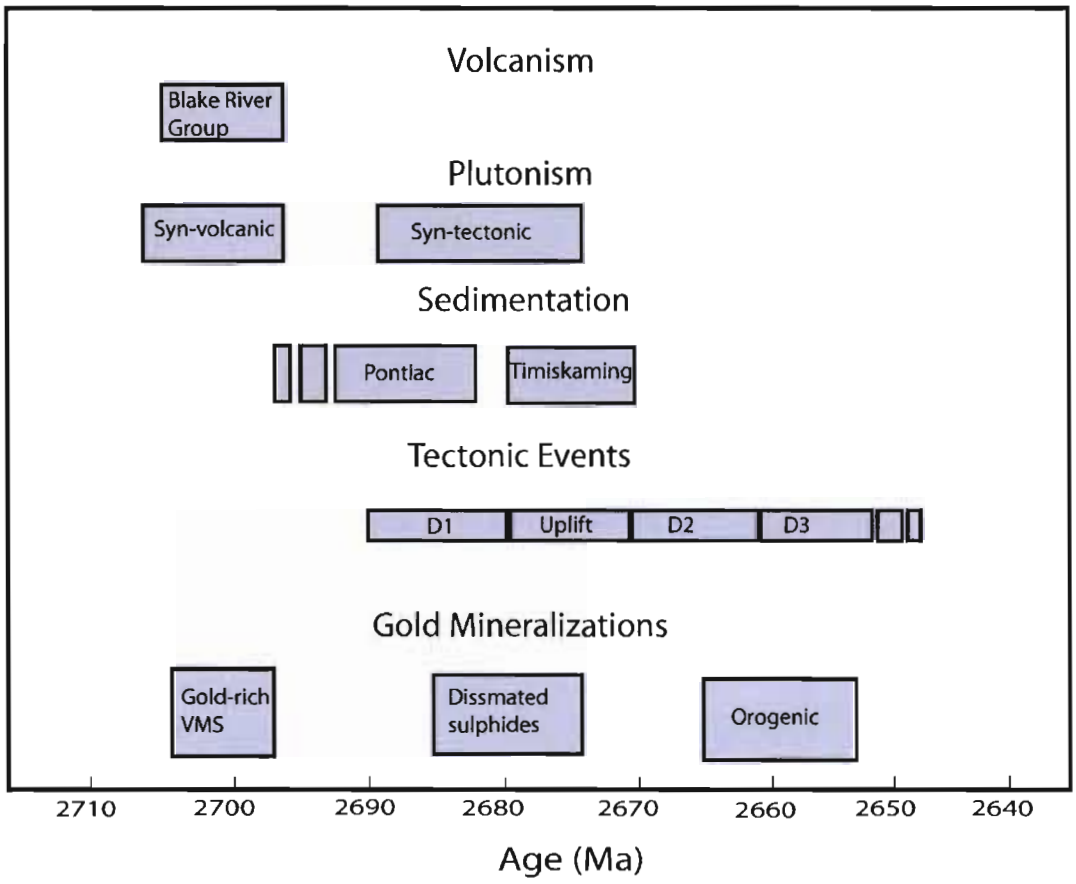

Figure 3-3: Timing of rock formations, tectonic events and gold mineralizations within the study area

Most of the gold mineralisation considered in this study belongs to a broad class of orogenic gold deposit type. The quartz-carbonates vein, replacement and veins associated to syenite types fit with this definition. These deposits are characterized by epigenetic, structurally controlled mineralization located in accretionary orogens that formed over a large crustal-depth range from deep seated fluids (Groves et al.,

1998). Orogenic type gold mineralizations are deposited by the circulation of a low salinity H_2O-CO_2 ± CH_4 ± N_2 fluid which transported the gold as a reduced sulphur complex (Groves et al., 2003). They are considered to post-date regional metamorphism, plutonism and early phases of orogenic deformation (Groves et al., 2000; Goldfarb et al. 2005). In the case of the southern Abitibi belt, orogenic gold deposits are believed to have formed at the end of the second thrusting event during the late dextral transpression (Robert et al., 2005) post-dating the formation of VMS type and disseminated sulphides gold deposits (fig. 3-3).

3.6 Geomechanical modeling

Hydrothermal ore formation is governed by fluid circulation. At greenschist facies rock permeability is low and fluids are over-pressured, the role of rock deformation is predominant in the hydraulic gradients that affect fluid flow (Oliver, 1996). The location of low stress zones or dilation zones is crucial for gold-bearing fluid circulation and focussing. Numerical techniques were developed over the years to study epigenetic ore deposits by modeling possible fluid pathways during deformation. Three types of approaches have been used to in the study of the distribution of structurally induced permeability and potential fluid flow by the use of numerical modeling. Table 3-1 outlines the main differences between these methodologies and the approach proposed in this paper. These methodologies focus

	Stress – Transfer Modeling	UDEC/ TRIDEC Paleo - stress	FLAC/ FLAC3D	Strain Modeling
Code	Finite element code	Finite difference code	Finite difference code	Finite element code
Stress Input	Slip movement along a designated fault	Regional Stress Field	Regional Stress Field	Displacements
Third Dimension	3D	2D/3D	2D/3D	3D
Material properties	Poro-elastic homogeneous	Elastic or elasto-plastic heterogeneous	Elasto-plastic heterogeneous	Elastic Heterogeneous
Discontinuities	Friction coefficient	Friction coefficient	Friction coefficient	Displacements
Fluid flow Modeling	-	-	yes	-
Dynamic/static	Static	Dynamic	Dynamic	Dynamic
Geological representation	Regular grid	Triangles/ tetrahedrons	squares/prism	Irregular grid tetrahedrons
Output	Zones of artershock close to rupture	Low minimum stress (σ_3) or mean stress	Evaluation of the intensity and localization of fluid flow	Dilation zones ($\Delta V/V$)

Table 3-1: Comparison between geomechanical modelling approaches used to identify zones of enhanced permeability in the study of epigenetic mineralizations

on the prediction of the pathways for mineralizing fluids but proceed with different approaches and theoretical framework. This section will briefly review these

methods and will compare them with the approach proposed in this paper. For further information on these techniques, the reader is invited to consult cited references.

Stress-transfer modeling (Mickelthwaite and Cox, 2004, 2006; Cox and Ruming, 2004) has been used in 2D with success to identify transiently permeable structures that focused fluid flow during repeated aftershock ruptures. This approach relies on the assumption that the distribution of aftershocks following rupture events controls fluid pathways by increased permeability. Areas close to failure are identified by calculating the stress change from a strike-slip event along a specific fault. Stress-transfer modeling is a static methodology and considers a homogeneous poro-elastic crust.

Another approach to the study hydrodynamics during rock deformation is stress mapping which models the mechanical response of a discontinuous jointed or fractured rock mass exposed to a regional stress field. This methodology considers area of low-minimum principal stress (σ_3) and low-mean stress (σ_m) during deformation as indicators of dilation and potential sites of fluid focussing (McLellan and Olivier, 2008). Most of these works were done using the UDEC (Universal Distinct Element Code; Itasca, 2000) or its three-dimensional version 3DEC. This method has efficiently been be used efficiently to target structurally controlled mineralizations at mine scale in regional studies in 2D (Jiang et al., 1997) Mcllelan and Olivier et al., 2008; Faure, 2003), on cross-sections (Mair et al, 2000) and at mine scale in three dimensions (Holyland, and Ojala 1997)

FLAC (Fast Lagrangian Analysis of Continua) is a finite difference code designed for the modeling of porous media. FLAC, or its 3D version FLAC3D, allows the coupling of fluid flow and deformation under a stress field. This approach has been used in 2D by Olivier et al. (2001) in the Mary Katleen U-REE deposit and at regional scale in the Mount Isa region. Potma et al. (2008) used this approach in three dimension for orogenic gold deposits in Stawell (Victoria) and Kundana (Western Australia).

3.6.1 3D Strain Modeling

All methodologies presented above except for Coulomb stress-transfer modeling compute the response to a rock mass to a regional stress field. These approaches imply an estimation of the magnitude and orientation of the regional stress field. This estimation has critical implication for the modeling process and is very difficult to perform. In fact, the stress field can induce movements along structural discontinuities that do not concord with field observations. Furthermore, in paleo-stress modeling and FLAC, movements along structural discontinuities are governed by friction and cohesion parameters. These parameters are very complicated to estimate since literature is very sparse on the subject. Potma et al. (2008) and others have addressed the problem by an iterative approach. The method presented allows avoiding external constraints and attributing fault geomechanical parameters implying a more realistic movement of structural blocs that respects structural

observations. Strain modeling is based on 3D geomechanical modeling which relies on a displacement vector or displacement field implying that structural field observations are accommodated for each discontinuity (faults or contacts). The strain is then calculated a by finite element code within the rest of the modeled study area according to the displacement imposed.

As strain modeling, stress transfer modeling relies on an evaluation of displacement from a slip event. This displacement is only entered for a predetermined fault and the static transfer is then calculated through the rest of the modeled area...In strain modeling, the displacement can be entered for numerous faults at the same time. Furthermore, stress transfer modeling makes the assumption that the studied rock mass encloses lithologies with homogeneous mechanical properties as opposed to strain modeling which allows the modeling of an heterogeneous rock mass.

The geomechanical modeling is performed in the Gocad software package using the Restoration Suite plug-in (Muron, 2005) recently modified by Titeux (2009). This software uses a grid representation named the solid models (Lepage, 2003) to model deformation. A Solid represents a volume composed of tetrahedrons divided in regions. The Solid model is composed of 0D (points), 1D (lines), 2D (surfaces) and 3D (volumes) regions. Each of these regions is paired, for example, the 2D region representing the CLLF is represented by 2 surfaces, a slave and a master. Both of these surfaces have four 1D regions (borders) also paired as master and a slave line

and so on. The slave region always moves on the master region. The Restoration suite relies on the finite-element method which consists in the division of a complex physical system in a number of more simple discrete elements corresponding to different material property is used to solve mechanical equations. This software was developed for the petroleum industry where it is mainly used for backward structural modeling also known as structural restoration. This study utilizes this technology in a context of forward structural modeling meaning that the movement of structural blocs is continued correspondingly as the last phase of deformation.

The proposed approach allows regional study in a realistic three dimensional model. As opposed to a 2D environment, the 3D approach offers the benefit of considering dips and more complex block movements and the irregular tetrahedral representation allows a realistic rendering of discontinuities compared to a regular grid composed of cells. Furthermore, the 3D representation offers a better distance calculation during the measure of spatial association with gold grades and alteration indexes.

3.7 3D Geological Model and Strain Modeling applied to the CLLF

The geological and structural contexts of the study area are well defined (Rabeau et al., 2009; Legault and Rabeau, 2006, 2007; Daigneault et al., 2004; Couture et al. 1996) and its proximity to the prolific Rouyn-Noranda central camp provides access

to a multitude of high quality data for the sector. A 3D geological model of the study area was built by for a mineral potential study Rabeau et al (2009); the reader is referred to this paper for further details on the modeling technique. For calculation purposes, the size of the original; model was reduced and structural and lithological discontinuities were simplified. All lithologies were grouped into six rock types with contrasting mechanical properties. The rock types considered for the study are: andesite/basalt, tuff, grauwacke/conclomerate, schist and gabbro. All post-Archean lithologies were eliminated from the model since their formation post-dates the gold mineralization, these include: the Gowganda Formation sediments and diabase dykes that cross cut the study area. Their physical properties are presented in table 3-2. Faults with the most important lateral extent were considered in the model and the late North-South brittle fractures were not taken into account (table 3-3).

The resulting model has a dimension of 11.7 x 7.2 x 1 km and is composed of 6 surfaces including 2 faults (Fig. 3-4a and 3-4b). From these triangulated surfaces, a solid model containing 11 329 tetrahedrons connected by 3022 points was built for the study area. The average length of the edge of the tetrahedrons composing the solid model is 419 m. The solid model was divided in 3 3D regions (Figure 3-5) separated by the two structural discontinuities (2D regions), the Cadillac-Larder Lake Fault and the Wasamac Fault. The physical parameters of each lithology involved were assigned to the nodes composing the volume occupied by the corresponding

lithology. The attribution was made using the triangulated surfaces presented in figure 3-4.

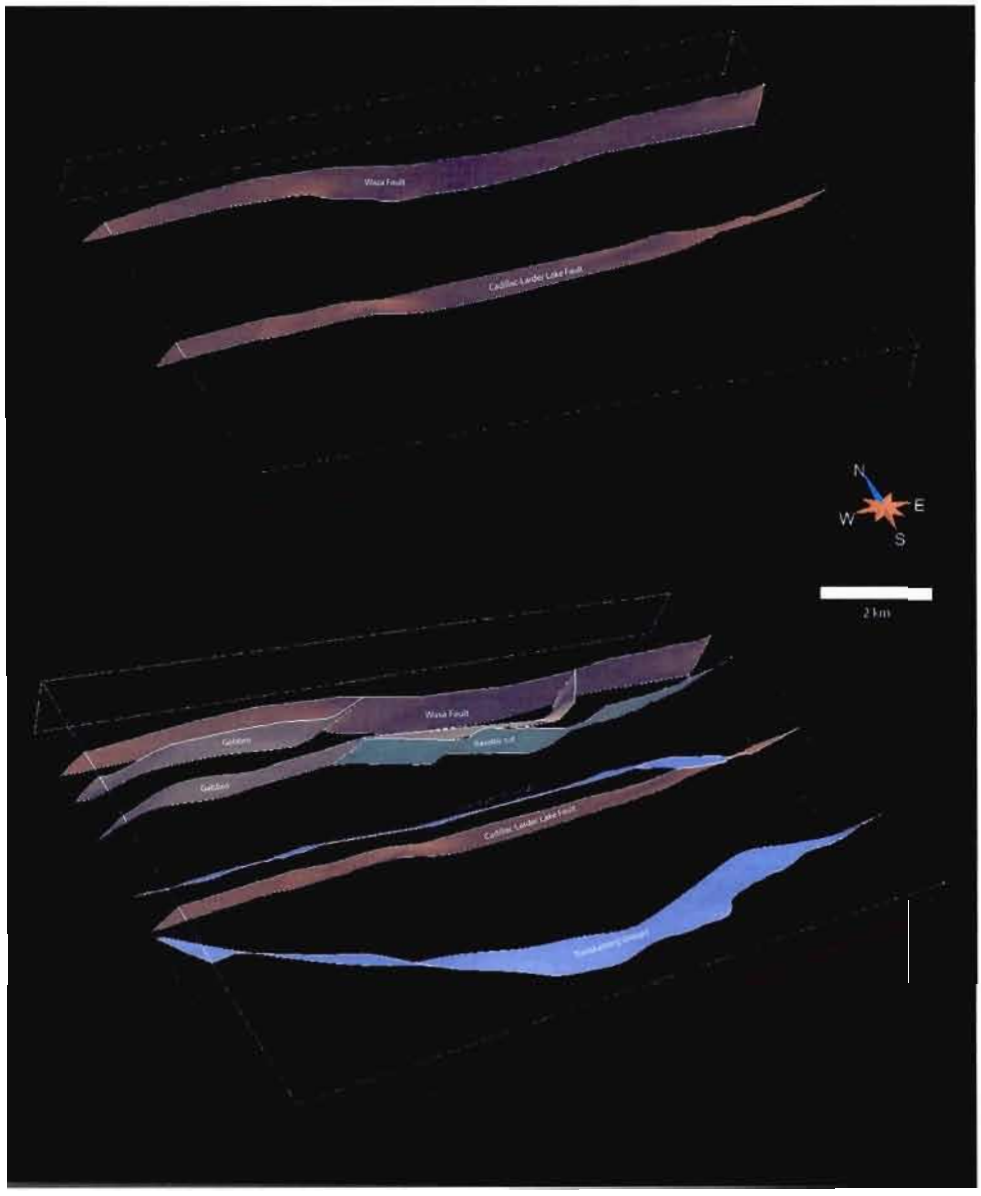

Figure 3-4: (A) Surfaces defining the structural boundaries within the geomechanical model. (B) Surfaces defining the lithological contacts shown with the Wasa and Cadillac Larder Lake Faults

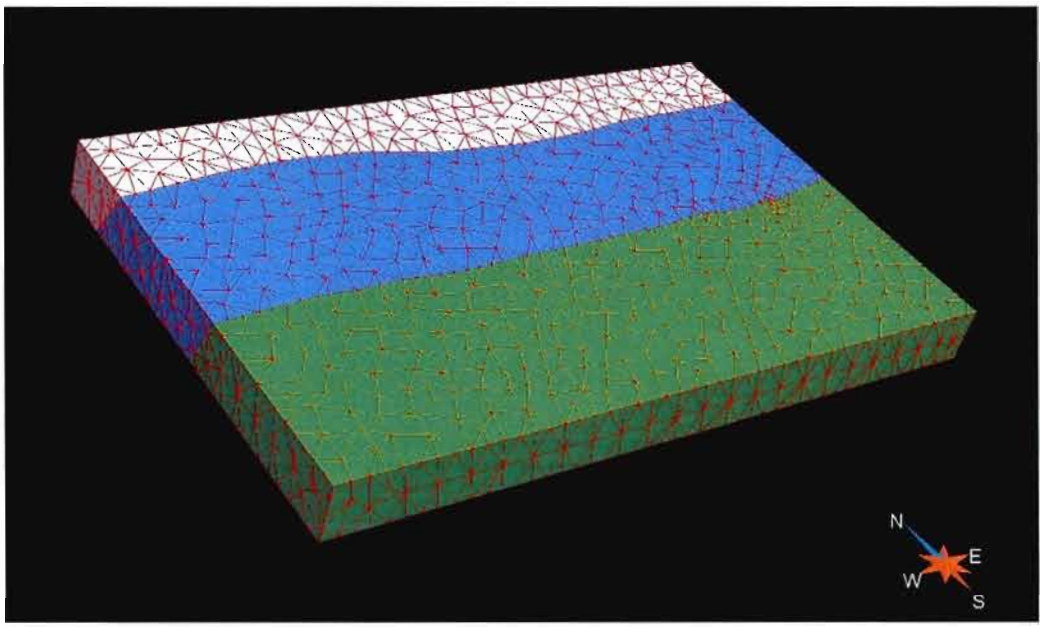

Figure3-5: Solid Model divided in 3 regions by the 2 structural discontinuities

3.7.1 Modeling parameters

All regions of the model are considered as linear, isotropic and elastic materials implying that they are regarded as obeying Hooke's Law. The mechanical properties of rocks present in the study area were calculated using the data base of the Geological Survey of Canada from which *P-wave* and *S-wave* velocities were calculated for rocks in the Abitibi Greenstone Belt. The depth system is about 10 km since regional metamorphism is at the green schist facies (Jolly, 1978), considering

that mechanical properties vary with pressure, all properties were evaluated at 200 MPa. Mechanical properties also vary with temperatures but the data was unavailable for the lithologies involved in this model. The parameters available still allow the production of a realistic model.

Rock Type	ρ (Kg/m^3)	E (GPa)	σ	λ	μ	K
Andesite/basalt	2.82	93.05	0.26	39.78	37.00	64.45
Diorite/Gabbro	2.90	104.47	0.23	38.20	42.32	66.42
Grauwacke / conglomerate	2.73	80.51	0.26	35.17	31.93	56.45
Biotite Schist	2.75	76.06	0.22	25.38	31.05	46.08
Mafic Tuff	2.79	96.62	0.22	30.73	39.65	57.16

Table 3-2: Mechanical properties of the different rock types present in the model. ρ = density, E = Young modulus, σ = Poisson coefficient, λ = Lamé's constant, μ = Shear modulus, K = Bulk modulus

Strain modeling approach is based on structural field observations; movement is imposed based on the last movement recorded by cinematic indicators on faults. The distance of displacement also has to be evaluated for each fault and is a critical parameter. The evaluation of the amount of displacement along each fault is the most

challenging parameter to determine. Two faults will accommodate the movement by imposing displacement fields on the model: the Cadillac-Larder Lake Fault and the Wasa Fault. The direction of each displacement observed along each fault is presented in table 3-3. The main indicators on the Wasa fault (steeply dipping lineations) suggest an inverse movement while the main movement on FCLL is a dextral shear seen by subhorizontal lineations.

Tectonic regime	***Faults***	***Movement***
Transition between D2 and D3	Cadillac-Larder Lake Fault[1,2,3]	Dextral subhorizontal shear (**+X, ØY, ØZ**)
	Wasa Fault[2]	Inverse (**ØX, -Y, +Z**)
D2 compression	Cadillac-Larder Lake Fault[1,2,3]	Inverse (**ØX, -Y, +Z**)
	Wasa Fault[2]	Inverse (**ØX, -Y, +Z**)
D3 dextral slip	Cadillac-Larder Lake Fault[1,2,3]	Dextral subhorizontal shear (**+X, ØY, ØZ**)
	Wasa Fault	--------

Table 3-3: Orientation of the displacement vector for each fault considered in the study. 1 Daigneault (1994), 2 Daigneault et al. (2002), 3 Legault and Rabeau (2009)

Metalogenic studies cited earlier suggest that the main mineralizing event is situated at the end of the compressive event and the beginning of the dextral transpression. This tectonic transition represents a process that could have extended on a long period of time. The strain modeling will be calculated for the two movements made simultaneously (inverse movement on the Wasa Fault and dextral slip on the CLLF) as if they occurred simultaneously. For comparison purposes, the strain modelling of the inverse displacement along both structural discontinuities representing the N-S compression known as D2 and and the slip event along the CLLF representing D3 were also modelled independently.

3.7.2 Boundary conditions

Each of these deformation phases have to be modeled using boundary conditions in order to obtain a solvable problem for the finite element code. Boundary conditions that are too sparse will result in model that is not kinetically admissible and with infinity of solutions. On the other hand, boundary conditions that are too constraining will block any possible deformation. Figures 3-6 and 3-7 summarize the boundary conditions used for the strain modeling of each movement.

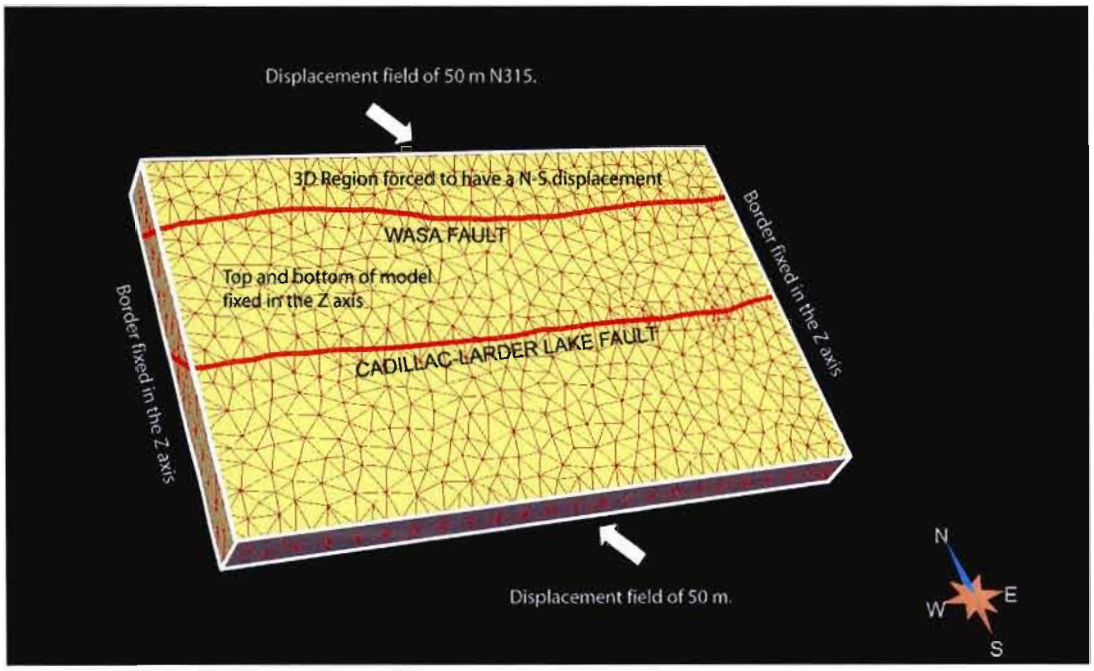

Figure 3-6: Boundary conditions applied to model the strain along the Wasa Fault and the CLLF simultaneously

At first, the transition phase between compression and slip was modeled by an inverse displacement on the Wasa Fault and the dextral slip movement along the CLLF (fig. 3-6). A displacement vector of 50 m N315 in the XY plane was fixed. The 3D region located north of the Wasa fault was forced to move in the North-South axis in order to obtain an inverse displacement along the Wasa Fault. The eastern and western borders as well as the top and bottom surfaces were blocked in the Z axis. Finally, both surfaces representing the two structural discontinuities were forced to stay together during displacement.

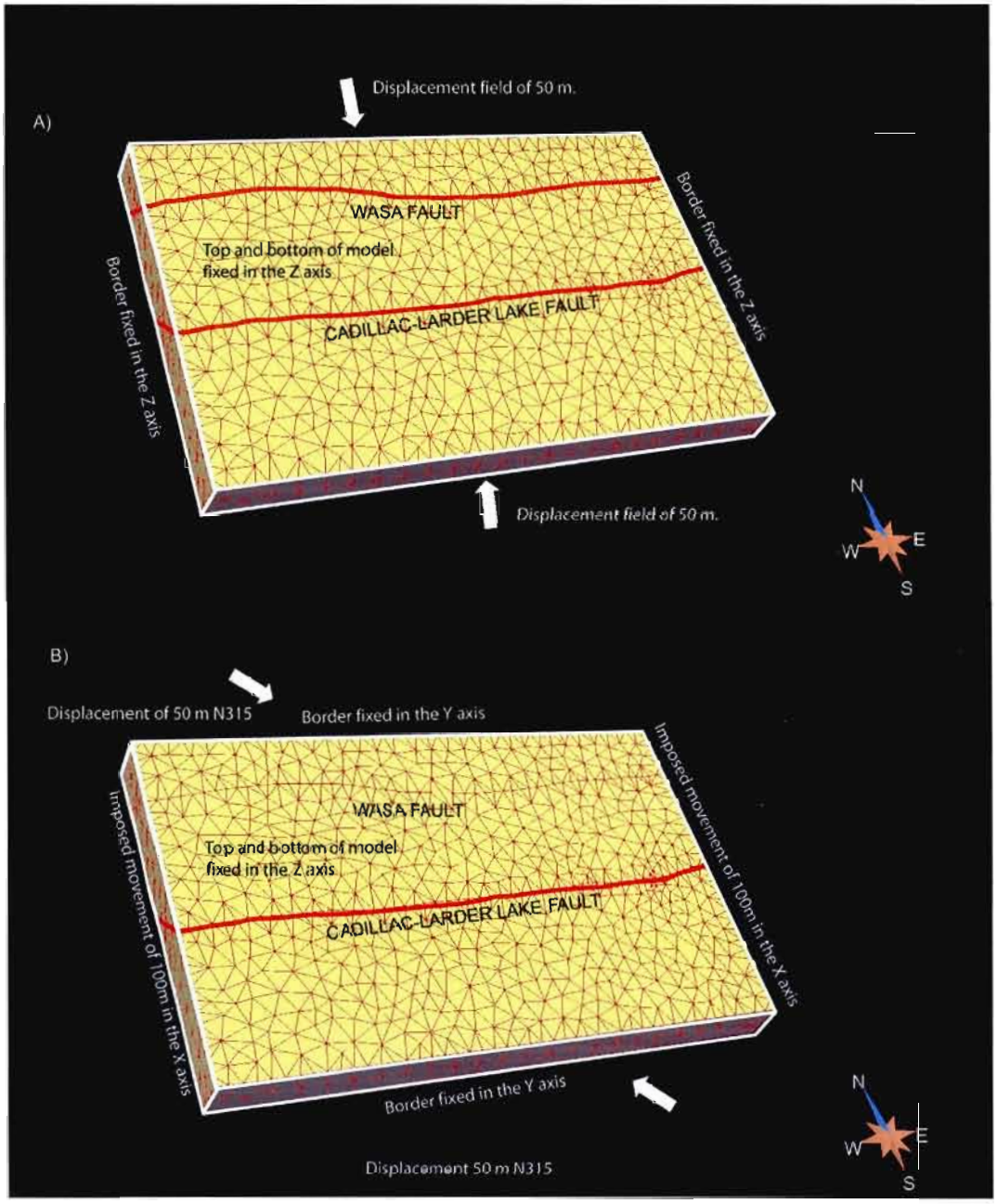

Figure 3-7: A) Boundary conditions given to model the strain in 3D for the compressive phase, B) : Boundary conditions given to model the strain in 3D for the transpressive phase

In order to better define the role of each displacement in the distribution of dilatant sites. The N-S shortening associated to D2 (fig. 3-3) was also modelled. The boundary conditions are synthesised in figure 3-7A. Both structural discontinuities were affected by this compression so a North/South displacement field of 50m was used for the strain modelling A. The top and bottom of the solid model were fixed in de Z direction meaning that movement is only allowed in the X and Y directions while the eastern and western sides were fixed in Y and Z. Finally the northern and southern borders of the models were forces to move of 50 m in opposite directions on the Y axis. A 0D region was also created from a point located on the top of the model to constraint movements in the Z and Y axis. Finally, a constraint was added to tie the slave and master surfaces together to force them to stay in contact during displacement.

As mentioned above, the last deformation phase recorded was mainly concentrated on the CLLFZ. This deformation phase, known as D3 (fig 3-3) was mainly marked by a dextral strike slip movement. The boundary conditions used for strain modelling for this deformation phase are synthesised in figure 3-7A. To model this de formation ,a displacement vector of 100 m was fixed for this important fault zone. Since only the CLLF was affected by this displacement, both of the 2D regions representing the Wasa Fault were welded together meaning that the discontinuity only acts as a competency contrast between the lithologies located on both sides. The region located south of the CLLF was fixed on all three axis. The top and bottom of the

solid model were fixed on the Z axis. The northern and southern borders were fixed in the Y axis. A displacement of 100 m was imposed on the Eastern and western borders in the positive direction of the X axis

3.8 Results

A 3D strain analysis is generated for each point of the tetrahedral model once the geomechanical modeling has been performed. From this analysis the value and direction of principal deformation can be obtained. Furthermore, zones in dilation are identified by comparing the initial volume of each tetrahedron to its volume after the deformation. The dilation is computed by subtracting the final volume to the initial volume and dividing the result by the initial volume. Each of these properties is stored in the points composing the model.

The distribution of dilation zones obtained by the geomechanical modeling can be interpreted has representing area of potential fluid focussing during deformation. In fact volume changes during deformation can be considered as zones of enhanced porosity (Ord and Olivier, 1997). In a context of over-pressured fluids, these sites are likely to focus the fluid flow. Figure 3-8 presents the spatial distribution of dilatant zones for each modeled displacement:

A) Compression on the Wasa Fault and dextral slip on the CLLF

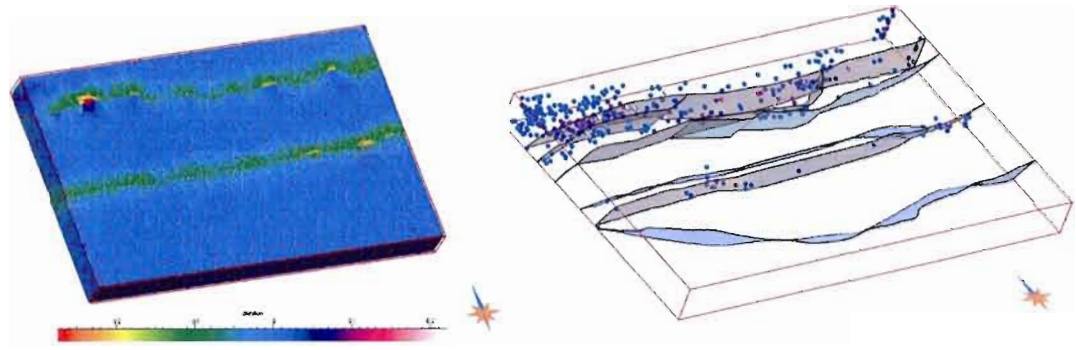

B) Compression on the Wasa Fault and the CLLF

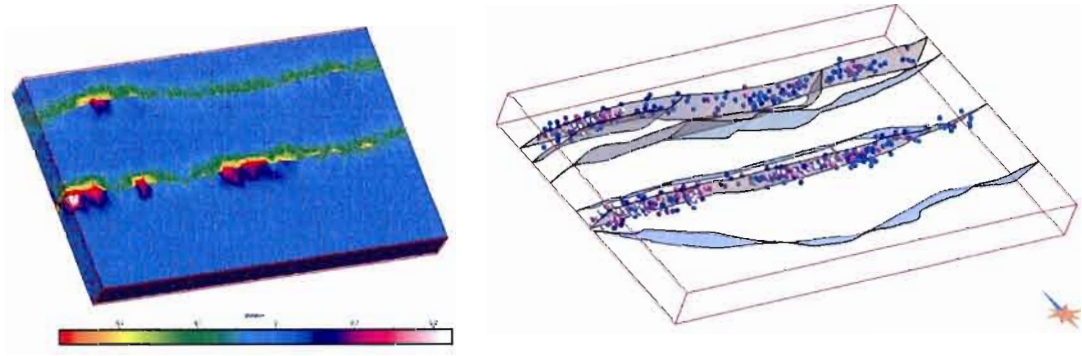

C) Dextral slip on the CLLF

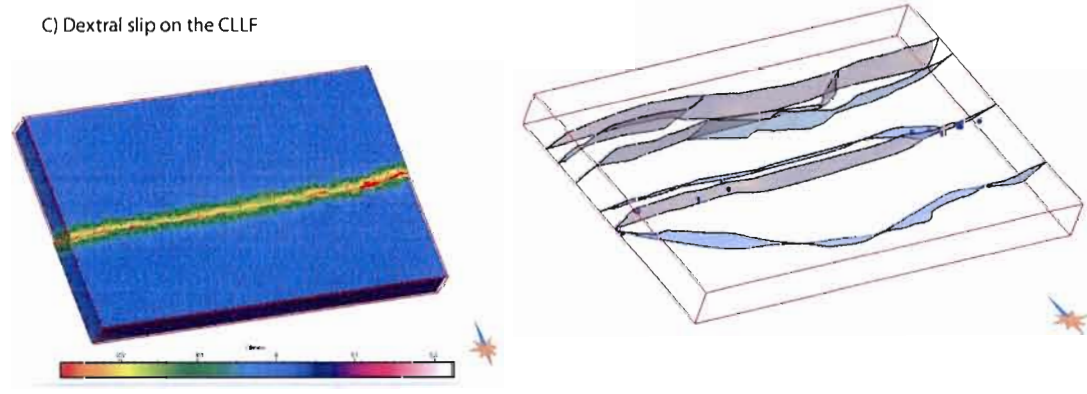

Figure 3-8: Results from the strain modelling. Each deformation phases are presented with dilation painted on the deformed solid model and by a point set

representing zones where the initial volume of the surrounding tetras increased of more than 1%. A) Strain modelling for the combination of two displacements, compression on the Wasa Fault and dextral slip on the CLLF. These movements represent the transition between the compressive and transpressive regimes (D2 and D3). B) Compression on both structural discontinuities (D2). 3) Dextral slip on the CLLF (D3).

The distribution of the dilatant zones is very different form one tectonic regime to another. The strain modeling of the transition phase between the compressive (D2) and transpressive (D3) regimes combining an inverse displacement on the Wasa Fault and a slip movement on the CLLF presents dilatational sites near both structural discontinuities (fig. 3-8). Most important dilatational sites (approaching 0.1) are located in the gabbroic unit near the Wasa Fault. In fact, the competency contrast between this unit and the ones surrounding it seems crucial in the distribution these sites. The strong concentration of dilatant sites in the north-western corner of the modeled area is interpreted as a border effect resulting form the boundary conditions that force the northern bloc to move on the N-S axis. The dilatant sites along the CLLF correspond to orientation or dip changes along the fault.

The stain modeling for the compressive phase (D2) presents a distribution of dilatant sites that is located along the two structural discontinuities. Dilatant sites are more

present along the length of the CLLF in comparison to the Wasa Fault, this could be explained by the fact that the dip of the CLLF is slightly les steep than the Wasa Fault (and average of 70 degrees N vs. 65 degrees N). Competency contrast between lithological units seems to have less influence in this tectonic regime. This could be explained by the general North-South orientation of the different units.

Finally, the strain modelling of the dextral slip presents the less dilation sites of the three phases modeled. The dilation sites correspond in general to the sites located in the vicinity of the CLLF from the D2/D3 model. Since the displacement is concentrated on the CLLF, the rest of the model almost moves as two homogeneous blocks.

3.8.1 Spatial association between mineralized sites and dilatant zones

To compare the location of dilatant sites and the location of mineralized occurrences, it is important to point out the fact that the "dilation" property is stored and exposed in the nodes joining the tetrahedrons which have borders with a 400 m mean length. This implies that the node presents a mean of the tetrahedrons surrounding it. Further more, the deposits used to test the spatial association are represented by points of about 150 m, the majority of these deposits have a bigger lateral extent.

The Granada site was not predicted by any episode of strain modeling (Fig. 3-9). This can be explained by the fact that this gold deposit is intimately associated to a

syenitic body (Couture et al., 1996) which was too small to be modelled in the present work The competency contrast between the syenite and the surrounding Temiskaming sediments is most likely to have caused fracturation which is responsible for the location of this deposit. The Durbar deposit is also outside of the prediction zones of all three models. This deposit is located near a small E-W fault which was not taken into account in the model construction phase. The absence of this fault within the model could explain the absence of dilation zones on this site.

From the modeled deformation phases, the transition between D2 and D3 seems to present the best spatial association between known mineralized occurrences and the position of dilatant sites (fig. 3-9A). The location of dilatant sites distribution in the model is within a less than 500m of the location of the Bazooka, Augmito, Lac Pelletier Forbex and Stadaconna sites. The compressive deformation phase also presents a good match between the location of dilatant sites and the emplacement of known orogenic type gold deposits but it fails to predict the Lac Pelletier deposit since the dilation zones associated to the modeling of this deformation phase are concentrated along the two fault zones. Finally, the simple dextral slip only the Bazooka deposit is located less than 500 m away of a dilatant site which makes it the least predictive of all three models.

In the case of orogenic gold deposits, the mineralizing fluid is a low-salinity CO_2 rich aqueous solution (Ridley and Diamond, 2000). The main evidence of a CO_2 rich hydrothermal fluid circulation is the presence of carbonates. A normative mineral

alteration index using major elements chemistry (NORMAT; Piché and Jébrak, 2007) was used to evaluating the carbonate content of 2463 whole rocks analysis. Figure 3-10 presents the samples presenting an IPAF alteration index of more than 50 (on a scale of 0 to 100) with zones of more than 1% volume change when performing stain modeling of the transition phase. When looking at this figure, the reader must keep in mind that the location of whole rock analysis where not equally distributed in the study area. Most of the samples were taken in the Blake River Group north of the CLLF. With this information in mind, the top view of the study area exposes a fairly good correspondence between the high IPAF values and the dilatant sites.

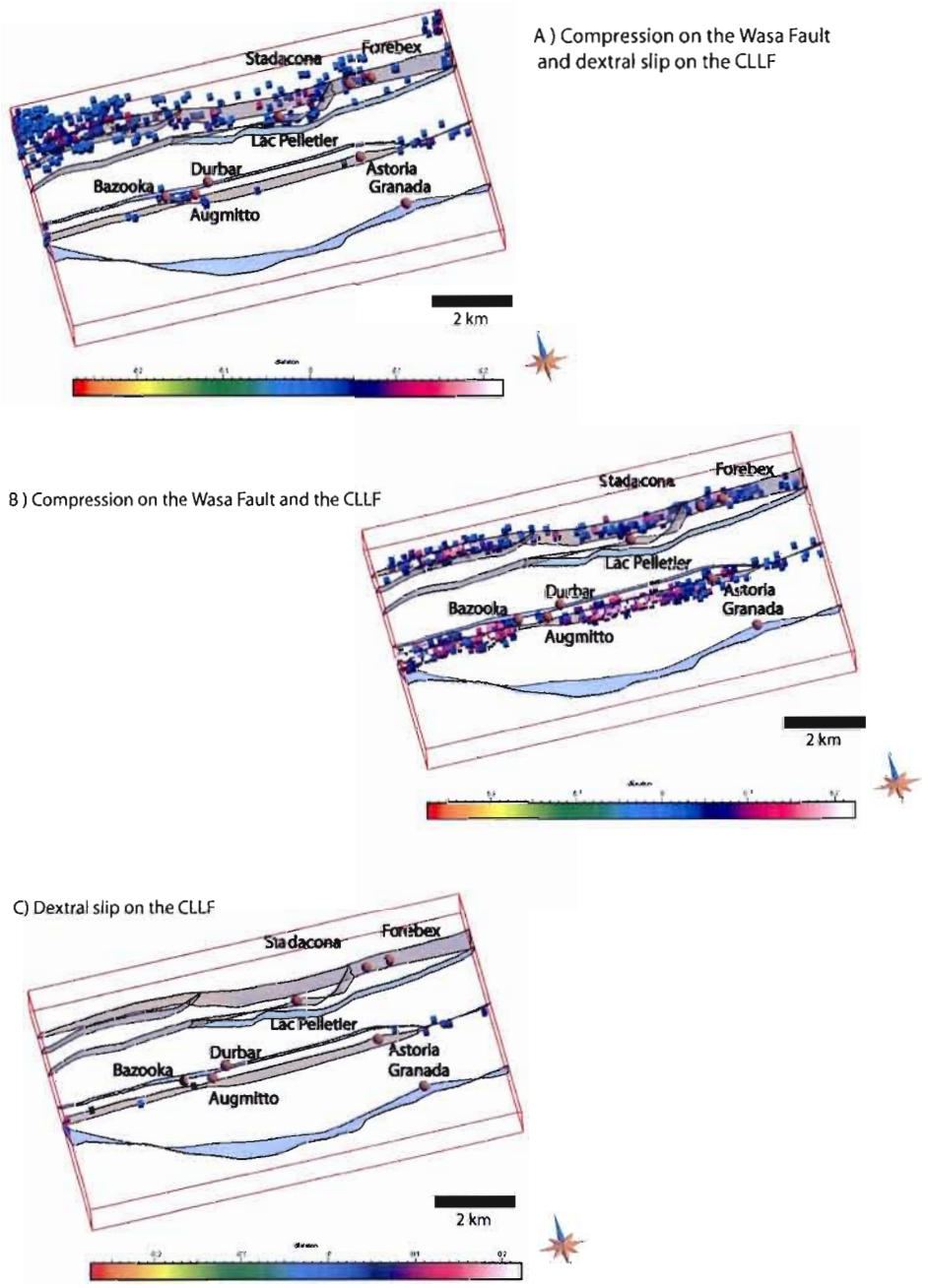

Figure 3-9: Correspondence between the important orogenic gold mineralizations located within the study area (red sphere) and the dilatant sites of each deformation phase modelled.

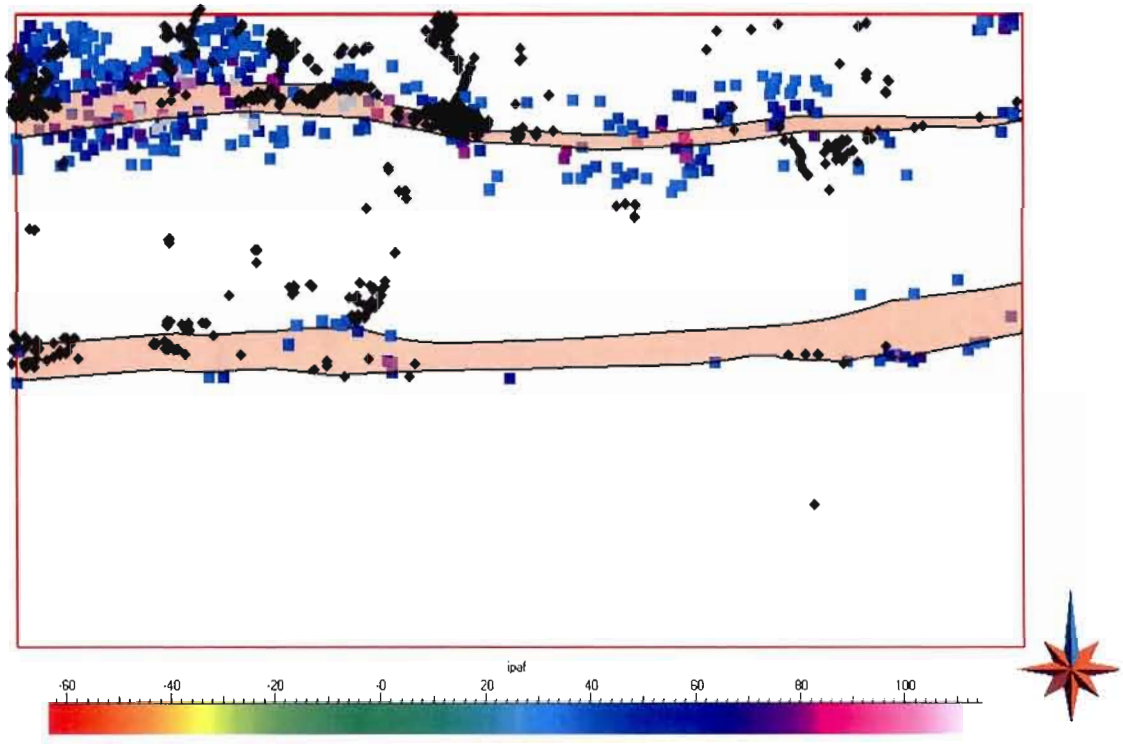

Figure 3-10: Distribution of IPAF (Piché and Jébrak, 2007) values of more than 50 (black diamonds) with zones of more than 1% volume change when performing strain modeling of the transition phase (cubes).

3.9 Discussion

The methodology presented in this paper can be perceived as a valuable regional exploration tool that takes into account structural field observations. It allows the modeling of strain while respecting displacements observed along structural discontinuities. The use of this methodology requires a very detailed knowledge of

the geology and 3D geometry of the units hosting the gold deposits. Furthermore, it requires a thorough structural analysis of the sector since the methodology relies on field observations.

The results presented above, confirm the strong structural control on the location of orogenic type gold deposits. In fact all the main dilatant sites identified are located along fault zones. The results of this study are also in agreement with most of the literature on orogenic gold deposits in terms of timing. In fact, the best match between the location of known orogenic gold deposits or zones enriched with carbonates and dilatant zones is obtained when performing strain modelling with a dextral slip on the CLLF and an inverse movement on the Wasa Fault. These displacements can be associated to o the transition between the D2 compression and D3 transpression which represents the tectonic phase associated to these mineralizations (Robert et al. 2005).

3.9.1 Limitations:

The use of a modeling approach implies a simplification of reality and assumptions on certain parameters in order to be able to perform calculations on strain distribution. An important geological assumption made in strain modeling concerns the relative timing of orogenic gold mineralizations within the southern Abitibi belt. The use of this computer based methodology involves that observable faults and

lithologies were present with a similar geometry during the main mineralizing event and that all of the present structural features where active during the last phase of deformation. As mentioned earlier, most orogenic type gold mineralization postdates major tectonic event, at local scale, displacement may be observed on ore but at regional scale the displacement should be minor. It has been argued (Goves et al., 2003; Goldfarb et al., 2001) that the relative late timing of orogenic gold deposits in terms of tectonic evolution implying that the present structural geometry within the host terranes approximates that at the time of gold deposition.

Modelling natural objects also implies many simplifications. For instance, all the 3D regions of the model are considered as linear, isotropic and elastic materials implying that they are regarded as obeying Hooke's Law. Further more, no fracturation where taken into account and deformation is modeled as happening in a single event. Finally, fluid pressure and its potential influence on strain repartition were not considered in this study.

This methodology also assumes that overpressurized fluids will circulate in dilatant zones. As in stress mapping or stress transfer modeling, the methodology presented here does not offer a quantification of fluid flow nor consider the influence of fluid pressures on deformation and strain repartition. Furthermore, many factors other than the location of dilatant sites have a significant influence on the spatial distribution of orogenic gold deposits. Even if hydrothermal fluid circulation is critical for the

formation of orogenic gold deposits near crustal scale fault zones, the distribution of these deposits also depends on factors such as chemical reactions that are not considered in this approach.

3.10 Conclusion

The work presented in this paper confirms that 3D geomechanical modeling can be a valuable tool for the prediction of the location of epithermal deposits and for diminishing exploration targeting risks. The proposed approach based on structural field observations has proven useful to predict the location of most known deposit in the sector as well as evidence of hydrothermal activity by locating dilatant zones during the deformation phase that is contemporaneous to gold emplacement.

Furthermore, the approach presented allowed to confirm certain facts on orogenic gold mineralizations. The methodology was tested on a segment of the Cadillac-Larder Lake Fault by modelling three tectonic regimes: NS compression, dextral slip and the transition phase between compression and slip. The transitional phase was confirmed as being the most likely to be contemporaneous to orogenic gold type mineralizations. In terms of implications for the distribution of orogenic gold deposits, the study confirms the strong structural control on these deposits.

3.11 Acknowledgements

This research has been funded by the Divex Fund and the Fondation de l'Université du Québec en Abitibi- Témiscamingue. We acknowledge the help of Jean Goutier (Ministère des Resources naturelles et de la Faune du Québec) and Marc Legault (CÉGEP de l'Abitibi-Témiscamingue) through very useful discussions. We also would like to thank Gilles Bellefleur of the Geological Survey of Canada for providing us with part of the physical properties needed for this study. The help of Anne-Laure Tertois from Paradigm and of Christophe Antoine from the Gocad Research Group was much appreciated in generating the tetrahedral Solid Model.

3.12 References

Dubé, B., Gosselin, P. Greenstone-hosted quartz-carbonate vein deposits, in Godfellow, W.D, ed., Mineral Deposits of Canada: A Synthesis of Major Deposit-Types, District Metallogeny, the Evolution of Geological Provinces, and Exploration MethodsGeological Association of Canadca, Mineral Deposit Division, Special Publication No. 5, 46-73.

Corfu, F. 1993. The Evolution of the Southern Abitibi Greenstone Belt in Light of Precise U-Pb Geochronology. Economic Geology 88(6), 1323-1340.

Corfu, F., Krogh, T. E., Jensen, L.S., U–Pb zircon geochronology in the southwestern Abitibi greenstone belt, Superior Province, Canadian Journal of Earth Sciences 26(9), p. 1747–1763

Couture, J.-F. 1996. Gisements metalliques du district de Rouyn-Noranda. In: Métalogénie et évolution de la région de Rouyn-Noranda (edited by Couture, J.-F. and Goutier, J.) MB 96-06. Ministère des Ressources naturelles du Québec, 11-18.

Couture, J.-F. and Pilote, P. 1993. The Geology and Alteration Patterns of a Disseminated Shear Zone-Hosted Mesothermal Gold Deposits: The Francoeur 3 Deposit, Rouyn-Noranda, Quebec. Economic Geology 88(6), 1664-1684.

Couture, J.-F. and Willoughby, N. O. 1996. Géologie du gisement Granada. In: Métallogénie et évolution de la région de Rouyn-Noranda (edited by Couture, J.-F. and Goutier, J.) MB 96-06. Ministère des Ressources naturelles du Québec, 77-80.

Couture, J.-F., Goutier, J., and Peloquin, A.S.,. 1996. Géologie de la region de Rouyn-Noranda. In: Métallogénie et évolution de la région de Rouyn-Noranda (edited by Couture, J.-F. and Goutier, J.) MB 96-06. Ministère des Ressources naturelles du Québec, 77-80.

Couture, J.-F. , Marquis, P., 1996 , Les minéralisations en Mo,Cu,Au associées aux intrusions alcalines tardi,tectoniques, secteur de la baie Renault. Dans: Métallogénie et évolution tectonique de la région de Rouyn,Noranda (Couture, J.-F. , Goutier, J. (éditeurs) . Ministère des Ressources naturelles du Québec; MB 96,06, pages 91-94

Cox, S. F., Knackstedt, M. A. & Braun, J. 2001. Principles of structural control on permeability and fluid flow in hydrothermal systems. In: Structural controls on ore genesis (edited by Richards, J. P. & Tosdal, R. M.). Reviews in Economic geology. volume 14. Society of Economic Geologists.

Cox, S. F. , Ruming, K., 2004. The St Ives mesothermal gold system, Western Australia - a case of golden aftershocks?, Journal of Structural Geology, V. 26, 6-7, p. 1109-1125

Daigneault, R. and Mueller, W. U. 2004. Abitibi greenstone belt plate tectonics: the diachronous history of arc development, accretion and collision. In: The Precambrian Earth: Tempos and events (edited by Eriksson, P., Altermann, W., Nelson, D., Mueller, W. U., Catuneaunu, O. and Strand, K.). Development in Precambrian Geology 12. Elsevier, 88-103.

Daigneault, R., Mueller, W. U. and Chown, E. H. 2002. Oblique Archean subduction: accretion and exhumation of an oceanic arc during dextral transpression, Southern

Volcanic Zone, Abitibi Subprovince, Canada. Precambrian Research 115(1-4), 261-290.

Daigneault R, 1996, Couloirs de déformation de la Sous-Province de l'Abitibi. Ministère des Ressources naturelles du Québec, Québec, p 115

Davis, D. W. 2002. U-Pb geochronology of Archean metasedimentary rocks in the Pontiac and Abitibi subprovinces, Quebec, contraints on timing, provenance and regional tectonics. Precambrian Research 115, 97-117.

Dimroth, E., Imreh, L., Rocheleau, M. and Goulet, N. 1982. Evolution of the south-central part of the Archean Abitibi Belt, Quebec. Part I: Stratigraphy and paleogeographic model. Canadian Journal of Earth Sciences 19(9), 1729-1758.

Eisenlohr, B. N., Groves, D. I. and Partington, G. A. 1989. Crustal-scale shear zones and their significance to Archaean gold mineralization in Western Australia. Mineralium Deposita 24, 1-8.

Fairbairn, H. W., Hurley, P. M., Card, K. D. and Knight, C. J. 1969. Corroletion of Radiometric Ages of Nipissin Diabase and Huronian Metasediments with Proterozoic Orogenic Events in Ontario. Canadian Journal of Earth Sciences 6, 489-497.

Faure, S., 2003, Analyse des champs filoniens aurifères avec le modeleur geomecanique UDEC, Projet du Consortium de recherché en exploration minérale 2002-4 , 30 p

Goldfarb, R. J., Groves, D. I. and Gardoll, S. 2001. Orogenic gold and geological time: a global synthesis. Ore Geology Reviews 18, 1-75.

Groves, D. I. 1993. The crustal continuum model for late-Archean lode-gold deposits of the Yilgarn Block, Western Australia. Mineralium Deposita 28(6), 366-374.

Groves, D. I., Goldfarb, R. J., Gebre-Mariam, M., Hageman, S. G. and Robert, F. 1998. Orogenic gold deposits: A proposed classification in the context of the crustal distribution and relationship to other deposit types. Ore Geology Reviews 13(1-5), 7-27.

Groves, D. I., Goldfarb, R. J., Knox-Robinson, C. M., Ojala, J., Gardoll, S., Yun, G. Y. and Holyland, P. 2000. Late-kinematic timing of orogenic gold deposits and significance for computer-based exploration techniques with emphasis on the Yilgarn Block, Western Australia. Ore Geology Reviews 17, 1-38.

Groves, D. I., Goldfarb, R. J., Robert, F., Hart, C. R. J. &. 2003. Gold deposits in metamorphic belts: overview of current understanding, outstanding problems, future research, and exploration significance. Economic Geology 98, 1-29.

Hodgson, C. J. 1993. Mesothermal Lode-gold Deposits. In: Mineral Deposit Modeling (edited by Kirkham, R. V., Sinclair, W. D., Thorpe, R. I. and Duke, J. M.) Special Paper 40. Geological Association of Canada, 635-678.

Holyland, P.W., Ojala, V. J., 1997, Computer-aided structural targeting in mineral exploration: Two- and three-dimensional stress mapping, Australian Journal of Earth Sciences, Volume 44, Issue 4 August 1997 , pages 421 - 432

Jiang, Z, Oliver, N.H.S., Barr, T. D., Power W.L., Ord, A., 1997, Numerical modeling of fault-controlled fluid flow in the genesis of tin deposits of the Malage ore field, Gejiu mining district, China, Economic Geology;; v. 92; no. 2; p. 228-247

Jolly, W.T., 1978 – Metamorphic history of the Archean Abitibi belt. In: Metamorphism in the Canadian Shield. Geological Survey of Canada; Paper 78-10, pages 63-78.

Kerrich, R., Goldfarb, R. J., Groves, D. I. and Garwin, S. 2000. The Geodynamics of World-Class Gold Deposits: Characteristics, Space-Time Distribution, and Origins.

In: Gold in 2000 (edited by Hageman, S. G. and Brown, P. E.) 13. Reviews in Economic geology, 500-551.

Lafrance, B., Davis, D.W., Goutier, J., Moorhead, J., Pilote, P., Mercier-Langevin, P., Dubé, B., Galley, A.G., and Mueller, W.U., 2005, Nouvelles datations isotopiques dans la portion Québécoise du Groupe de Blake River et des unités adjacentes: Ministères des Ressourcesnaturelles et de la Faune, Québec; RP 2005-01, 15 p.

Legault, M. and Lalonde A., in prep, Discrimination des syenites associés aux gisements aurifères de la Sous-province de l'Abitibi, Québec, Canada, Ministère des Ressources naturelles, RP-2008-XX

Legault, M. and Rabeau, 2007, Étude métallogénique et modélisation 3D dans la region de la Faille Cadillac dans le secteur de Rouyn-Noranda (phase 2), Ministère des Ressources Naturelles et de la Faune du Québec, 11 p.

Legault, M. and Rabeau, 2006, Étude métallogénique et modélisation 3D dans la region de la Faille Cadillac dans le secteur de Rouyn-Noranda (phase 1), Ministère des Ressources natureelle et de la Faune du Québec , 11 p.

Lapage, F 2003, Generation de maillages tridimentionnels pour la simulation des phenomènes physiques en geosciences. PhD thesis, INPL, Nancy, France. 200 p.

Mair, J. L., Ojala, V. J., Salier , B. P., Groves, D.I., Brown, S.M., 2000, Application of stress mapping in cross-section to understanding ore geometry, predicting ore zones and development of drilling strategies, Australian Journal of Earth Sciences, V. 47,- 5, p. 895 - 912

Mclellan, J.G., Oliver, N.H.S., 2008, Discrete element modeling applied to mineral prospectivity analysis in the eastern Mount Isa Inlier Precambrian Research, V. 163 1-2, p. 174-188

McNicoll, V., Dubé, B., Goutier, J., Mercier-Langevin, P., Dion, C., Monecke, T., Ross, P.S., Thurston, P, Percival, J., Legault, M., Pilote, P., Débard, J. Leclerc, F., Gibson, H., Ayer, J., 2008, New U-Pb Geochronology from theTGI-3 Abitibi/plan cuivre : Implications for geological Interpretations and Base Metal Exploration, abstract, GAC-MAC, Quebec 2008, p.110.

Micklethwaite, S., Cox, S.F., 2004, Fault-segment rupture, aftershock-zone fluid flow, and mineralization, Geology, v. 32; no. 9; p. 813-816

Micklethwaite, S., Cox, S.F., 2006, Progressive fault triggering and fluid flow in aftershock domains: Examples from mineralized Archaean fault systems, Earth and Planetary Science Letters, v 250,- 1-2, Pages 318-330

Mueller, W.U., Friedman, R., Daigneault, R., Mortensen, J.K., The Blake River Caldera Complex : comstraints on Volcanic Stratigraphy, Subaqueous Volcanism and Synvolcanic Pluton History, abstract, GAC-MAC, Quebec 2008, p.118.

Muron, 2005, Méthodes numériques de restauration des structures faillées, Unpublished thesis, Institut national polytechnique de Lorraine, 131 p.

Olivier N.H.S., Review and classification of structural controls on fluid flow during regional metamorphism, Journal of Metamorphic Geology, Volume 14, 4, Pages 477 - 492

Ord, A., Olivier, N. H. S.,1997, Mechanical controls on fluid flow during regional metamorphism: some numerical models, Journal of Metamorphic Geology, Vol. 15, Issue 3, p.345 - 359

Piché, M., Jébrak, M., Normative minerals and alteration indices developed for mineral exploration, Journal of Geochemical Exploration, V. 82, Issues 1-3, Pages 59-77

Potma; W., Roberts; P. A., Schaubs, P. M., Sheldon, H. A, Zhang,Y., Hobbs, B. E., Ord, A., 2008, Predictive targeting in Australian orogenic-gold systems at the deposit

to district scale using numerical modelling, Australian Journal of Earth Sciences ; Volume 55, 1, p. 101 – 122

Poulsen, K. H., Robert, F. and Dubé, B. 2000. Geological classification of Canadian gold deposits. Geological Survey of Canada, 106 p.

Rabeau, O, Legault, M., Cheilletz, A., Jébrak, M. Royer, J. J., Cheng, L. Z., 2009, Gold potential of a hidden Archean fault zone: the case of the Cadillac-Larder Lake Fault, accepted in Journal of Exploration and Mining Geology

Ridley, J.R. and Diamond, L. W., 2000, Fluid chemistry of orogenic Lode Gold Deposits and Implications for Genetic Models, SEG REviews, V.13, p. 141-162.

Robert, F. 2001. Syenite-associated disseminated gold deposits in the Abitibi greenstone belt, Canada. Mineralium Deposita 36, 503-516.

Robert, F., Poulsen, H.K., Cassidy, K.F., Hodgson, J., 2005, Gold Metallogeny of the Superior and Yilgarn Cratons Economic Geology, 100th Anniversary Volume, p. 1001-1035

Titeux, M.O.,2009, Restauration et incertitudes structurales : changement d'échelles

des propriétés mécaniques et gestion de la tectonique salifère. PhD Thesis, INPL, Nancy, 200 p.

Thurston, P.C., Goutier, J., McNichol, V., Legault, M., 2008, Mafic Dykes cutting the Blake River Group, Abitibi Subprovince, abstract, GACMAC 20008

Weinberg, R. F., Hodkiewicz, P. F. & Groves, D. I. 2004. What controls gold distribution in Archean terranes? Geology 32(no. 7), 545-548.

Thurston, P. C., . Ayer, J. A, Goutier ,J., Hamilton, M. A., 2008, Depositional Gaps in Abitibi Greenstone Belt Stratigraphy: A Key to Exploration for Syngenetic Mineralization, Economic Geology; v. 103; no. 6; p. 1097-1134

Conclusions

Plusieurs études ont abordé le sujet de l'or de type orogénique et de ses modes de formation. (Groves, 1998; Groves et al. 2003; Kerrich et al., 2000; Goldfarb et al., 2005; Dubé and Gosselin, 2007). Il est bien établi, que ces dépôts épigénétiques sont soumis à un contrôle structural très important, et que les failles de premier ordre jouent un rôle prédominant dans leur formation. De plus, leur contexte de formation, la nature des fluides minéralisateurs ainsi que le mode de transport de l'or sont relativement bien compris. Par contre, l'exploration de ces gisements reste très complexe puisque leur distribution en périphérie des failles majeures paraît hétérogène et irrégulière.

Contrairement à une approche ciblée sur certains gisements, cette thèse a misé sur une approche numérique novatrice et intégratrice afin de définir les principaux facteurs régissant la distribution spatiale des gisements aurifères près d'un couloir de déformation majeur au sein d'une ceinture de roche verte et d'en tirer des méthodologies permettant de mieux cibler les secteurs à haut potentiel. Ces travaux ont été effectués à diverses échelles : de la faille de premier ordre à certains segments choisis de cette faille. Les méthodes numériques sont bien adaptées à l'étude de ce type de gisement considérant que Groves et al. (2000, 2003) ont démontré que les minéralisations d'or de type orogénique sont très tardives dans l'évolution tectonique.

Ce constat permet de supposer que la géométrie structurale observable dans la ceinture de roche verte de l'Abitibi est très similaire à celle présente lors de la circulation des fluides minéralisateurs et la mise en place des gisements d'or de type orogénique.

Le premier constat de cette thèse est que l'emplacement des gisements aurifères de type orogénique ne semble pas indépendant de celui de ses voisins. Pour arrivée à cette fin, une méthodologie qui utilise la distance inter-gisements en suivant le tracé de la faille, appelée distance curviligne, a été développée. Il a été possible de démontrer une loi de type log-uniforme entre l'interdistance curviligne entre les gisements et la fréquence cumulative. Il est possible de déduire de ce constat que la nature des lithologies le long d'une faille de premier ordre a peu d'influence sur la distribution spatiale des gisements d'or de type orogénique à l'échelle régionale. De plus, ce constat permet d'évaluer une zone d'influence des relâchements de pression hydrostatique le long de la faille de Cadillac-Larder Lake qui serait d l'ordre de 5 km. Finalement, une distribution spatiale prévisible permet de dresser une carte de potentiel à petite échelle.

Cette thèse a aussi permis de développer une méthode de ciblage en 3D sur un segment d'une faille archéenne majeure enfoui sous couverture protérozoïque. Le secteur de cette étude a été délimité en utilisant les conclusions du premier chapitre. Cette méthodologie utilise la méthode du *poids de la preuve* afin de déterminer

l'association spatiale entre les gisements d'or orogéniques et certains facteurs géologiques à une échelle plus locale. Les associations spatiales les plus fortes ont par la suite permis de cibler des secteurs sous les sédiments.

Finalement, cette thèse s'est penchée sur une approche géomécanique en 3D dans afin d'identifier les zones en dilatation lors des événements tectoniques rattachés à la mise en place de l'or de type orogénique. En se basant sur la notion que les pressions tectoniques et lithostatiques infligées à un volume rocheux entraînent des migrations de fluides des zones à hautes pressions vers les zones à basses pressions, un outil de modélisation de la déformation basé sur les déplacements a été mis au point. Cet outil permet une approche très intégratrice est peu s'avérer très prometteur en tant qu'aide à la prospection et pour expliquer l'emplacement de certains gisements.

Certains travaux futurs qui pourraient éclaircir des points qui restent en suspend suite à ces travaux. Il serait par exemple important de tester la distribution spatiale des gisements de type orogéniques en utilisant la distance curviligne sur d'autres failles d'importance crustale à l'extérieur de la ceinture de roche verte de l'Abitibi. Des emplacements comme le craton du Yilgarn en Australie pourraient être intéressants à tester. Des examens de la distribution des gisements sur les segments de deuxième et de troisième ordre permettraient eux aussi d'apporter des éléments de réponse au rôle des failles dans la formation de ces gisements. Finalement, un raffinement de l'approche géomécanique dans le but de réaliser des modélisations de déformation sur

des modèles plus détaillés et avec une meilleure résolution permettrait de grandement de bonifier l'approche

Références

Dubé, B., Gosselin, P., 2007, Greenstone-hosted quartz-carbonate vein deposits, in : Mineral Deposits of Canada: A Synthesis of Major Deposit-Types, District Metallogeny, the Evolution of Geological Provinces, and Exploration Methods, Godfellow, W.D, ed., Geological Association of Canadca, Special Pubublication. No. 5, p. 46-73.

Goldfarb, R. J., Baker, T., Dubé, B., Groves, D. I., Hart, C.J.R., and Gosselin, P., 2005, Distribution, character and genesis of gold deposits in metamorphic terranes. *In:* Economic geology 100th Anniversary volume. Society of Economic Geologists, p. 407-450.

Groves, D. I., Goldfarb, R. J., Gebre-Mariam, M., Hageman, S. G., and Robert, F., 1998, Orogenic gold deposits: A proposed classification in the context of the crustal distribution and relationship to other deposit types: Ore Geology Reviews, v. 13, p. 7-27.

Groves, D. I., Goldfarb, R. J., Knox-Robinson, C. M., Ojala, J., Gardoll, S., Yun, G. Y., and Holyland, P., 2000, Late-kinematic timing of orogenic gold deposits and significance for computer-based exploration techniques with emphasis on the Yilgarn Block, Western Australia: Ore Geology Reviews, v. 17, p. 1-38.

Groves, D. I., Goldfarb, R. J., Robert, F., Hart, C. R. J. &. 2003. Gold deposits in metamorphic belts: overview of current understanding, outstanding problems, future reaserch, and exploration significance. *Economic Geology* 98, 1-29.

Kerrich, R., Goldfarb, R. J., Groves, D. I., and Garwin, S., 2000, The Geodynamics of World-Class Gold Deposits: Characteristics, Space-Time Distribution, and Origins., in Hageman, S. G., and Brown, P. E., eds., Gold in 2000, 13, Reviews in Economic geology, p. 500-551.